Title

Neural Circuits Underlying Social Touch Deficits in Mouse Models of Autism Spectrum Disorders

Author

Chari, Trishala

Publication Date

2024

Peer reviewed|Thesis/dissertation

UNIVERSITY OF CALIFORNIA

Los Angeles

Neural Circuits Underlying Social Touch Deficits in Mouse Models of Autism Spectrum Disorders

A dissertation submitted in partial satisfaction of the requirements for the degree Doctor of Philosophy in Neuroscience

by

Trishala Chari

2024

ABSTRACT OF THE DISSERTATION

Neural Circuits Underlying Social Touch

Deficits in Mouse Models of Autism Spectrum Disorders

by

Trishala Chari

Doctor of Philosophy in Neuroscience

University of California, Los Angeles, 2024

Professor Carlos Portera-Cailliau, Chair

Social touch, an important aspect of social interaction and communication, is essential to kinship across animal species. Although often perceived as pleasurable, social touch can become considered aversive under certain contexts and often in individuals with Autism Spectrum Disorders (ASD). However, little is known about the neural circuits that contribute to social touch aversion in ASD. Rodent models provide an opportunity to interrogates these circuits, but social touch has not been thoroughly investigated in rodents, in part due to the lack of appropriate assays. We designed a novel head-fixed assay for social touch in mice, in which the experimenter has complete control to elicit highly stereotyped bouts of social touch between two animals. The user determines the number, duration, context, and type of social touch interactions, while monitoring an array of complex, aversive behavioral responses with high resolution cameras. We validated this assay in two different models of autism spectrum disorder (ASD), the *Fmr1* knockout (KO) model of Fragile X Syndrome and maternal immune activation mice. We observed higher rates of avoidance running, hyperarousal, and aversive facial expressions (AFEs) to social touch than to object touch, in both ASD models compared to controls. Because this new social touch assay for head-fixed mice can be used to record neural activity during repeated bouts of social touch, we assessed how social touch is encoded in the relevant vS1, tS and BLA circuits and how

social touch encoding is perturbed in *Fmr1* KO mice. We find that vS1 in wild type mice can distinguish social from non-social touch, thereby encoding differences in texture. tS activity reflects salience encoding, such that the firing of cells is driven more by social than object touch when touch is voluntary and vice-versa when touch is forced. Finally, activity in the BLA is only driven by touch that is strongly aversive (i.e. forced object touch). In *Fmr1* KO mice, vS1 and tS activity are similarly modulated by social and object touch suggesting that these regions cannot discriminate between the two types of touch. The inability to distinguish between social and non-social touch is also reflected at the behavioral level in the FXS mouse model. Furthermore, *Fmr1* KO mice have a similar proportion of cells responding to aversive behaviors during social and object across vS1, tS and BLA. These experiments shed light on how the inability of cortical, striatal and amygdalar circuits to distinguish social touch from aversive non-social touch may contribute to the emergence of social touch aversion in ASD mouse models.

The dissertation of Trishala Chari is approved.

Weizhe Hong

Laura Anne Wilke

Sotiris Masmanidis

Shafali Jeste

Carlos Portera-Cailliau, Committee Chair

TABLE OF CONTENTS

LIST OF FIGURES

LIST OF ABBRIEVIATIONS

ASD: Autism Spectrum Disorder

NDC: Neurodevelopmental condition

FXS: Fragile X Syndrome

KO: Knockout

WT: Wildtype

MIA: Maternal immune activation

PBS: Phosphate buffered saline

PFA: Paraformaldehyde

Poly(I:C): Polyinosinic:polycytidylic acid

Intraperitoneally: i.p.

AFE: Aversive facial expressions

DLC: DeepLabCut

2P: 2-photon

TRAP: Targeted Recombination in Active Populations

tdTom: tdTomato

vS1: Vibrissal primary somatosensory cortex

Layer 2/3, 4, 5/6: L2/3, L4, L5/6

tS: Tail of the striatum

BLA: Basolateral amygdala

ACCx: Anterior cingulate cortex

NAc: Nucleus accumbens

InsCx: Insular cortex

CeA: Central amygdala

MeA: Medial amygdala

PVT: Paraventricular nucleus of the thalamus

PvtH: Paraventricular nucleus of the hypothalamus

PAG: Periaqueductal grey

MC: Motor cortex

V1: Primary visual cortex

DiI: 1,1'-Dioctadecyl-3,3,3',3'-tetramethylindocarbocyanine perchlorate

PSTH: Peristimulus time histogram

PCA: Principal component analysis

ROC: Receiver operating characteristic

SVM: Support vector machine

ACKNOWLEDGEMENTS

First and foremost, I'd like to thank Dr. Carlos Portera-Cailliau, my advisor throughout my graduate training. Your mentorship allowed me to thrive as an independent researcher, always thinking outside the box and trying new ideas even if they seemed crazy or insane. That support for creative thinking and scientific rigor was crucial for me to grow in the scientist that I am today.

I'd also like to thank my fellow labmates in the Portera-Cailliau lab: Nazim Kourdougli, Anand Suresh, Irma Tello García, Carlos Sánchez-León, Zoë Dobler, Michelle Wu. Even if we were all working on our own separate projects, we always found ways to help each other out and this speaks to the collaborative environment that fostered my graduate training. I would also like to thank João Couto as a collaborator from Anne Churchland's lab and who helped me immensely in setting up Neuropixels chronic recordings in mice in the Portera-Cailliau lab and with initial analysis pipeline for the electrophysiological data.

My thesis work was supported by the UCLA T32 Training in Neurotechnology Translation Predoctoral Award (NIH T32NS115753). I thank the T32 directors Drs. Nanthia Suthana, Daniel Lu and Dejan Markovic for their leadership and providing a unique training program that allows basic researchers to apply their research work to translational Neuroscience. My work is also supported by the Achievement in Rewards for College Scientists (ARCS) Fellowship and a NIH Eunice Kennedy Shriver National Institute of Child Health and Human Development PhD Fellowship (NIH F31HD108042). I am grateful for the support that these funding sources have provided during my graduate training.

My training would not have been possible without the support of my doctoral committee. Thank you Drs. Weizhe Hong, Laura Anne Wilke, Sotiris Masmanidis and Shafali Spurling Jeste for pushing me to think about my data analytically and rigorously through your unique perspectives in different research areas of Neuroscience.

As a PhD student in UCLA's Neuroscience Interdepartmental Program (NSIDP), I was provided a lot for support from leadership and administration. I'd like to thank Drs. Felix Schweizer and Tom O'Dell as Chair and Vice-Chair of NSIDP. Dr. Schweizer always provide a space where I could speak freely about research and the trials and tribulations that came with it. I also appreciated all resources and opportunities he would provide to support my training and growth as a scientist. I'd also like to thank Jenny Lee, the NSIDP graduate advisor, and Aftin Whitten, the NSIDP program coordinator. Jenny was a beacon for financial advice. course opportunities and even recommendations for a day out in Los Angeles. I appreciate the work she put to ensure that I was well-supported as a student at UCLA. I also thank my fellow NSIDP students, especially the Social Committee, for providing a social space to talk about the trials and tribulations of our graduate training. Our annual Joshua Tree trips always provided a brief getaway from our studies to reflect on our trainings and years in the program.

I'd like to thank the Graduate Programs in Bioscience (GPB) team, specifically Drs. Alex Bui, Director of GPB, and Diana Azurdia, Director of Mentoring and Inclusion for Bioscience Research Training. I appreciate their efforts to bring together the students from all the programs in GPB to foster a community for scientists from all backgrounds.

I would like to thank my NSIDP program cohort. Being one of the few cohorts that went through the COVID pandemic, I always appreciated our Zoom get-togethers and how we were able to encourage and help each other on our research projects even from a distance.

I thank my friends that I met through the program and Neuroscience community at UCLA. Thank you to Benjamin Liu, Juan Luis Romero Sosa and Sukriti Gupta. You are the best roommates that I could ever ask for and provided the encouragement I needed to get through the past few years of my graduate training. I also thank Katherine Espinoza, Conor Dorian and Roy McReynolds III, my fellow NSIDP cohort that lives down the block. I am so glad that we found each other during graduate school and our hotpot dinners are proof of the strong friendship we've built over the years as fellow scientists.

I'd also like to thank my friends and fellow scientists across the globe. I would especially like to thank Leire Ledahawsky, my roommate back in Edinburgh. Our 10+ year friendship is proof that even with distance, we can find ways to support one another as Neuroscientists.

Lastly, I'd like to thank my family – my brother Varun, my sister-in law Saankhya and my parents, Shanti and Govind Chari. Thank you to my mom especially for always making the effort to chat weekly even when there were times I would get flooded with tons of work during my PhD. You always knew the importance of keeping family close. Thank you all for being the strongest support system in my life.

VITA

EDUCATION

2012 - 2016	School of Biomedical Sciences, University of Edinburgh
2016 - 2018	Harvard Extension School, Harvard University
2018 - 2024	David Geffen School of Medicine, University of California, Los Angeles Interdepartmental Program in Neuroscience

RESEARCH EXPERIENCE

2013	Summer Undergraduate Research Intern (Marco Gallio, Ph.D., advisor) Weinberg College of Arts & Sciences, Northwestern University
2014	Summer Undergraduate Research Intern (Daniel Corcos, Ph.D., advisor) Feinberg School of Medicine, Northwestern University
2015	Amgen Scholars Program (Anton Sirota, Ph.D., advisor) Faculty of Biology, Ludwig Maximilian Universirty of Munich
2016	Undergraduate Honors Project (Peter Brophy, Ph.D., advisor) Centre for Discovery Brain Sciences, University of Edinburgh
2016-2018	Research Assistant (Michela Fagiolini, Ph.D., advisor) F.M. Kirby Neurobiology Center, Boston Children's Hospital
2019	Rotation Project (Lindsay De Biase, Ph.D., advisor) Department of Physiology, UCLA
2019	Rotation Project (Elaine Hsiao, Ph.D., advisor) Integrative Biology & Physiology, UCLA
2019-2024	Ph.D. Dissertation Project (Carlos Portera-Cailliau, Ph.D., advisor) Department of Neurology, UCLA

PUBLICATIONS

1. **Chari T**, Hernandez A, Couto J, Portera-Cailliau C. (*in prep*). Neocortical, striatal, and amygdalar neurons differentially encode social versus non-social touch.

2. Dobler Z, Suresh A, **Chari T**, Mula S, Portera-Cailliau C. (*under revision*). Adapting and facilitating responses of layer 2/3 neuron populations in mouse somatosensory cortex are dynamic and shaped by experience across days.
3. **Chari T**, Hernandez A, Portera-Cailliau C. (2023). A novel head-fixed assay for social touch in mice uncovers aversive responses in two autism models. *J Neurosci*. PMID: 37669860.
4. **Chari T**, Griswold S, Andrews NA, Fagiolini M. (2020). The stage of the estrus cycle is critical for interpretation of female mouse social interaction behavior. *Front Behav Neurosci*. 14:113. PMID: 32714163.

PRESENTATIONS

Selected Invited Talks

1. **Chari T**. Neural circuits underlying social touch deficits in mouse models of autism spectrum disorder**.** Society for Neuroscience Meeting, Nov 2023
2. **Chari T**. A novel behavioral assay to investigate social touch deficits in mouse models of autism. NIH/NINDS T32 PI/Trainee Annual Meeting, June 2023

Selected Oral Poster Presentations

1. **Chari T**, Hernandez A, Portera-Cailliau C. Neural circuits underlying social touch behavioral deficits in mouse models of autism. Lake Conference on Neural Dynamics and Coding, Sept 2023.
2. **Chari T**, Dobler Z, Portera-Cailliau C. A novel behavioral assay to investigate social touch deficits in mouse models of autism. Barrels Society Meeting, Oct 2020.
3. Andrews N, **Chari T**, Griswold S, Fagiolini M. Phenotyping mouse models of neurodevelopmental disorders at the Neurodevelopmental Behavior Core in Boston Children's Hospital. Translational Neuroscience Symposium, April 2017.

SELECTED HONORS AND AWARDS

2020 UCLA T32 Training in Neurotechnology Translations Predoctoral Award (NIH T32NS115752)

2020 Achievement in Rewards for College Scientists (ARCS) Fellowship

2022 NIH Eunice Kennedy Shriver National Institute of Child Health and Human Development F31 Ruth L. Kirschstein Individual Predoctoral NRSA for PhD Fellowship (NIH F31HS108042)

2023 UCLA Brain Research Institute Travel Award

CHAPTER 1: Introduction

1.1: Social touch in animals and humans

Social communication and interaction rely on a multitude of sensory stimuli between two or more animals or humans. These sensory cues vary and can come in the form of auditory (vocalizations or language), visual (body language, facial expression cues), olfactory (pheromones) and tactile (grooming, comforting, caressing) information[1,2]. Tactile social information, including social facial touch, is particularly relevant in human and animal social interaction and communication (even mating), and it allows for the development of strong kinship bonds[1,3-7]. Touch allows animals of the same species to comfort one another, provide information about corresponding internal states and build or develop new or existing relationships[3,6,8,9]. Social touch behaviors in humans are diverse and include kissing, hugging, grooming, caressing and even tickling[3]. Similar touch behaviors are also observed in animal species during mutual grooming (including allogrooming) or social play[10-13]. Although often perceived as pleasurable or pleasant, social touch can translate into an aversive stimulus under certain contexts (e.g., when a child is kissed or hugged by an adult stranger). Social touch is often perceived as aversive by individuals with neurodevelopmental conditions (NDC), including Autism Spectrum Disorders (ASD)[3].

1.2: Aversion to social touch in ASD

ASD represents a prevalent subtype of NDC that is characterized by deficits in social interaction, repetitive behaviors, and differences in sensory processing[14]. Decreases in quality of life for autistic individuals are primarily attributed to social deficits, which can be associated with (or even triggered by) atypical processing of sensory stimuli[3,15,16]. Sensory hypersensitivity has been observed in children with ASD with increased physiological arousal, gaze avoidance & aversion towards seemingly innocuous stimuli (loud noises or touch from another person)[14,17,18]. Studies have reported that sensory hypersensitivity may be due to a combination of changes in the detection threshold and adaptation to sensory stimuli[19-22]. Tactile hypersensitivity can also

contribute to social behavioral problems, either as tactile stimuli becoming distractors during social interaction or by heightening the responsivity to social touch[17,23,24]. In fact, aversion to social touch, including affective touch, has been reported through variety of different behavioral manifestations that mirror the manifestations of tactile hypersensitivity, including physiological changes, gaze avoidance and anxiety[25-29]. Research has also shown that ASD individuals are unable to differentiate social from non-social touch either by texture or by the affective importance, suggesting they cannot perceive the rewarding nature of social touch[19,30-32]. In general, children with ASD with aversion to social touch leading to social inexperience may also be susceptible to other behavioral symptoms, such as anxiety and isolation[5,33]. While these maladaptive responses to social touch are well recognized in ASD, little is known about the neural circuits involved.

1.3: Tactile hypersensitivity and social deficits in rodent ASD models

Rodent models of ASD could be used to understand the neural circuits or brain regions that contribute to social touch aversion, but research on social touch and the resulting aversive behaviors in rodent models remains in its infancy. Fortunately, both tactile hypersensitivity and social interaction deficits have been well described in these models. As such, certain models may be more suitable to study social touch aversion than others based on if they exhibit a combination of tactile hypersensitivity and social deficits. The models in which most of these behavioral manifestations have been described represent single gene disorders of autism (for example those caused by mutations in *Fmr1*, *Shank3*, or *Mecp2*), but these behaviors have also been described in select environmental models[34,35].

Tactile hypersensitivity has been observed in a variety of different rodent models. The Fragile X Syndrome (FXS) *Fmr1* knockout (KO) model of autism will avoid or display defensive grabbing to passive whisker stimulation at 10 Hz[21,36]. This frequency of tactile stimulation is within the range at which mouse whiskers move when they naturally explore their environment,

suggesting this model displays hypersensitivity to mild tactile stimuli[37]. Tactile hypersensitivity also impairs learning in the *Fmr1* KO model[38]. Similarly, the *Shank3* genetic mouse model of ASD displays tactile hyperreactivity to weak deflections of their whiskers during a tactile discrimination behavioral task. The *Syngap1*, 16p11.2 deletion & *Mecp2* genetic mouse models of autism also show evidence of sensory hypersensitivity[39-41]. Interestingly, the *Cntnap2* model of autism doesn't show tactile hypersensitivity, reflecting the variability also observed across ASD individuals in how they respond to innocuous tactile stimuli.

Compared to tactile hypersensitivity, social interaction deficits have been more widely observed across both genetic and environmental rodent models of autism. Social deficits have mainly been assessed based on social preference for other conspecifics or by abnormal ultrasonic vocalizations (USVs), which is used as social communication between rodents[42]. The BTBR inbred mouse strain, the *Fmr1*, *Mecp2*, *Shank3b, and Cntnap2* mutant mice*,* and the maternal immune activation (MIA) environmental model are but a subset of mouse models of NDC that show reduced social preference towards a stranger conspecific on the three-chamber assay[41,43-46]. Additionally, studies have reported that the MIA, Tuberous Sclerosis (*Tsc2*$^{+/-}$), *Shank3, Nrxn1* KO and *Fmr1* KO models of autism show differences in the frequency and temporal dynamics of USVs towards their mother during development and towards other mice in adulthood[47-50]. Interestingly, one study found that the MIA model shows abnormal development of the dysgranular zone of the primary somatosensory cortex and this may be associated with reduced social preference and abnormal USVs in MIA mice[51]. Another study has also suggested that prosocial behaviors, such as huddling, may be reduced in the 16p11.2 deletion model of autism[52]. Based on these findings, the *Fmr1* KO, *Shank3*, *Mecp2* and 16p11.2 deletion genetic models and the MIA environmental model of ASD may be suitable to study social touch aversion due to the presence of both tactile hypersensitivity and social interaction deficits in these models.

It should also be noted there are cases in which individuals with ASD show tactile hyposensitivity and may engage in sensory seeking behaviors towards social and non-social touch to enhance sensory experience[53,54]. Interestingly, this behavioral phenomenon appears to occur in at least the *Shank3* rodent model of autism, where they display repetitive grooming as a means for sensory stimulation, and warrants further investigation with assays that could quantify sensory seeking to social touch[55,56].

While tactile hypersensitivity and social interactions have been studied extensively in rodent models of autism, this has not been the case for hypersensitivity and aversion to social touch. The dearth of research on aversion to social touch in rodent models may in part be due to the limitations of current behavioral assays for assessing social touch.

1.4: Assays for quantifying behavioral responses to social touch in rodent models

Previous studies have employed behavioral assays ranging from freely moving to head-restrained assays to study how rodent models respond to social touch[57-62]. One of the more established assays for quantifying the degree of social interactions between two mice is the three-chamber social preference assay. In this assay, the test mouse is placed in the middle of a three-chambered arena. One of the side chambers (either left or right) contains a cylindrical compartment (an inverted pencil cup holder) containing a novel mouse (i.e., a stranger mouse that the test mouse has never been exposed to). The other side chamber has a similar compartment but instead contains a novel object (of any shape, size, texture, or color) that the test mouse has never seen before. The test mouse is assessed for how long it spends with the compartment containing the stranger mouse or the novel object upon being placed in the middle chamber. The three-chamber assay can also be modified by placing a familiar mouse instead of a novel object in one of the compartments to assess if mice prefer social novelty and spend more time in the chamber containing the novel mouse than the chamber with the familiar mouse. While this assay provides the advantage of assessing naturalistic, freely moving

behaviors of the test mouse, the assay does limit the social touch behaviors that the test mouse elicits with the novel or familiar mouse due to the barrier for the cylindrical compartment. Aversive behaviors to social touch are often not present because the test mouse can choose to avoid the novel or familiar mouse altogether. The decision not to engage in social approach is a consistent limitation across freely moving assays for studying social touch aversion. Furthermore, the complexity of behaviors that can be measured is limited as the camera for recording the interactions of the test mouse with the other mouse or object is above the three-chamber[63].

The open-field test has also been adapted to assess freely moving social touch interactions between two mice or rats[62,64]. One of the animals is placed in a cylindrical compartment similar to the three-chamber assay[64] or both animals can be allowed to freely move in the chamber[62]. However, the open-field social interaction (OFSI) test has similar limitations as the three-chamber test in that the interacting animals may be prevented from engaging in more social touch behaviors and that the placement of the camera above the open-field arena limits the complexity of the behaviors that can be assessed.

In addition to the three-chamber assay and OFSI test, the gap paradigm for social touch has also been established as a social touch behavioral assay in rats. The social touch gap paradigm allows a “chooser” rat to freely interact in an arena with up to two “test” rats, that are barred from one another by a wall, but are only separated by a 10-20 cm gap from the “chooser” rat. A very fast frame rate (250 Hz) camera is mounted above the arena along with standard infrared lights. This setup allows the experimenter to record videos that can then be analyzed to track when the “chooser” rat makes social touch contact with either test rat and measure whisking dynamics, such as whisking motion and the angular displacement of whiskers, between the two rats with high precision[57,58,65,66] . Ultrasound microphones can also be mounted in the gap paradigm to track vocalizations when two rats make social facial contact[66].

While the gap paradigm is a robust freely moving assay that allows the experimenter to assess more complex social touch behaviors, it is still limited as other freely moving assays are in the diversity of behaviors that can be measured. Freely moving assays can also be susceptible to a mix of different touch interactions occurring simultaneously (e.g. anogenital sniffing, whisker-whisker contact, allo-grooming). Furthermore, freely-moving assays are not particularly high-throughput because the interactions depend on the animals' decisions to engage (or not) in social touch, and because interaction duration and frequency can vary across animals that are tested. Finally, freely moving assays limit experimenters from recording neuronal activity in vivo with techniques that yield many neurons to record from, such as 2-photon (2P) calcium imaging and electrophysiological recordings with silicon probes.

In recent years, studies have attempted to address these limitations. Machine learning techniques and depth sensing have been integrated with video tracking in freely-moving assays to allow for the detection and quantification of socially-relevant touch behaviors, such as allo-grooming or attacking between two mice or rats[67,68]. The emergence of novel behavioral analyses with machine learning in freely-moving paradigms has also been compounded by the emergence of deep-learning frameworks for pose tracking that can track the position of individual body parts of interacting animals in videos[69,70]. Finally, high-throughput recording techniques have evolved to be compatible with freely moving assays, such as calcium imaging with one-photon miniaturized microscopes and chronically implanted silicon probes[71-73].

Although not considered naturalistic relative to freely-moving assays, head-restrained, or head-fixed, behavioral assays can circumvent some of the limitations that freely moving behavioral assays face when assessing social touch behaviors (e.g., the lack of complex behaviors that can be assessed, the inability to use high-throughput, in vivo recording techniques for neural activity and the absence of trial-based social touch interactions). Head-fixed behavioral assays for social touch have either one animal head-restrained while assessing its interaction with an unrestrained conspecific or both animals head-restrained[59,60]. These

head-fixed paradigms allow the experimenter to record neural activity with either 2-photon calcium imaging or silicon probes and can measure more subtle behaviors, such as whisker movements, sniffing, or pupil dynamics, during social contact[59,61]. Head-fixed behavioral assays have also been modified to be able to present social interactions between two animals in a trial-based manner, in which the experimenter also has control over the duration of the interaction and the interactions are more standardized. For example, two-photon calcium imaging can be performed on a test mouse while it is presented repeatedly with another male or female mouse that is in a chamber that can move on a linear motor for a specific duration before being shuttled away. The delivery of these social stimuli can be done multiple times to provide repetitive bouts of interaction on a trial basis, but limits direct contact between the two animals and cannot control for type of social touch interaction (i.e. if the interaction is via whiskers or snouts) the test mouse engages in with the social stimulus[74].

Although current head-fixed assays can address some of the limitations of freely moving assays, most are unable to solve all the issues that plague freely moving behavioral assays for social touch. Furthermore, the main disadvantage with head-fixed assays is that the social touch interactions are not naturalistic and thus may not adequately reflect how animals perceive social touch. However, a head-fixed assay for social touch might be well-suited to understanding social touch aversion in mouse models of autism given that it can 1. be designed to allow for trial-based social touch interactions in which the experimenter has control over the duration and type of interaction, 2. allow either the test animal or the presented animal (or both) to engage in touch behaviors, 3. provide the experimenter with the ability to assess more complex, aversive behaviors and 4. be used in combination with high-throughput neural recording techniques to probe the neural circuits underlying social touch aversion.

1.5: Neural circuits underlying social touch

While the neural circuits underlying avoidance/aversion to social touch have not been studied extensively under normal conditions in wild type mice, and even less in the context of autism, there is a body of research that has identified circuits involved in the encoding of whisker touch, social behaviors, and aversion to pain and other unpleasant stimuli. The circuits that have been interrogated include those required for tactile sensory processing, as well as those required for prosocial behaviors and pleasurable touch. These circuits could be modulated differently by aversive social touch, especially if they share connections with emotionally relevant brain regions.

The primary somatosensory cortex (S1) is particularly important for encoding social touch given that it encodes all types of tactile information received from the periphery both in humans and animals[75]. In humans S1 has been shown to be strongly activated by pleasant social caress[76,77]. The subregion of the S1 required for encoding whisker-mediated touch in rodents, also known as vibrissal S1 (vS1) or barrel cortex, is essential for mice and rats to navigate their environment and distinguish between different tactile stimuli[78]. vS1 includes neurons whose activity is increased or suppressed by social facial touch. Trimming of whiskers in rodents attenuates changes in vS1 activity to social touch[57]. vS1 can also distinguish differences in social touch based on the conspecific's sex[79].

Beyond S1, other cortical regions have also been implicated in encoding social touch and social touch behaviors. In humans, both prefrontal and insula cortices show increased activation to social touch from others[77]. The anterior cingulate cortex (ACCx) is strongly activated in mice when they engage in allogrooming or allolicking, social touch behaviors that reduce stress and provide comfort in mice[80,81]. These consolation behaviors are dependent on serotonergic signaling in the ACCx[82]. In addition to ACCx, social snout to snout, snout to body or anogenital touch are highly represented in the insular cortex (InsCx)[83].

The ventral striatum has also been associated with pleasurable social touch and social reward[84,85]. The nucleus accumbens (NAc) of the ventral striatum receives dopaminergic

signaling from the ventral tegmental area during affective and sexual social touch, suggesting this circuit contributes to encoding pleasant social touch[86].

The encoding of social, affective touch is additionally shown to be highly represented across amygdalar nuclei in humans[87]. In primates, amygdalar neurons, including those in the central amygdala, are activated during grooming[88]. However, hyperactivation of the basolateral amygdala (BLA) reduced social touch contact between primates[89]. Beyond humans and primates, rodents also show evidence of social touch representations in their amygdala. Tachykinin-expressing, GABAergic neurons in medial amygdala (MeA) encode social affiliative touch from allogrooming between mice. Optogenetic activation of these MeA neurons increases allogrooming behaviors[90].

Together, these findings have mainly focused on neural circuits required for encoding pleasurable and affiliative touch. vS1 appears to be one of the few regions that responds to social touch in general, but may represent social touch differently when it becomes aversive. To determine what circuits might contribute to translating social touch from something pleasant to aversive in ASD, we must also review the neural circuits required for encoding aversive stimuli and how they would be associated with social touch aversion.

1.6: The potential role of aversive-encoding neural circuits in social touch aversion

Aversion state encoding in rodents exists across the brain, including in the amygdala, hippocampus (HPC) and prefrontal (PFC) regions[91,92]. However, there are specific circuits that have been tightly linked in assigning social sensory stimuli to a negative emotional valence. There are two common examples in which social sensory stimuli may translate to something aversive: 1. Social aggression and 2. social avoidance.

Social aggression is one example in which social sensory information becomes designated with a negative valence. Aggression involves the translation of olfactory cues in mice, auditory and visual cues in birds, or multisensory cues in humans and primates into an

unpleasant stimulus that drives aggression and fighting behaviors[93]. The MeA has been considered the first brain region in the neural pathway for aggression in mice at which all olfactory cues converge[93]. Optogenetic stimulation of excitatory neurons in the MeA can trigger aggression and increases attack behavior by males in the resident-intruder assay. Additionally, hypothalamic nuclei, specifically the ventromedial (VMHvl), has been associated with social aggression and receives projections from the medial preoptic area required for suppressing aggression in male mice[94]. Both the MeA and VMHvl are interconnected, along with the midbrain and HPC, and are thought to represent the core aggression circuit[93].

In recent years, studies have also addressed social avoidance, though not specifically to touch alone. The neural circuitry underlying social avoidance encompasses many of the brain regions involved in social aggression[95,96]. For example, the lateral septum, known to increase attacks between rodents when lesioned, also shows heightened activity in mice with chronic social defeat stress (CSDS). The CSDS mouse model shows social avoidance even in a typically non-threatening social environment[97-99]. While these circuits for social aggression and avoidance might be potential avenues of investigation as they relate to social touch aversion, it is also worth noting the circuits that integrate the positive and negative valence of social stimuli together. If social touch, often considered pleasurable, now becomes aversive in ASD, then these regions may play a role in inappropriately assigning valence to social touch.

The InsCx is one of the brain regions known to directly link sensory stimuli to a positive or negative emotional context. InsCx receives sensory inputs attributed to all modalities while also sharing connections with brain regions associated with social aggression and avoidance[100]. Furthermore, activation of InsCx in rodents drives aversive behaviors and avoidance while silencing InsCx prevents affective preference to a stressed conspecific[101]. It is worth noting that the BLA shares similar functional properties to and has shared connectivity with InsCx[100,102]. The BLA encodes aversive and painful stimuli while also containing neuronal ensembles that are modulated by social exploration[103-105]. Elevated BLA activity and abnormal enlargement of BLA

nuclei have also been reported in individuals with ASD and both are highly correlated with the degree of social deficits[106,107].

Together, these research findings indicate potential brain regions and circuits that could explain social touch aversion in ASD.

1.7: Summary

Social touch, while often considered pleasurable and comforting, may become unpleasant and aversive under certain contexts. Furthermore, aversion to social touch is much more prominent in individuals with ASD[3,17,29,30,34,53]. This aversion to social touch in ASD individuals may be associated with hypersensitivity to tactile stimuli or the inability to engage in social interaction and communication altogether. The neural circuits underlying social touch aversion have not been well studied, but rodent models of ASD provide an opportunity to interrogate the circuits involved[108]. While there are several rodent behavioral assays that could be used to assess aversive and avoidance behaviors to social touch, each of these assays come with limitations that would prevent a thorough investigation of aversive behaviors to social touch and the underlying neural circuitry in ASD rodent models. Finally, there is evidence of specific brain regions that could be associated with social touch and aversive behaviors to social touch and these areas could be useful starting points towards characterizing the neural circuit for social touch aversion.

1.8: Rationale for thesis project

It remains unclear how ASD rodent models exhibit social touch aversion and which neural circuits contribute to the translation of social touch into an aversive stimulus. Our understanding of the neural circuits involved in social touch aversion is also limited by the fact that the neural circuits for the perception of social touch have not been fully characterized.

Social touch may be encoded differently in humans or animals when they have the flexibility to engage in social touch versus are forced to engage in social touch.

First, a novel behavioral assay is required to assess aversive and avoidance behaviors to social touch and if these behaviors are more prominent in ASD rodent models. This assay could be adapted from existing behavioral assays developed for evaluating social touch behaviors in freely moving and head-restrained rodents. Furthermore, the recent development of novel machine learning tools and pose estimation techniques means that complex behaviors can now be analyzed more quickly and with less human bias from videos of an animal's face or body[68-70,109,110]. Thus, we initially sought to develop an improved assay for monitoring responses to social touch in mice.

Second, given that there is little research on the neural circuits involved in social touch perception and aversion in ASD, a thorough investigation of the neuronal dynamics across multiple brain regions is essential and would require large-scale recordings of neuronal activity. These large-scale recordings can be done with 2P calcium imaging to acquire neural data from hundreds or thousands of neurons simultaneously, though at the cost of temporal resolution and limited access to subcortical brain regions[111]. Alternatively, in vivo electrophysiology with silicon probes maximizes temporal resolution across multiple brains regions but limits the quantity of neurons that can be recorded[112]. In vivo electrophysiology can also be used for recordings of cortical and subcortical brain regions simultaneously, which would be more advantageous for studying circuits related to social touch aversion[112]. Hence, we specifically designed a novel behavioral assay for social touch such that we could record neural activity in relevant brain regions over multiple social interactions. This allowed us to average activity over dozens of repeated stereotyped social touch trials.

Using this novel behavioral assay and in vivo electrophysiology, I have carried out a dissertation project that investigates the neural circuits underlying aversion to social touch in

both wild type (WT) mice and in two mouse models of autism: the MIA environmental model and the *Fmr1* KO genetic model.

With the experiments carried out in the chapters of this dissertation, I aim to answer the following questions: 1) Do mouse models of ASD show avoidance and aversive behaviors to social touch in a novel head-fixed behavioral assay? 2) How is social facial touch encoded in cortical, striatal and amygdalar circuits in WT mice? 3) How is social touch differentially represented in the cortical, striatal and amygdalar circuits in the *Fmr1* KO mouse model of autism?

In Chapter 2, I provide a detailed description of the novel head-fixed behavioral assay I designed to evaluate how two mouse models of ASD respond to social touch (with a stranger mouse) versus object touch (with a novel object) relative to control mice. I demonstrate that this assay for social touch in mice uncovers similar hyperarousal, avoidance responses and aversive facial expressions in MIA and *Fmr1* KO mice. I also show how restricting the ability to voluntarily engage in touch using the assay (through forced interactions) affects the degree to which mice exhibit avoidance and aversive behaviors. In Chapter 3, I characterize how neurons in vS1 and BLA, as well as tail of the striatum (tS), of WT mice respond to social versus object touch differently and examine the role of each of these regions in discriminating social from non-social touch. In Chapter 4, I provide evidence that social touch is differentially represented in vS1, tS and BLA neurons of a mouse model of ASD. I also indicate how neuronal dynamics at the circuit level reflect the behavioral responses to social touch in this ASD model.

1.9: References

1. Chen, P., and Hong, W. (2018). Neural Circuit Mechanisms of Social Behavior. Neuron *98*, 16-30. 10.1016/j.neuron.2018.02.026.

2. Prior, N.H., Bentz, E.J., and Ophir, A.G. (2022). Reciprocal processes of sensory perception and social bonding: an integrated social-sensory framework of social behavior. Genes Brain Behav *21*, e12781. 10.1111/gbb.12781.

3. Cascio, C.J., Moore, D., and McGlone, F. (2019). Social touch and human development. Dev Cogn Neurosci *35*, 5-11. 10.1016/j.dcn.2018.04.009.

4. Keysers, C., Knapska, E., Moita, M.A., and Gazzola, V. (2022). Emotional contagion and prosocial behavior in rodents. Trends Cogn Sci *26*, 688-706. 10.1016/j.tics.2022.05.005.

5. Dunbar, R.I. (2010). The social role of touch in humans and primates: behavioural function and neurobiological mechanisms. Neurosci Biobehav Rev *34*, 260-268. 10.1016/j.neubiorev.2008.07.001.

6. Adolphs, R. (2009). The social brain: neural basis of social knowledge. Annu Rev Psychol *60*, 693-716. 10.1146/annurev.psych.60.110707.163514.

7. Bales, K.L., Witczak, L.R., Simmons, T.C., Savidge, L.E., Rothwell, E.S., Rogers, F.D., Manning, R.A., Heise, M.J., Englund, M., and Arias Del Razo, R. (2018). Social touch during development: Long-term effects on brain and behavior. Neurosci Biobehav Rev *95*, 202-219. 10.1016/j.neubiorev.2018.09.019.

8. Keysers, C., Kaas, J.H., and Gazzola, V. (2010). Somatosensation in social perception. Nat Rev Neurosci *11*, 417-428. 10.1038/nrn2833.

9. de Waal, F.B.M., and Preston, S.D. (2017). Mammalian empathy: behavioural manifestations and neural basis. Nat Rev Neurosci *18*, 498-509. 10.1038/nrn.2017.72.

10. Jablonski, N.G. (2021). Social and affective touch in primates and its role in the evolution of social cohesion. Neuroscience *464*, 117-125. 10.1016/j.neuroscience.2020.11.024.

11. Riters, L.V., Spool, J.A., Merullo, D.P., and Hahn, A.H. (2019). Song practice as a rewarding form of play in songbirds. Behav Processes *163*, 91-98. 10.1016/j.beproc.2017.10.002.

12. Achterberg, E.J.M., and Vanderschuren, L. (2023). The neurobiology of social play behaviour: Past, present and future. Neurosci Biobehav Rev *152*, 105319. 10.1016/j.neubiorev.2023.105319.

13. Kohl, J., Babayan, B.M., Rubinstein, N.D., Autry, A.E., Marin-Rodriguez, B., Kapoor, V., Miyamishi, K., Zweifel, L.S., Luo, L., Uchida, N., and Dulac, C. (2018). Functional circuit architecture underlying parental behaviour. Nature *556*, 326-331. 10.1038/s41586-018-0027-0.

14. Robertson, C.E., and Baron-Cohen, S. (2017). Sensory perception in autism. Nat Rev Neurosci *18*, 671-684. 10.1038/nrn.2017.112.

15. Landa, R.J., Gross, A.L., Stuart, E.A., and Faherty, A. (2013). Developmental trajectories in children with and without autism spectrum disorders: the first 3 years. Child Dev *84*, 429-442. 10.1111/j.1467-8624.2012.01870.x.

16. Thye, M.D., Bednarz, H.M., Herringshaw, A.J., Sartin, E.B., and Kana, R.K. (2018). The impact of atypical sensory processing on social impairments in autism spectrum disorder. Dev Cogn Neurosci *29*, 151-167. 10.1016/j.dcn.2017.04.010.

17. Green, S.A., Hernandez, L.M., Bowman, H.C., Bookheimer, S.Y., and Dapretto, M. (2018). Sensory over-responsivity and social cognition in ASD: Effects of aversive sensory stimuli and attentional modulation on neural responses to social cues. Dev Cogn Neurosci *29*, 127-139. 10.1016/j.dcn.2017.02.005.

18. Jung, J., Zbozinek, T.D., Cummings, K.K., Wilhelm, F.H., Dapretto, M., Craske, M.G., Bookheimer, S.Y., and Green, S.A. (2021). Associations between physiological and neural measures of sensory reactivity in youth with autism. J Child Psychol Psychiatry *62*, 1183-1194. 10.1111/jcpp.13387.

19. Puts, N.A., Wodka, E.L., Tommerdahl, M., Mostofsky, S.H., and Edden, R.A. (2014). Impaired tactile processing in children with autism spectrum disorder. J Neurophysiol *111*, 1803-1811. 10.1152/jn.00890.2013.

20. Bryant, L.K., Woynaroski, T.G., Wallace, M.T., and Cascio, C.J. (2019). Self-reported Sensory Hypersensitivity Moderates Association Between Tactile Psychophysical Performance and Autism-Related Traits in Neurotypical Adults. J Autism Dev Disord *49*, 3159-3172. 10.1007/s10803-019-04043-8.

21. He, C.X., Cantu, D.A., Mantri, S.S., Zeiger, W.A., Goel, A., and Portera-Cailliau, C. (2017). Tactile Defensiveness and Impaired Adaptation of Neuronal Activity in the Fmr1 Knock-Out Mouse Model of Autism. J Neurosci *37*, 6475-6487. 10.1523/jneurosci.0651-17.2017.

22. Williams, Z.J., He, J.L., Cascio, C.J., and Woynaroski, T.G. (2021). A review of decreased sound tolerance in autism: Definitions, phenomenology, and potential mechanisms. Neurosci Biobehav Rev *121*, 1-17. 10.1016/j.neubiorev.2020.11.030.

23. Kojovic, N., Ben Hadid, L., Franchini, M., and Schaer, M. (2019). Sensory Processing Issues and Their Association with Social Difficulties in Children with Autism Spectrum Disorders. J Clin Med *8*. 10.3390/jcm8101508.

24. Hamilton, A., and Pelphrey, K. (2018). Sensory and social features of autism - can they be integrated? Dev Cogn Neurosci *29*, 1-3. 10.1016/j.dcn.2018.02.009.

25. Innocenti, A., De Stefani, E., Bernardi, N.F., Campione, G.C., and Gentilucci, M. (2012). Gaze direction and request gesture in social interactions. PLoS One *7*, e36390. 10.1371/journal.pone.0036390.

26. Stuart, N., Whitehouse, A., Palermo, R., Bothe, E., and Badcock, N. (2023). Eye Gaze in Autism Spectrum Disorder: A Review of Neural Evidence for the Eye Avoidance Hypothesis. J Autism Dev Disord *53*, 1884-1905. 10.1007/s10803-022-05443-z.

27. Mammen, M.A., Moore, G.A., Scaramella, L.V., Reiss, D., Ganiban, J.M., Shaw, D.S., Leve, L.D., and Neiderhiser, J.M. (2015). Infant Avoidance During a Tactile Task Predicts

Autism Spectrum Behaviors in Toddlerhood. Infant Ment Health J *36*, 575-587. 10.1002/imhj.21539.

28. South, M., and Rodgers, J. (2017). Sensory, Emotional and Cognitive Contributions to Anxiety in Autism Spectrum Disorders. Front Hum Neurosci *11*, 20. 10.3389/fnhum.2017.00020.

29. Bufo, M.R., Guidotti, M., Mofid, Y., Malvy, J., Bonnet-Brilhault, F., Aguillon-Hernandez, N., and Wardak, C. (2022). Atypical Response to Affective Touch in Children with Autism: Multi-Parametric Exploration of the Autonomic System. J Clin Med *11*. 10.3390/jcm11237146.

30. Lee Masson, H., Pillet, I., Amelynck, S., Van De Plas, S., Hendriks, M., Op de Beeck, H., and Boets, B. (2019). Intact neural representations of affective meaning of touch but lack of embodied resonance in autism: a multi-voxel pattern analysis study. Mol Autism *10*, 39. 10.1186/s13229-019-0294-0.

31. Cascio, C.J., Moana-Filho, E.J., Guest, S., Nebel, M.B., Weisner, J., Baranek, G.T., and Essick, G.K. (2012). Perceptual and neural response to affective tactile texture stimulation in adults with autism spectrum disorders. Autism Res *5*, 231-244. 10.1002/aur.1224.

32. Clements, C.C., Zoltowski, A.R., Yankowitz, L.D., Yerys, B.E., Schultz, R.T., and Herrington, J.D. (2018). Evaluation of the Social Motivation Hypothesis of Autism: A Systematic Review and Meta-analysis. JAMA Psychiatry *75*, 797-808. 10.1001/jamapsychiatry.2018.1100.

33. Gliga, T., Farroni, T., and Cascio, C.J. (2019). Social touch: A new vista for developmental cognitive neuroscience? Dev Cogn Neurosci *35*, 1-4. 10.1016/j.dcn.2018.05.006.

34. Schaffler, M.D., Middleton, L.J., and Abdus-Saboor, I. (2019). Mechanisms of Tactile Sensory Phenotypes in Autism: Current Understanding and Future Directions for Research. Curr Psychiatry Rep *21*, 134. 10.1007/s11920-019-1122-0.

35. Kazdoba, T.M., Leach, P.T., and Crawley, J.N. (2016). Behavioral phenotypes of genetic mouse models of autism. Genes Brain Behav *15*, 7-26. 10.1111/gbb.12256.

36. Kourdougli, N., Suresh, A., Liu, B., Juarez, P., Lin, A., Chung, D.T., Graven Sams, A., Gandal, M.J., Martínez-Cerdeño, V., Buonomano, D.V., et al. (2023). Improvement of sensory

deficits in fragile X mice by increasing cortical interneuron activity after the critical period. Neuron. 10.1016/j.neuron.2023.06.009.

37. Sofroniew, N.J., and Svoboda, K. (2015). Whisking. Curr Biol *25*, R137-140. 10.1016/j.cub.2015.01.008.

38. Arnett, M.T., Herman, D.H., and McGee, A.W. (2014). Deficits in tactile learning in a mouse model of fragile X syndrome. PLoS One *9*, e109116. 10.1371/journal.pone.0109116.

39. Michaelson, S.D., Ozkan, E.D., Aceti, M., Maity, S., Llamosas, N., Weldon, M., Mizrachi, E., Vaissiere, T., Gaffield, M.A., Christie, J.M., et al. (2018). SYNGAP1 heterozygosity disrupts sensory processing by reducing touch-related activity within somatosensory cortex circuits. Nat Neurosci *21*, 1-13. 10.1038/s41593-018-0268-0.

40. Yang, M., Mahrt, E.J., Lewis, F., Foley, G., Portmann, T., Dolmetsch, R.E., Portfors, C.V., and Crawley, J.N. (2015). 16p11.2 Deletion Syndrome Mice Display Sensory and Ultrasonic Vocalization Deficits During Social Interactions. Autism Res *8*, 507-521. 10.1002/aur.1465.

41. Orefice, L.L., Zimmerman, A.L., Chirila, A.M., Sleboda, S.J., Head, J.P., and Ginty, D.D. (2016). Peripheral Mechanosensory Neuron Dysfunction Underlies Tactile and Behavioral Deficits in Mouse Models of ASDs. Cell *166*, 299-313. 10.1016/j.cell.2016.05.033.

42. Arakawa, H. (2020). From Multisensory Assessment to Functional Interpretation of Social Behavioral Phenotype in Transgenic Mouse Models for Autism Spectrum Disorders. Front Psychiatry *11*, 592408. 10.3389/fpsyt.2020.592408.

43. Endo, N., Makinodan, M., Somayama, N., Komori, T., Kishimoto, T., and Nishi, M. (2019). Characterization of behavioral phenotypes in the BTBR T(+) Itpr3(tf)/J mouse model of autism spectrum disorder under social housing conditions using the multiple animal positioning system. Exp Anim *68*, 319-330. 10.1538/expanim.18-0177.

44. Mines, M.A., Yuskaitis, C.J., King, M.K., Beurel, E., and Jope, R.S. (2010). GSK3 influences social preference and anxiety-related behaviors during social interaction in a mouse model of fragile X syndrome and autism. PLoS One *5*, e9706. 10.1371/journal.pone.0009706.

45. Yu, B., Yuan, B., Dai, J.K., Cheng, T.L., Xia, S.N., He, L.J., Yuan, Y.T., Zhang, Y.F., Xu, H.T., Xu, F.Q., et al. (2020). Reversal of Social Recognition Deficit in Adult Mice with MECP2 Duplication via Normalization of MeCP2 in the Medial Prefrontal Cortex. Neurosci Bull *36*, 570-584. 10.1007/s12264-020-00467-w.

46. Reed, M.D., Yim, Y.S., Wimmer, R.D., Kim, H., Ryu, C., Welch, G.M., Andina, M., King, H.O., Waisman, A., Halassa, M.M., et al. (2020). IL-17a promotes sociability in mouse models of neurodevelopmental disorders. Nature *577*, 249-253. 10.1038/s41586-019-1843-6.

47. Choi, G.B., Yim, Y.S., Wong, H., Kim, S., Kim, H., Kim, S.V., Hoeffer, C.A., Littman, D.R., and Huh, J.R. (2016). The maternal interleukin-17a pathway in mice promotes autism-like phenotypes in offspring. Science *351*, 933-939. 10.1126/science.aad0314.

48. Young, D.M., Schenk, A.K., Yang, S.B., Jan, Y.N., and Jan, L.Y. (2010). Altered ultrasonic vocalizations in a tuberous sclerosis mouse model of autism. Proc Natl Acad Sci U S A *107*, 11074-11079. 10.1073/pnas.1005620107.

49. Toledo, M.A., Wen, T.H., Binder, D.K., Ethell, I.M., and Razak, K.A. (2019). Reversal of ultrasonic vocalization deficits in a mouse model of Fragile X Syndrome with minocycline treatment or genetic reduction of MMP-9. Behav Brain Res *372*, 112068. 10.1016/j.bbr.2019.112068.

50. Molloy, C.J., Cooke, J., Gatford, N.J.F., Rivera-Olvera, A., Avazzadeh, S., Homberg, J.R., Grandjean, J., Fernandes, C., Shen, S., Loth, E., et al. (2023). Bridging the translational gap: what can synaptopathies tell us about autism? Front Mol Neurosci *16*, 1191323. 10.3389/fnmol.2023.1191323.

51. Shin Yim, Y., Park, A., Berrios, J., Lafourcade, M., Pascual, L.M., Soares, N., Yeon Kim, J., Kim, S., Kim, H., Waisman, A., et al. (2017). Reversing behavioural abnormalities in mice exposed to maternal inflammation. Nature *549*, 482-487. 10.1038/nature23909.

52. Walsh, J.J., Christoffel, D.J., Heifets, B.D., Ben-Dor, G.A., Selimbeyoglu, A., Hung, L.W., Deisseroth, K., and Malenka, R.C. (2018). 5-HT release in nucleus accumbens rescues social deficits in mouse autism model. Nature *560*, 589-594. 10.1038/s41586-018-0416-4.

53. Cascio, C., McGlone, F., Folger, S., Tannan, V., Baranek, G., Pelphrey, K.A., and Essick, G. (2008). Tactile perception in adults with autism: a multidimensional psychophysical study. J Autism Dev Disord *38*, 127-137. 10.1007/s10803-007-0370-8.

54. Foss-Feig, J.H., Heacock, J.L., and Cascio, C.J. (2012). Tactile Responsiveness Patterns and their Association with Core Features in Autism Spectrum Disorders. Res Autism Spectr Disord *6*, 337-344. 10.1016/j.rasd.2011.06.007.

55. Peça, J., Feliciano, C., Ting, J.T., Wang, W., Wells, M.F., Venkatraman, T.N., Lascola, C.D., Fu, Z., and Feng, G. (2011). Shank3 mutant mice display autistic-like behaviours and striatal dysfunction. Nature *472*, 437-442. 10.1038/nature09965.

56. Kalueff, A.V., Stewart, A.M., Song, C., Berridge, K.C., Graybiel, A.M., and Fentress, J.C. (2016). Neurobiology of rodent self-grooming and its value for translational neuroscience. Nat Rev Neurosci *17*, 45-59. 10.1038/nrn.2015.8.

57. Bobrov, E., Wolfe, J., Rao, R.P., and Brecht, M. (2014). The representation of social facial touch in rat barrel cortex. Curr Biol *24*, 109-115. 10.1016/j.cub.2013.11.049.

58. Wolfe, J., Mende, C., and Brecht, M. (2011). Social facial touch in rats. Behav Neurosci *125*, 900-910. 10.1037/a0026165.

59. Jeon, Y.S., Jeong, D., Kweon, H., Kim, J.H., Kim, C.Y., Oh, Y., Lee, Y.H., Kim, C.H., Kim, S.G., Jeong, J.W., et al. (2023). Adolescent Parvalbumin Expression in the Left Orbitofrontal Cortex Shapes Sociability in Female Mice. J Neurosci *43*, 1555-1571. 10.1523/jneurosci.0918-22.2023.

60. Jennings, J.H., Kim, C.K., Marshel, J.H., Raffiee, M., Ye, L., Quirin, S., Pak, S., Ramakrishnan, C., and Deisseroth, K. (2019). Interacting neural ensembles in orbitofrontal cortex for social and feeding behaviour. Nature *565*, 645-649. 10.1038/s41586-018-0866-8.

61. Willmore, L., Minerva, A.R., Engelhard, B., Murugan, M., McMannon, B., Oak, N., Thiberge, S.Y., Peña, C.J., and Witten, I.B. (2023). Overlapping representations of food and social stimuli in mouse VTA dopamine neurons. Neuron *111*, 3541-3553.e3548. 10.1016/j.neuron.2023.08.003.

62. Tang, Y., Benusiglio, D., Lefevre, A., Hilfiger, L., Althammer, F., Bludau, A., Hagiwara, D., Baudon, A., Darbon, P., Schimmer, J., et al. (2020). Social touch promotes interfemale communication via activation of parvocellular oxytocin neurons. Nat Neurosci *23*, 1125-1137. 10.1038/s41593-020-0674-y.

63. Crawley, J.N. (2012). Translational animal models of autism and neurodevelopmental disorders. Dialogues Clin Neurosci *14*, 293-305. 10.31887/DCNS.2012.14.3/jcrawley.

64. Fetcho, R.N., Hall, B.S., Estrin, D.J., Walsh, A.P., Schuette, P.J., Kaminsky, J., Singh, A., Roshgodal, J., Bavley, C.C., Nadkarni, V., et al. (2023). Regulation of social interaction in mice by a frontostriatal circuit modulated by established hierarchical relationships. Nat Commun *14*, 2487. 10.1038/s41467-023-37460-6.

65. Lenschow, C., and Brecht, M. (2015). Barrel cortex membrane potential dynamics in social touch. Neuron *85*, 718-725. 10.1016/j.neuron.2014.12.059.

66. Rao, R.P., Mielke, F., Bobrov, E., and Brecht, M. (2014). Vocalization-whisking coordination and multisensory integration of social signals in rat auditory cortex. Elife *3*. 10.7554/eLife.03185.

67. Hong, W., Kennedy, A., Burgos-Artizzu, X.P., Zelikowsky, M., Navonne, S.G., Perona, P., and Anderson, D.J. (2015). Automated measurement of mouse social behaviors using depth sensing, video tracking, and machine learning. Proc Natl Acad Sci U S A *112*, E5351-5360. 10.1073/pnas.1515982112.

68. Wiltschko, A.B., Tsukahara, T., Zeine, A., Anyoha, R., Gillis, W.F., Markowitz, J.E., Peterson, R.E., Katon, J., Johnson, M.J., and Datta, S.R. (2020). Revealing the structure of pharmacobehavioral space through motion sequencing. Nat Neurosci *23*, 1433-1443. 10.1038/s41593-020-00706-3.

69. Mathis, A., Mamidanna, P., Cury, K.M., Abe, T., Murthy, V.N., Mathis, M.W., and Bethge, M. (2018). DeepLabCut: markerless pose estimation of user-defined body parts with deep learning. Nat Neurosci *21*, 1281-1289. 10.1038/s41593-018-0209-y.

70. Pereira, T.D., Tabris, N., Matsliah, A., Turner, D.M., Li, J., Ravindranath, S., Papadoyannis, E.S., Normand, E., Deutsch, D.S., Wang, Z.Y., et al. (2022). SLEAP: A deep learning system for multi-animal pose tracking. Nat Methods *19*, 486-495. 10.1038/s41592-022-01426-1.

71. Guo, C., Blair, G.J., Sehgal, M., Sangiuliano Jimka, F.N., Bellafard, A., Silva, A.J., Golshani, P., Basso, M.A., Blair, H.T., and Aharoni, D. (2023). Miniscope-LFOV: A large-field-of-view, single-cell-resolution, miniature microscope for wired and wire-free imaging of neural dynamics in freely behaving animals. Sci Adv *9*, eadg3918. 10.1126/sciadv.adg3918.

72. Luo, T.Z., Bondy, A.G., Gupta, D., Elliott, V.A., Kopec, C.D., and Brody, C.D. (2020). An approach for long-term, multi-probe Neuropixels recordings in unrestrained rats. Elife *9*. 10.7554/eLife.59716.

73. Juavinett, A.L., Bekheet, G., and Churchland, A.K. (2019). Chronically implanted Neuropixels probes enable high-yield recordings in freely moving mice. Elife *8*. 10.7554/eLife.47188.

74. Cox, J., and Witten, I.B. (2019). Striatal circuits for reward learning and decision-making. Nat Rev Neurosci *20*, 482-494. 10.1038/s41583-019-0189-2.

75. O'Connor, D.H., Krubitzer, L., and Bensmaia, S. (2021). Of mice and monkeys: Somatosensory processing in two prominent animal models. Prog Neurobiol *201*, 102008. 10.1016/j.pneurobio.2021.102008.

76. Gazzola, V., Spezio, M.L., Etzel, J.A., Castelli, F., Adolphs, R., and Keysers, C. (2012). Primary somatosensory cortex discriminates affective significance in social touch. Proc Natl Acad Sci U S A *109*, E1657-1666. 10.1073/pnas.1113211109.

77. Lee Masson, H., Pillet, I., Boets, B., and Op de Beeck, H. (2020). Task-dependent changes in functional connectivity during the observation of social and non-social touch interaction. Cortex *125*, 73-89. 10.1016/j.cortex.2019.12.011.

78. Petersen, C.C. (2007). The functional organization of the barrel cortex. Neuron *56*, 339-355. 10.1016/j.neuron.2007.09.017.

79. Ebbesen, C.L., Bobrov, E., Rao, R.P., and Brecht, M. (2019). Highly structured, partner-sex- and subject-sex-dependent cortical responses during social facial touch. Nat Commun *10*, 4634. 10.1038/s41467-019-12511-z.

80. Burkett, J.P., Andari, E., Johnson, Z.V., Curry, D.C., de Waal, F.B., and Young, L.J. (2016). Oxytocin-dependent consolation behavior in rodents. Science *351*, 375-378. 10.1126/science.aac4785.

81. Zhang, M., Wu, Y.E., Jiang, M., and Hong, W. (2024). Cortical regulation of helping behaviour towards others in pain. Nature *626*, 136-144. 10.1038/s41586-023-06973-x.

82. Li, L., Zhang, L.Z., He, Z.X., Ma, H., Zhang, Y.T., Xun, Y.F., Yuan, W., Hou, W.J., Li, Y.T., Lv, Z.J., et al. (2021). Dorsal raphe nucleus to anterior cingulate cortex 5-HTergic neural circuit modulates consolation and sociability. Elife *10*. 10.7554/eLife.67638.

83. Miura, I., Sato, M., Overton, E.T.N., Kunori, N., Nakai, J., Kawamata, T., Nakai, N., and Takumi, T. (2020). Encoding of social exploration by neural ensembles in the insular cortex. PLoS Biol *18*, e3000584. 10.1371/journal.pbio.3000584.

84. Elias, L.J., and Abdus-Saboor, I. (2022). Bridging skin, brain, and behavior to understand pleasurable social touch. Curr Opin Neurobiol *73*, 102527. 10.1016/j.conb.2022.102527.

85. Daniel, R., and Pollmann, S. (2014). A universal role of the ventral striatum in reward-based learning: evidence from human studies. Neurobiol Learn Mem *114*, 90-100. 10.1016/j.nlm.2014.05.002.

86. Elias, L.J., Succi, I.K., Schaffler, M.D., Foster, W., Gradwell, M.A., Bohic, M., Fushiki, A., Upadhyay, A., Ejoh, L.L., Schwark, R., et al. (2023). Touch neurons underlying dopaminergic pleasurable touch and sexual receptivity. Cell *186*, 577-590.e516. 10.1016/j.cell.2022.12.034.

87. Gothard, K.M., and Fuglevand, A.J. (2022). The role of the amygdala in processing social and affective touch. Curr Opin Behav Sci *43*, 46-53. 10.1016/j.cobeha.2021.08.004.

88. Martin, A.B., Cardenas, M.A., Andersen, R.K., Bowman, A.I., Hillier, E.A., Bensmaia, S., Fuglevand, A.J., and Gothard, K.M. (2023). A context-dependent switch from sensing to feeling in the primate amygdala. Cell Rep *42*, 112056. 10.1016/j.celrep.2023.112056.

89. Wellman, L.L., Forcelli, P.A., Aguilar, B.L., and Malkova, L. (2016). Bidirectional Control of Social Behavior by Activity within Basolateral and Central Amygdala of Primates. J Neurosci *36*, 8746-8756. 10.1523/jneurosci.0333-16.2016.

90. Wu, Y.E., Dang, J., Kingsbury, L., Zhang, M., Sun, F., Hu, R.K., and Hong, W. (2021). Neural control of affiliative touch in prosocial interaction. Nature *599*, 262-267. 10.1038/s41586-021-03962-w.

91. Calhoon, G.G., and Tye, K.M. (2015). Resolving the neural circuits of anxiety. Nat Neurosci *18*, 1394-1404. 10.1038/nn.4101.

92. Malezieux, M., Klein, A.S., and Gogolla, N. (2023). Neural Circuits for Emotion. Annu Rev Neurosci *46*, 211-231. 10.1146/annurev-neuro-111020-103314.

93. Lischinsky, J.E., and Lin, D. (2020). Neural mechanisms of aggression across species. Nat Neurosci *23*, 1317-1328. 10.1038/s41593-020-00715-2.

94. Wei, D., Osakada, T., Guo, Z., Yamaguchi, T., Varshneya, A., Yan, R., Jiang, Y., and Lin, D. (2023). A hypothalamic pathway that suppresses aggression toward superior opponents. Nat Neurosci *26*, 774-787. 10.1038/s41593-023-01297-5.

95. Alfieri, V., Mattera, A., and Baldassarre, G. (2022). Neural Circuits Underlying Social Fear in Rodents: An Integrative Computational Model. Front Syst Neurosci *16*, 841085. 10.3389/fnsys.2022.841085.

96. Gellner, A.K., Voelter, J., Schmidt, U., Beins, E.C., Stein, V., Philipsen, A., and Hurlemann, R. (2021). Molecular and neurocircuitry mechanisms of social avoidance. Cell Mol Life Sci *78*, 1163-1189. 10.1007/s00018-020-03649-x.

97. Wong, L.C., Wang, L., D'Amour, J.A., Yumita, T., Chen, G., Yamaguchi, T., Chang, B.C., Bernstein, H., You, X., Feng, J.E., et al. (2016). Effective Modulation of Male Aggression through Lateral Septum to Medial Hypothalamus Projection. Curr Biol *26*, 593-604. 10.1016/j.cub.2015.12.065.

98. Li, L., Durand-de Cuttoli, R., Aubry, A.V., Burnett, C.J., Cathomas, F., Parise, L.F., Chan, K.L., Morel, C., Yuan, C., Shimo, Y., et al. (2023). Social trauma engages lateral septum circuitry to occlude social reward. Nature *613*, 696-703. 10.1038/s41586-022-05484-5.

99. Leroy, F., Park, J., Asok, A., Brann, D.H., Meira, T., Boyle, L.M., Buss, E.W., Kandel, E.R., and Siegelbaum, S.A. (2018). A circuit from hippocampal CA2 to lateral septum disinhibits social aggression. Nature *564*, 213-218. 10.1038/s41586-018-0772-0.

100. Gogolla, N. (2017). The insular cortex. Curr Biol *27*, R580-r586. 10.1016/j.cub.2017.05.010.

101. Rogers-Carter, M.M., Varela, J.A., Gribbons, K.B., Pierce, A.F., McGoey, M.T., Ritchey, M., and Christianson, J.P. (2018). Insular cortex mediates approach and avoidance responses to social affective stimuli. Nat Neurosci *21*, 404-414. 10.1038/s41593-018-0071-y.

102. Kayyal, H., Yiannakas, A., Kolatt Chandran, S., Khamaisy, M., Sharma, V., and Rosenblum, K. (2019). Activity of Insula to Basolateral Amygdala Projecting Neurons is Necessary and Sufficient for Taste Valence Representation. J Neurosci *39*, 9369-9382. 10.1523/jneurosci.0752-19.2019.

103. Corder, G., Ahanonu, B., Grewe, B.F., Wang, D., Schnitzer, M.J., and Scherrer, G. (2019). An amygdalar neural ensemble that encodes the unpleasantness of pain. Science *363*, 276-281. 10.1126/science.aap8586.

104. Fustiñana, M.S., Eichlisberger, T., Bouwmeester, T., Bitterman, Y., and Lüthi, A. (2021). State-dependent encoding of exploratory behaviour in the amygdala. Nature. 10.1038/s41586-021-03301-z.

105. Mazuski, C., and O'Keefe, J. (2022). Representation of ethological events by basolateral amygdala neurons. Cell Rep *39*, 110921. 10.1016/j.celrep.2022.110921.

106. Seguin, D., Pac, S., Wang, J., Nicolson, R., Martinez-Trujillo, J., and Duerden, E.G. (2021). Amygdala subnuclei development in adolescents with autism spectrum disorder: Association with social communication and repetitive behaviors. Brain Behav *11*, e2299. 10.1002/brb3.2299.

107. Procyshyn, T.L., Lombardo, M.V., Lai, M.C., Jassim, N., Auyeung, B., Crockford, S.K., Deakin, J.B., Soubramanian, S., Sule, A., Terburg, D., et al. (2022). Oxytocin enhances basolateral amygdala activation and functional connectivity while processing emotional faces: preliminary findings in autistic vs non-autistic women. Soc Cogn Affect Neurosci *17*, 929-938. 10.1093/scan/nsac016.

108. Silverman, J.L., Thurm, A., Ethridge, S.B., Soller, M.M., Petkova, S.P., Abel, T., Bauman, M.D., Brodkin, E.S., Harony-Nicolas, H., Wöhr, M., and Halladay, A. (2022). Reconsidering animal models used to study autism spectrum disorder: Current state and optimizing future. Genes Brain Behav *21*, e12803. 10.1111/gbb.12803.

109. Nath, T., Mathis, A., Chen, A.C., Patel, A., Bethge, M., and Mathis, M.W. (2019). Using DeepLabCut for 3D markerless pose estimation across species and behaviors. Nat Protoc *14*, 2152-2176. 10.1038/s41596-019-0176-0.

110. Syeda, A., Zhong, L., Tung, R., Long, W., Pachitariu, M., and Stringer, C. (2023). FaceMap: a framework for modeling neural activity based on orofacial tracking. Nat Neurosci. 10.1038/s41593-023-01490-6.

111. Lecoq, J.A., Boehringer, R., and Grewe, B.F. (2023). Deep brain imaging on the move. Nat Methods *20*, 495-496. 10.1038/s41592-023-01808-z.

112. Wei, Z., Lin, B.J., Chen, T.W., Daie, K., Svoboda, K., and Druckmann, S. (2020). A comparison of neuronal population dynamics measured with calcium imaging and electrophysiology. PLoS Comput Biol *16*, e1008198. 10.1371/journal.pcbi.1008198.

CHAPTER 2: A Novel Head-Fixed Assay Uncovers Aversive Responses in Two Autism Models

2.1: Introduction

Across animal species and humans, social touch is an important component of social interaction and communication that allows for the development of strong kinship bonds[1-3]. Touch may be experienced under different contexts, such as between parent and offspring, siblings, friends, or even strangers[4]. How animals experience social touch as pleasant versus aversive, and the degree to which their behavioral responses differ from those related to touching inanimate objects is largely unknown. Moreover, the neural circuits encoding social touch or how activity within those circuits relates to the behavioral repertoire animals exhibit in response to social touch are not fully understood.

Animal studies have begun to address these questions, especially in rodents, using a variety of behavioral paradigms. Unfortunately, the social touch assays currently available have certain limitations. Those that favor naturalistic interactions in freely moving rodents lack temporal and spatial control over individual touch interactions and typically the data collected reflects a mix of different interactions occurring simultaneously (e.g., anogenital sniffing, whisker-whisker contact, allo-grooming)[5-9]. Head-fixed social interaction assays do exist and can allow for the experimenter to track complex behaviors while recording neural activity; however, recent assays lack control over both the duration and type of interaction the mouse engages in[10-12]. To overcome these problems, we sought to design a novel head-fixed social touch behavioral assay for rodents, in which we could control the duration, number, context, and type of social touch interactions with high precision, while at the same time monitoring an array of complex behavioral responses (facial expressions, pupillary changes, locomotion, etc.) using high frame rate cameras (**Fig. 2-1**). We focused on a single type of social touch interaction (face-to-face), as opposed to the equally prevalent anogenital sniffing interactions in mice[4,13], because we felt it had more translational relevance to humans. We took care to ensure that the experimenter had complete control to directly elicit highly stereotyped bouts of social touch between animals.

To validate our new assay, we used it to identify differences in behavioral responses to social touch in mouse models of autism spectrum disorder (ASD), prevalent NDCs in which social touch aversion has been well documented[14,15]. Apprehension to social touch in ASD could be caused by tactile hypersensitivity[16-19], which is a strong predictor of future social deficits[20]. Avoidance of social touch by ASD children could prevent them from forming social relationships as adults[21,22]. In certain rodent models of autism, tactile sensitivity and social interaction deficits also appear to be linked[23,24], and, in some cases, differences in the development of primary somatosensory cortex (S1) are associated with social deficits [25,26]. Thus, further research into social touch in ASD models is warranted.

In this chapter, we tested two distinct mouse models of ASD (the *Fmr1* knockout model of Fragile X Syndrome – FXS and maternal immune activation mice) in our novel head-fixed social touch assay. We quantified various behavioral responses in the test animal during social touch with a stranger mouse. We observed increased avoidance, hyperarousal (pupil dilation), and more aversive facial expressions (AFEs) to social touch in both ASD models compared to their healthy controls. Furthermore, we found that *Fmr1* KO mice showed greater avoidance and AFEs to forced social touch (with familiar or stranger mice) than wild type controls, but less so to mice of the opposite sex. Our results suggest that this new social touch assay can parse out maladaptive and aversive behavioral responses to social touch in ASD mouse models and might also be of use to the larger neuroscience community.

2.2: Materials and Methods

2.2.1: Experimental model and animal details

Male and female C5BL/6 mice at postnatal day 60-90 on the day of behavioral testing were used for behavioral experiments and were derived from the following mouse lines based on prior publications: wildtype (WT) B6J (JAX line 000664), *Fmr1* KO (JAX line 003025), and wild-type B6NTac (Taconic line) [16,25-28]. The group/genotypes used for behavioral testing are as

follows: WT and *Fmr1* KO mice (JAX line) and PBS and maternal immune activation (MIA) mice (Taconic line). Mice were group-housed with access to food and water *ad libitum* under a 12 hour light cycle (12 hours light/12 hours dark) in controlled temperature conditions. All experiments were done in the light cycle and followed the U.S. National Institutes of Health guidelines for animal research under an animal use protocol ARC #2007-035 approved by the Chancellor's Animal Research Committee and Office for Animal Research Oversight at the University of California, Los Angeles.

2.2.2: Maternal immune activation (MIA)

We followed established protocols[27,29]. Wildtype B6NTac pregnant dams were injected intraperitoneally with polyinosonic:polycytidylic acid (Poly(I:C)) for MIA or with phosphate buffered saline (PBS; control) at embryonic day 12.5 (E12.5). A small blood sample of the dams was collected from the submandibular vein 2.5 h after injection and centrifuged to isolate serum. Serum was run through an interleukin-6 (IL-6) enzyme-linked immunosorbent assay (ELISA) kit (Invitrogen). Successful immune activation in Poly(I:C) injected dams was confirmed by demonstrating significantly elevated levels of interleukin 6 (IL-6) in the dams compared to PBS-injected dams[30].

2.2.3: Characterization of MIA model

To first characterize the MIA model, we tested whether progeny of Poly(I:C)-injected dams exhibit behavioral deficits previously observed in this model[25,27,29,31]. We tested their offspring (male and female) in a battery of three behavioral assays (however, these initial cohort was not tested in the social touch assay). The MIA offspring were tested for the presence of ultrasonic vocalizations at P7-9, in the 3-chamber social interaction assay (which quantifies their preference to a novel mouse over an inanimate novel object) at P60-90, and in the marble burying assay (a measure of repetitive behaviors in rodents) also at P60-90[25,31-33]. PBS and MIA mice that were

tested on the social touch behavioral assay were only characterized for IL-6 levels and did not undergo this battery of three behavioral assays.

2.2.4: Surgical implantation of head bars

Adult mice were anesthetized with isoflurane (5% induction, 1.5-2% maintenance via nose cone v/v) and secured on a stereotaxic frame (Kopf) via metal ear bars. A 1 cm long midline skin incision was made above the skull under sterile conditions. A titanium U-shaped head bar (3.15 mm wide x 10 mm long) was placed on the skull just caudal to Lambda and permanently glued with dental cement. This bar was later used to secure the animal to a post for the head-fixed social touch behavioral assay. This surgery lasted ~15-20 min and mice fully recovered within 30 min after surgery and returned to group-housed cages.

2.2.5: Social touch assay in head-restrained mice

Following head bar implantation, mice were habituated to head restraint and to running on an air-suspended 200 mm polystyrene ball, as well as to the movement of a motorized stage that was used for repeated presentations of an inanimate object or a stranger mouse. The stage was controlled through MATLAB (Mathworks) in a custom-built, sound-attenuated behavioral rig (93 cm x 93 cm x 57 cm) that was dimly illuminated by two infrared lights (Bosch, 850 nm) (**Fig. 2-1a**). For habituation, test mice were placed on the ball for 20 min each day for 7-9 consecutive days before testing. In parallel, 'visitor' mice (stranger to the test mouse) were habituated to head-restraint in a plexiglass tube (diameter: 4 cm) secured to a motorized stage consisting of an aluminum bread board (15 x 7.6 x 1 cm) attached to a translational motor (Zaber Technologies, X-LSM100A). The stage translated at a constant speed of 1.65 cm/s. The neutral starting position was 6 cm away from the test mouse.

Following habituation, test mice were subjected to both voluntary and forced interactions with a visitor mouse or a novel inanimate object (a plastic 50 mL Falcon conical centrifuge tube,

Fisher Scientific) over the course of 2 d (**Fig. 2-1b**). Voluntary interactions meant that the test mouse was within whisker contact of the novel object or mouse, while in forced interactions the stage stopped at a position closer to the test mouse such that the tip of the object or snout of the visitor mouse was in direct contact with the snout of the test mouse. These positions were calibrated before each experiment. On day 1, test mice were placed on the ball and recorded for a 2 min baseline period (the plexiglass tube on the moving stage was empty). Next, we inserted the novel plastic object (50 mL Falcon tube) into the plexiglass tube on the motorized stage. For this control interaction the test mouse first experienced a 2 min period of no touch but was able to visualize the object in the neutral position (before touch, 6 cm away). Next, the motorized stage moved the object to within whisker reach of the test mouse for a total of 5 or 20 such presentations of voluntary object touch. Each bout lasted 5 s, with a 5 s interstimulus interval (ISI) during which the platform moved away by 1 cm and the object was out of reach of the test mouse. The total travel time for the platform was 1.2 s (for back and forwards). After this voluntary object touch session, the test mouse was returned to its cage to rest for at least 60 min before being head-restrained again on the ball to undergo voluntary or forced social touch (randomized) session with a visitor mouse. A same-sex, same age (P60-90) novel WT mouse (for WT and *Fmr1* KO test mice) or a novel PBS mouse (for PBS and MIA test mice) was head-restrained inside the plexiglass tube on the stage. Following a 2 min period in the neutral position where the test mouse could see but not touch the stranger mouse, the motorized stage moved to the position for voluntary social touch (whisker-to-whisker) or forced social touch (snout-to-snout) for 5 or 20 bouts of each (also lasting 5 s with a 5 s ISI where the mouse on the platform moved out of reach of the test mouse). The test mouse was then returned to its cage for 24 h. On day #2, the mouse was placed back on the ball again for a 2 min baseline period followed by a 2 min period of no touch with a different stranger mouse. Depending on if the test mouse received voluntary or forced social touch on day 1, the mouse received 5 or 20 presentations of the alternate touch type with the second stranger mouse (**Fig. 2-1c**).

Additionally, we tested a separate cohort of WT and *Fmr1* KO mice on 20 presentations of forced touch from a novel plastic object (a 50 mL Falcon tube), a novel inanimate furry toy mouse (PennPlax) onto which we glued Nylon whiskers (1.5 cm length, 0.5 cm thickness), a stranger mouse of the opposite sex, and a familiar same-sex mouse. In this cohort, the test animal received forced object touch followed by forced social touch on the same day. On the next day, the animal received touch from an inanimate toy mouse and on day 3, the animal received touch from a stranger mouse of the opposite sex. Finally, the test mouse received voluntary social touch from stranger mouse on day 4. 24 hours later, the test mouse received forced social touch from the same mouse used on day 4 (now 'familiar', given the repeated exposure).

2.2.6: Behavioral quantification and analyses

During the course of the assay, high-resolution videos (.mp4 or .avi files) were recorded of the test mouse's eye, face, and body with 3 cameras (either The Imaging Source, Monochrome USB3 or Teledyne Flir, Blackfly S USB3) at 50 FPS (Figs. 3-6) or 120 FPS (Figs. 7-8) for behavioral analyses. Avoidance running, aversive facial expressions, pupil diameter and locomotion were analyzed from these videos of the eye, face, and body (**Fig. 2-1d**). Running avoidance (backwards directed running), running speed and locomotion were analyzed from body videos using custom-written video analysis routines in MATLAB. Painted dots on the polystyrene ball (1 cm diameter) were used to measure the angle and distance based on the displacement of each dot at a frame to the closest dot 5 frames later (median angle and distance was calculated using all angles and distances for dots displaced for every 5 frames, or 0.1 s). Median angle was used to determine the direction the animal was moving toward, while distance was used to calculate running speed. All videos were visually inspected post-hoc to correct for values corresponding to grooming or other sudden movements (so that those would not be considered as directional running). Locomotion was characterized as whenever the animal was actively moving on the ball in the video. In a second cohort of *Fmr1* KO mice and WT controls, we used

recorded videos at 120 FPS, and used a modified manual scoring of avoidance running because automated detection of three or more dots on the ball was not possible due to lighting conditions or fading of painted dots[16]. Pupil diameter was quantified using *Facemap*[34] and MATLAB. Aversive facial expressions (AFEs; i.e., prolonged whisker protraction and orbital tightening) were analyzed using *DeepLabCut*[35,36]. Briefly, the network was trained on images from the face videos to identify markers on the mouse's whisker follicles. The displacement of the follicles was calculated using these markers to detect sustained (≥2 s) negative displacements from the resting position of the whiskers as aversive whisker protraction movements. Analysis of the whisker displacement was semi-automated; all videos were inspected post-hoc to exclude frames when grooming and other movements obscured the face or certain whisker movements interfered with the detection of sustained whisker protraction. We quantified overall active whisking during the assay by calculating the motion energy of whisking using *Facemap*. To quantify orbital tightening or eye squinting, a neural network was trained on still images from videos of the face to reliably identify markers along the mouse's eye. The area of the eye was calculated from these markers to quantify orbital tightening. For analysis of pupil diameter and orbital tightening, we excluded video frames when blinking, grooming, or other movements obscured the animal's face.

Because there are important sex differences in both the prevalence and symptoms of ASD[37,38], we distinguished males from females across all figures (squares = males, circles = females).

2.2.7: Statistical analyses

Statistical tests were performed in Prism software (GraphPad). Statistical analyses of normality (Lilliefors and Shapiro Wilk tests) were performed on each data set; if data deviated from normality ($p<0.05$) or not ($p>0.05$), appropriate non-parametric and parametric tests were performed. For parametric two-group comparisons, a Student's t-test (paired or unpaired) was used. For non-parametric tests, we used Mann-Whitney test (two groups) and the Kruskall-Wallis

test (repeated measures). Multiple comparisons across touch conditions and genotypes/groups were analyzed using two-way ANOVA with post-hoc Bonferroni's test. If data was non-normal, we applied a logarithmic transformation on the data and compared the two-way ANOVA with and without the transformation. Since the statistical output of the two-way ANOVA was similar for the transformed and the non-transformed, non-normal data, we used the statistical output from the latter. All experiments were conducted in at least two litters per genotype/group. Graphs either show data from each mouse per group or group means (averaged over different mice) superimposed on individual data points. In all figures, the error bars denote standard error of mean (s.e.m.).

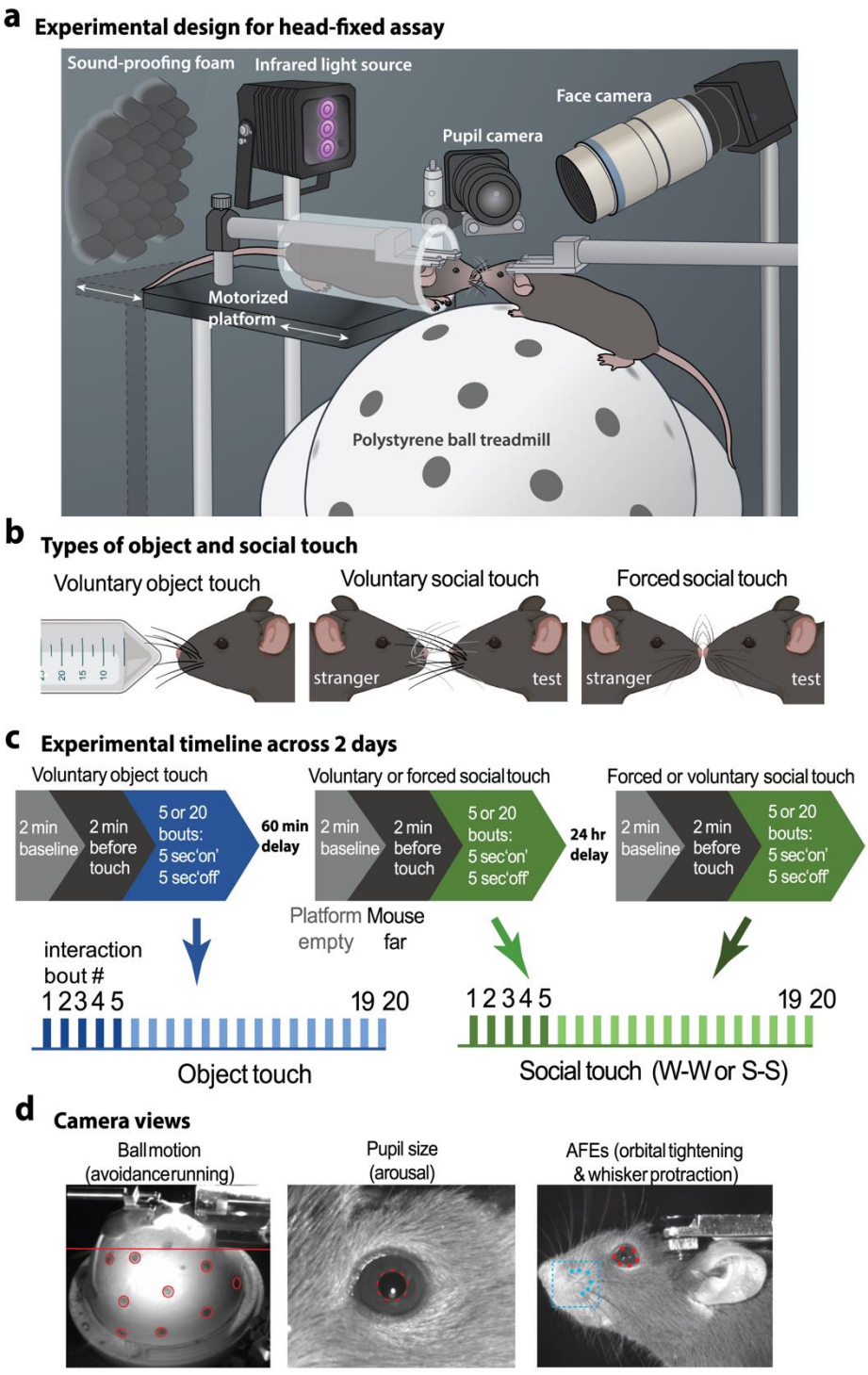
a
Experimental design for head-fixed assay
Sound-proofing foam
Infrared light source
Face camera
Pupil camera
Motorized platform
Polystyrene ball treadmill
b
Types of object and social touch
Voluntary object touch
Voluntary social touch
Forced social touch
stranger
test
stranger
test
c
Experimental timeline across 2 days
Voluntary object touch
Voluntary or forced social touch
Forced or voluntary social touch
2 min baseline
2 min before touch
5 or 20 bouts: 5 sec'on' 5 sec'off'
60 min delay
24 hr delay
Platform empty
Mouse far
interaction bout #
1 2 3 4 5
19 20
Object touch
Social touch (W-W or S-S)
d
Camera views
Ball motion (avoidance running)
Pupil size (arousal)
AFEs (orbital tightening & whisker protraction)

Fig. 2-1: Setup for social touch behavioral assay.

a. Overview of head-fixed setup for the social touch behavioral assay. A head-fixed test mouse can run on an air-suspended polystyrene ball while interacting with a stranger mouse restrained in a plexiglass tube secured to a motorized platform. The system is fully automated to move the stranger mouse to different distances away from the test mouse. Two cameras focus on the face and the eye/pupil, respectively, while a third camera that tracks the mouse and ball motion is overhead (not shown). An infrared light source provides optimal light for tracking behavioral responses. Acoustic foam is used for sound insulation.

b. We tested three types of touch: voluntary object (whisker-object), voluntary social (whisker-whisker), and forced social (snout-snout).

c. Duration of baseline (platform empty without object/mouse), no touch, and object social touch, as well as the number of stimulations and delay between each type of touch condition.

d. Camera views for tracking ball motion, pupil size and AFEs.

2.3: Results

2.3.1: A novel behavioral assay for social touch

To investigate how mice respond to social touch, and the circuits involved, one must consider the pros and cons of different behavioral assays. Inspired by prior designs of social touch assays for mice and rats[5,7,10,11], we designed a novel head-fixed behavioral assay in which we can control the frequency and duration of each social touch interaction, the type of touch (whisker-whisker vs. snout-snout), and the context (social vs. object). In this this assay, a head-restrained test mouse that is allowed to run on an air-suspended polystyrene ball is monitored with multiple cameras during repeated presentations of a novel mouse that is also head-fixed and resting on a motorized stage that brings it to predetermined positions at various distances away from the test mouse (see Materials and Methods, **Fig. 2-1a-c**). We tested three different positions of the stage to assess corresponding conditions of social touch: 1. Before touch, where the test animal can see the novel 'visitor' mouse but not touch it; 2. Voluntary social touch where the test mouse can interact with the visitor via its whiskers; 3. Forced social touch, where the visitor mouse is so close to the test mouse that their snouts are in direct physical contact.

By using high frame rate cameras to record the test animal's face and eyes, as well as ball motion, we can quantify different aspects of facial expressions (e.g., whisker movements, mouth opening, ear movements, eye size changes) and changes in pupil diameter or saccades, as well as locomotion (see Materials & Methods; **Fig. 2-1d**). Because we are interested social touch aversion in autism, we focused on behaviors that might indicate that the mouse experienced social touch as an unwanted aversive stimulus, by exhibiting avoidance, defensive behaviors, facial expressions of negative emotion, or hyperarousal. Indeed, these behavioral responses are observed in ASD individuals responding to social or affective touch and in mouse models of ASD responding to passive non-social touch[3,16,17,21,39-41]. Our assay also examines social touch that is potentially unpleasant, rather than allo-grooming, by including forced snout-snout interactions. This allowed us to explore how ASD mouse models might respond to social touch across different

contexts and how the tactile system engages with these stimuli behaviorally. However, this assay can be easily modified to change the presentation parameters, or the types of visitor and test mice (e.g., age, sex, genotype), in order to explore a myriad of interesting questions about social touch in rodents. We also designed the assay to be compatible with calcium imaging or silicon probe recordings of neural activity, to elucidate circuits that are activated by social touch, as well as those that mediate behavioral responses to social touch.

To demonstrate the utility of this novel social touch assay, we compared the behavioral responses of control wild-type (WT) mice to those of two mouse models of ASD. The first was the *Fmr1* knockout (*Fmr1* KO) mouse model of Fragile X Syndrome (FXS) (The Dutch-Belgian Fragile X Consortium, 1994), the leading single gene cause of intellectual disability and autism. The other was the Poly(I:C) maternal immune activation (MIA) model, which is widely used as a model of an environmental cause of autism[25,27,29]. Of note, we characterized the MIA model both as far as IL-6 levels in the dam and various behavioral deficits in the offspring (**Fig. 2-2**). We found that MIA mice exhibited reduced pup USV calls, reduced social preference, and increased marble burying compared to offspring of PBS-injected dams (**Fig. 2-2b**; marble burying: $p=0.010$; USVs: $p=0.043$; 3-chamber: $p < 0.0001$).

Below, we present results of our observations related to four major behavioral responses: 1. Avoidance running; 2. Pupil dilation; 3. Whisker protraction; and 4. Orbital tightening (squinting). Overall, we hypothesized that, compared to their respective controls, *Fmr1* KO and MIA mice would show increased avoidance, hyperarousal, and more AFEs (whisker protraction, eye squinting) to social touch that controls, but no differences for object touch. Furthermore, we expected that forced social touch (snout-snout) would be more aversive than voluntary social interactions (whisker-whisker) for ASD mice.

a **Interleukin-6 levels in pregnant dams at E12.5 following Poly(I:C) injection from two lots**

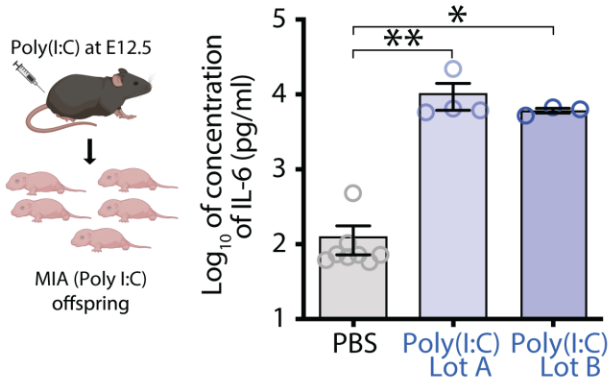

b **Offspring of Poly (I:C) dams with high IL-6 show behavioral deficits**

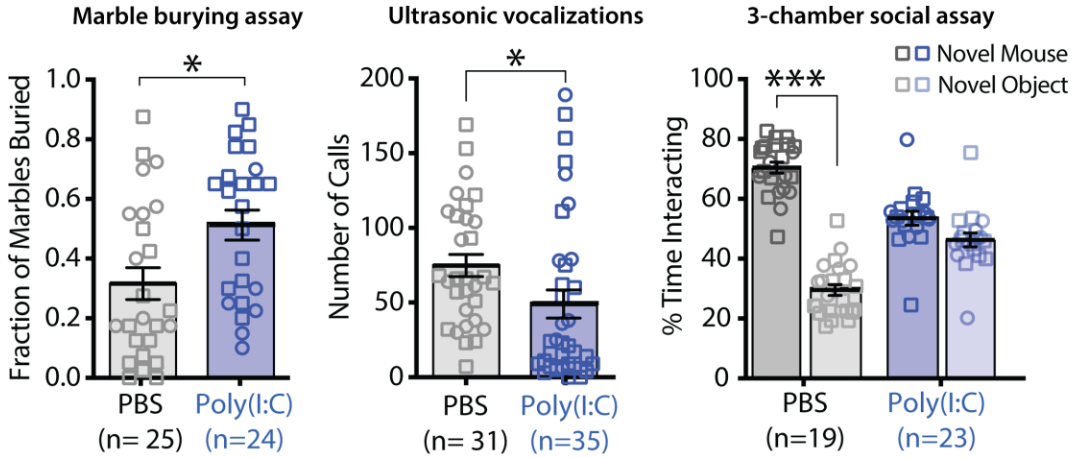

c **IL-6 levels in Poly(I:C) injected pregnant dams at E12.5 for social touch behavioral assay**

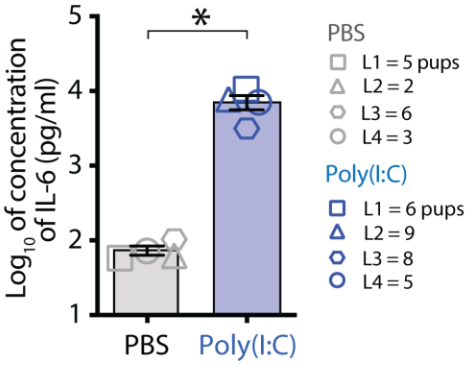

Fig. 2-2: Interleukin-6 levels are higher in pregnant dams injected with Poly(I:C) and their offspring show expected behavioral deficits.

a. MIA was induced in pregnant dams by intraperitoneally injecting Poly(I:C) at embryonic age 12.5 (E12.5). Interleukin-6 (IL-6) cytokine levels are higher in pregnant dams injected with Poly(I:C) at E12.5 compared to dams injected with PBS. Two different Poly(I:C) lots acquired from Sigma-Aldrich were tested and elicited significantly higher IL-6 levels in dams. **p<0.01, *p<0.05 for Mann-Whitney test.

b. Offspring of dams injected with Poly(I:C) from Lot A and B showed increased fraction of marbles buried in the marble burying assay at P60-90, reduced ultrasonic vocalizations recorded at P7-9, and no difference in preference for a novel mouse versus novel object in the 3-chamber social interaction assay. Squares = males, circles = females in panel b. ***p<0.001, *p<0.05, unpaired t-test for marble burying assay and USVs, two-way ANOVA with Bonferroni's for 3-chamber social assay.

c. IL-6 levels in PBS and Poly(I:C) injected pregnant dams whose offspring were used for the behavioral testing in the social touch assay. Poly(I:C) from Lot A and B were used in pregnant dams.

2.3.2: Greater avoidance running in Fmr1 KO and MIA mice during social touch but not object touch

Sensory hypersensitivity is very prevalent in ASD and is thought to contribute to maladaptive avoidance responses, such as tactile defensiveness and social avoidance[42,43]. Most children with FXS experience sensory over-reactivity, often leading to tactile defensiveness and gaze aversion[44,45]. However, avoidance to social touch per se has never been investigated in animal models of ASD or FXS. Previously, we demonstrated that *Fmr1* KO mice exhibit tactile defensiveness to repetitive whisker stimulation, which manifested as avoidance running[16]. To investigate whether social touch leads to avoidance, we quantified running direction of the test mouse relative to the novel object or stranger mouse (**Fig. 2-3a**). If the test animal was moving backward (either left or right), we categorized this as avoidance, in contrast to running forward, which was considered an adaptive response (seeking social interaction). We initially calculated the total time the mouse spent in locomotion, regardless of direction, to determine if group differences in running might skew the proportion of avoidance running. Although there are reports of hyperactivity in *Fmr1* KO mice[28], we have not found differences in total locomotion between adult *Fmr1* KO and WT mice either in response to whisker stimulation or while performing a visual discrimination task[16,46]. In the social touch assay, we observed that mice of all groups spent more time running when they transitioned from the baseline period (before touch) to the period of social touch ($p<0.05$), but there were no significant group differences ($p>0.05$ between WT vs *Fmr1* KO & PBS vs MIA, **Table 2-1**). There were also no differences in running speed during object or social touch between *Fmr1 KO* or MIA mice and their respective controls (**Fig. 2-3b**).

In contrast, when we compared the proportion of time that mice spent showing avoidance running as a proportion of total locomotion, we found that both *Fmr1* KO and MIA mice displayed higher avoidance during voluntary and forced social touch compared to controls, but not during voluntary object touch (**Fig. 2-3c**; WT vs. *Fmr1* KO: vol. object $p>0.05$, vol. social $p=0.006$, forc. social $p=0.047$; PBS vs. MIA: vol. object $p>0.05$, vol. social $p=0.002$, forc. social $p=0.002$). Thus,

considering overall running speed was similar between the two ASD models and their controls both before and during social touch, these differences in avoidance running could not be explained by hyperactivity.

Because there are important sex differences in both the prevalence and symptoms of ASD[37,38], we also compared avoidance between male and female mice in each group, but did not find any significant sex differences within genotype. We also looked at differences between litters in each genotype but did not see any obvious differences either, although the sample size per litter was small (2-9 mice per litter, median = 5 mice).

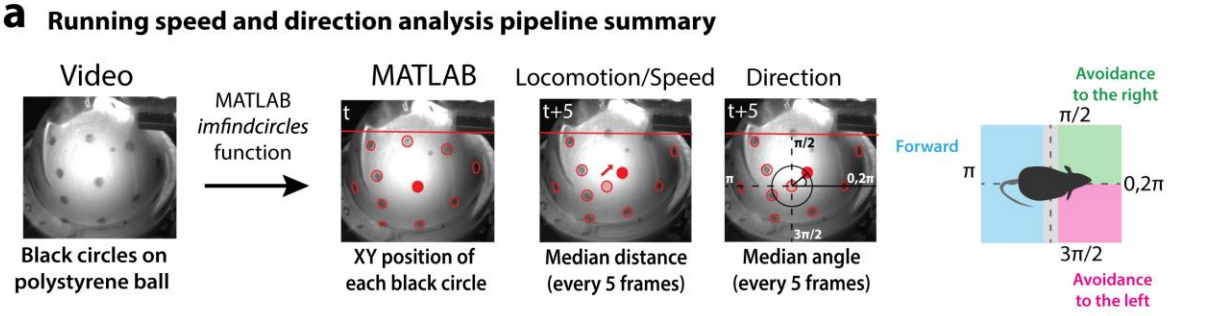
a
Running speed and direction analysis pipeline summary
Video
MATLAB
imfindcircles
function
MATLAB
Locomotion/Speed
Direction
Black circles on
polystyrene ball
XY position of
each black circle
Median distance
(every 5 frames)
Median angle
(every 5 frames)
Avoidance
to the right
π/2
Forward
π
0,2π
3π/2
Avoidance
to the left
*(All videos inspected to correct for grooming and non-directed ball movements; see Methods)

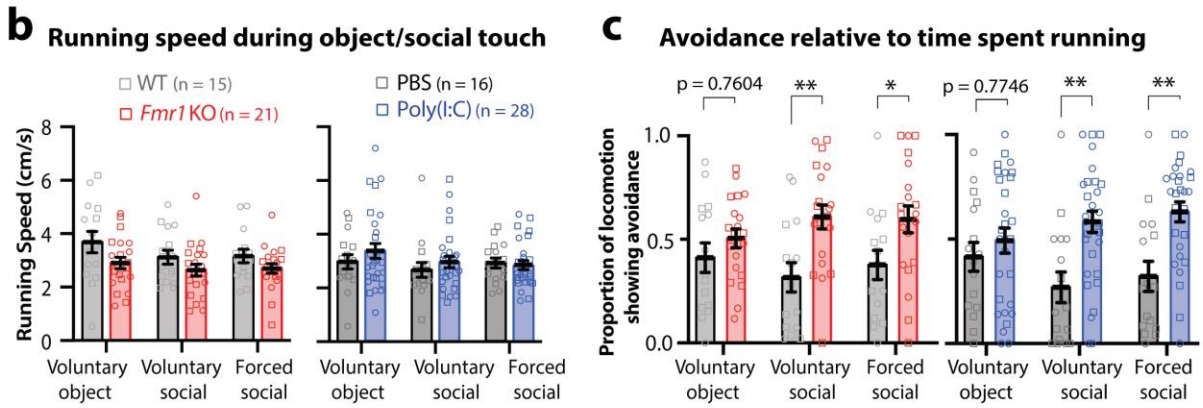
b
Running speed during object/social touch
WT (n = 15)
Fmr1 KO (n = 21)
PBS (n = 16)
Poly(I:C) (n = 28)
Running Speed (cm/s)
Voluntary object
Voluntary social
Forced social
c
Avoidance relative to time spent running
p = 0.7604
**
*
p = 0.7746
**
**
Proportion of locomotion showing avoidance
1.0
0.5
0.0

Fig. 2-3: Mouse models of autism show avoidance to social touch from a stranger mouse.

a. Analysis of locomotion and running speed and direction. Speed (cm/s) is calculated using the distance moved of a circle at time *t* to the closest circle in pixel space in time *t+5* every 5 frames (0.1 s). Direction of circle movement at time *t* to *t+5* frames is calculated from the angle between the circle at time *t* as the origin point relative closest circle at *t+5* in pixel space. Median speed and angle is calculated from distance and angle displacements of all circles every 5 frames (0.1 s). Locomotion is calculated by finding running speeds within 2 standard deviations of the mean speed. Example circle (red filled in time *t* and pink filled in *t+5*) moves to the right and up (red filled in time *t+5*, leftwards avoidance). Circles above red line are excluded from detection. Videos were inspected post-hoc to exclude frames when the animal was grooming or engaged in non-directed ball movements.

b. Average running speeds during all types of touch do not differ between ASD mice and control animals.

c. Running avoidance (backwards to left or right) is higher in *Fmr1 KO* and Poly(I:C) MIA mice compared to controls during voluntary and forced social touch but not object touch. Squares=males, circles females. **p<0.01, *p<0.05, two-way ANOVA with Bonferroni's. No outliers were detected with ROUT's analysis.

Table 2-1. Differences in Overall Locomotion

Locomotion Before vs During Touch		
Two-way ANOVA with Bonferroni's	Mean Proportion of Time ± SEM	p-value
WT (n = 15)		
Voluntary Object	0.51 ± 0.08 vs 0.63 ± 0.08	0.2740
Voluntary Social	0.40 ± 0.06 vs 0.67 ± 0.08	0.006
Forced Social	0.46 ± 0.08 vs 0.64 ± 0.06	0.0148
Fmr1 KO (n = 21)		
Voluntary Object	0.26 ± 0.05 vs 0.53 ± 0.05	<0.001
Voluntary Social	0.41 ± 0.06 vs 0.60 ± 0.067	0.0172
Forced Social	0.304 ± 0.055 vs 0.652 ± 0.069	<0.001
PBS (n = 16)		
Voluntary Object	0.301 ± 0.074 vs 0.704 ± 0.062	<0.001
Voluntary Social	0.298 ± 0.069 vs 0.473 ± 0.079	0.0508
Forced Social	0.285 ± 0.078 vs 0.571 ± 0.05	<0.001
Poly(I:C) (n = 28)		
Voluntary Object	0.438 ± 0.059 vs 0.506 ± 0.052	0.3124
Voluntary Social	0.385 ± 0.056 vs 0.620 ± 0.058	<0.001
Forced Social	0.320 ± 0.051 vs 0.563 ± 0.043	<0.001
Locomotion WT vs Fmr1 KO During Touch		
Voluntary Object	0.634 ± 0.083 vs 0.525 ± 0.052	0.4206
Voluntary Social	0.670 ± 0.075 vs 0.604 ± 0.067	0.7371
Forced Social	0.644 ± 0.064 vs 0.652 ± 0.069	0.9966
Locomotion PBS vs Poly(I:C) During Touch		
Voluntary Object	0.704 ± 0.062 vs 0.506 ± 0.052	0.0619
Voluntary Social	0.473 ± 0.079 vs 0.620 ± 0.058	0.2463
Forced Social	0.571 ± 0.05 vs 0.563 ± 0.043	>0.999

Table 2-1: Locomotion increases when mice engage in object or social touch and does not differ between mouse models of autism and their controls.

2.3.3: Pupil dilation with social touch lasts longer in Fmr1 KO, but not MIA mice

Autonomic hyperarousal, including elevated heart rate and pupil dilation, is observed in autistic individuals during tactile stimulation or affective touch, and is used as an indicator of tactile hypersensitivity[47-49]. We measured changes in pupil size as a proxy for arousal in response to social touch (**Fig. 2-4a**). We first compared pupil size as a mean of the first 5 presentations and found no differences between WT and *Fmr1* KO or between PBS and MIA mice, regardless of condition (object or social touch). Next, because pupils can dilate or constrict over short time scales, we compared pupil size at individual presentations of object or social touch[50,51]. We found that, in all groups, pupils significantly dilated to a similar extent after the first object/mouse presentation (**Fig. 2-4b)**. Interestingly, after repeated presentations of voluntary object touch, pupil size returned to baseline in all groups, presumably as a form of adaptation to a non-threatening situation (**Fig. 2-4b**). In contrast, pupils remained dilated for a longer period in *Fmr1* KO mice with both voluntary social touch and forced social touch whereas they constricted to baseline in MIA mice and controls. The difference was most pronounced with forced social touch, where pupils were significantly larger in *Fmr1* KO mice than in their controls on the 5th presentation (**Fig. 2-4b**; pupil size: WT vs. *Fmr1* KO $p<0.001$, PBS vs. MIA $p>0.05$).

In a subset of these mice that we tested up to 20 presentations of forced social touch, we found that pupil size in *Fmr1* KO and MIA mice eventually returned to baseline (**Fig. 2-4c**). We did not find any sex or litter differences in pupil size before or after social touch. Altogether, these findings indicate that *Fmr1* KO mice display more hyperarousal than WT mice to social touch.

a **Pupil size analysis summary**

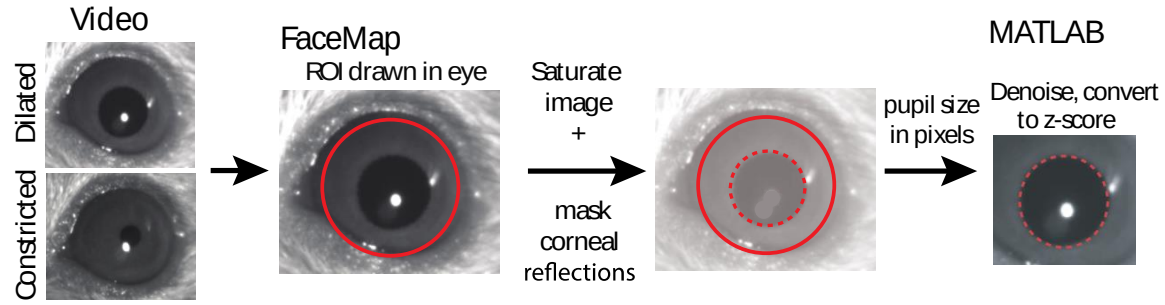

*(All videos inspected to exclude frames where the pupil is obscured due to grooming, blinking or body movements)

b **Pupil size changes across initial presentations of object/mouse**

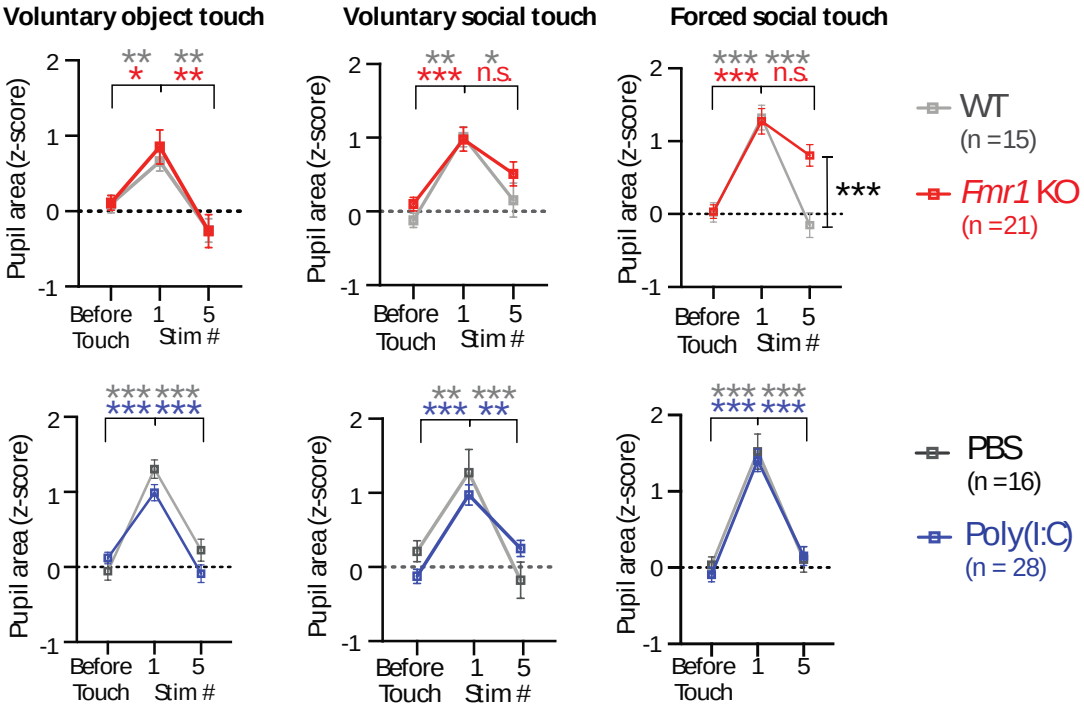

c **Pupil size across 20 presentations of forced social touch**

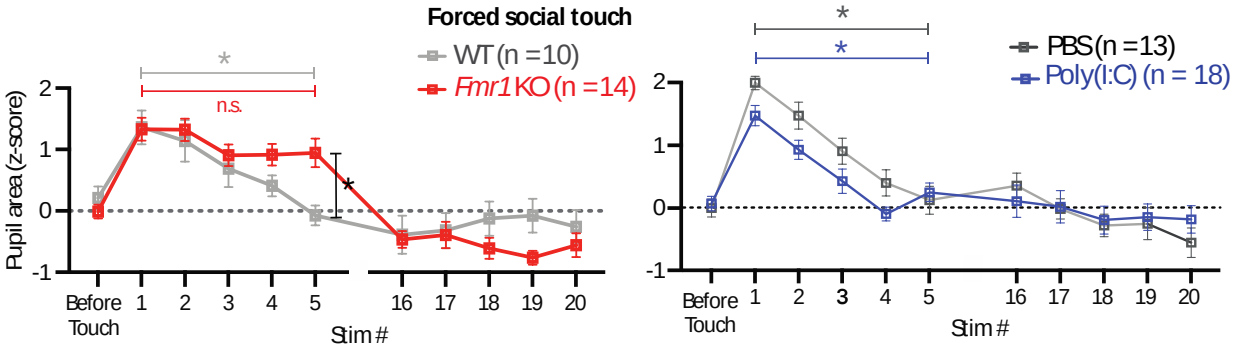

Fig. 2-4: Pupil dilation is prolonged during social touch in ASD mice

a. Summary of pupil size analysis using Facemap. A region of interest (ROI) is drawn in the Facemap graphical user interface in Python (red circle). Facemap detects the pupil within the ROI (red dashed circle) and generates pupil area in pixels, which is converted to z-score in MATLAB.

b. Pupil size does not decrease to baseline levels (before touch) in *Fmr1 KO*, but does in MIA mice and both controls, by the 5th stimulation of voluntary and forced social touch. ***p<0.001, ** p<0.01, *p<0.05, two-way ANOVA with Bonferroni's for pupil area before touch vs. 1st and 5th stimulation.

c. A subset of mice were tested for up to 20 presentations of forced social touch. *Fmr1* KO mice, but not MIA mice, show persistent pupil dilation compared to their controls. Squares = males, circles = females. ***p< 0.001, **p<0.01, *p<0.05, two-way ANOVA with Bonferroni's before touch vs. each stimulation. No outliers were detected with ROUT's analysis.

2.3.4: Aversive facial expressions (grimace) are more pronounced in Fmr1 KO and MIA mice during forced social touch

In humans, facial expressions are considered good indicators of emotional state[52]. Autistic individuals will grimace or wince to aversive sensory stimuli and will avert their gaze during social interactions[22,53,54]. Facial grimacing in the form of orbital tightening, changes in whiskers, or nose bulging, is also observed in rodents experiencing pain[55], but less is known about which facial expressions are associated with sensory hypersensitivity or unwanted social interactions. We posited that if ASD mice consider social touch as aversive, they would manifest facial grimacing. We focused on two facial features, whisker movement and orbital tightening, because they were easily detectable by cameras in our set-up and because analysis could be semi-automated using *DeepLabCut*[36,55]. For whisker movement, we quantified bouts of sustained whisker protraction, which is often seen in mice experiencing pain[55], in mice during active escape, and during aggression or immediate facial contact[56-59]. Prolonged whisker protraction is different from active whisking, which is an adaptive behavior in rodents as they explore their environment, both in terms of the speed and the direction of whisker movement. During active whisking, follicles are displaced forwards and backwards rapidly and rhythmically (8-12 Hz, for bouts lasting 1-2 seconds)[60]. In contrast, during aversive whisker protraction, the animal's whiskers are maintained in a fixed, forward position for bouts lasting up to several seconds.

We could distinguish between these two types of whisker movement using *DeepLabCut* and *Facemap* (**Fig. 2-5a**; see Methods). ASD mice and their controls showed more active whisking when presented with novel mice compared to before touch (**Fig. 2-5b,** $p<0.05$), but we did not find any significant differences in time spent actively whisking between groups or between voluntary or forced social touch. However, we found that *Fmr1* KO and MIA mice spent significantly more time than their controls displaying aversive whisker protraction during forced social touch (**Fig. 2-5c**, WT vs. *Fmr1* KO $p=0.013$, PBS vs. MIA $p=0.034$). In contrast, we saw no group differences in whisker protraction during object touch or voluntary social touch. There were

also no significant sex or litter differences in whisker protraction in any group across all touch conditions.

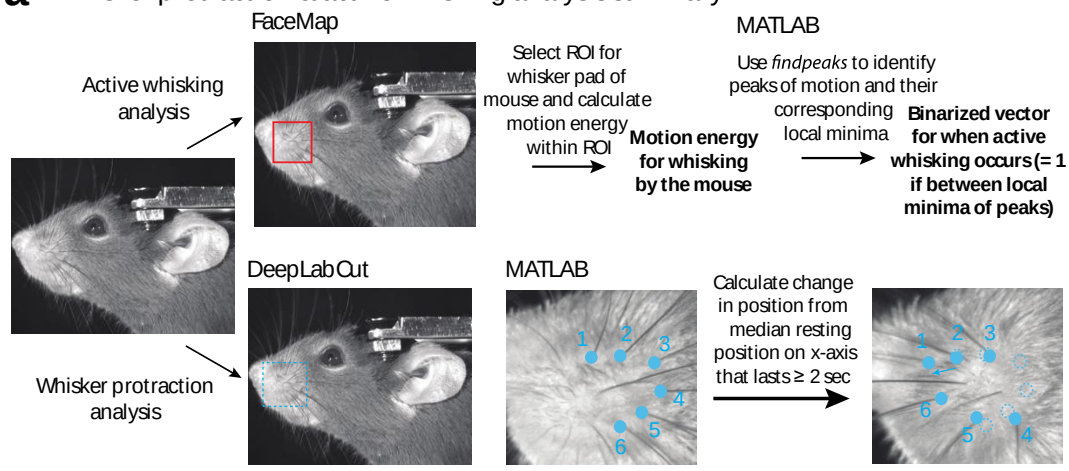

*(All videos inspected to exclude frames where grooming/other movements obscured the face and to conf rm whisker movements were occurring)

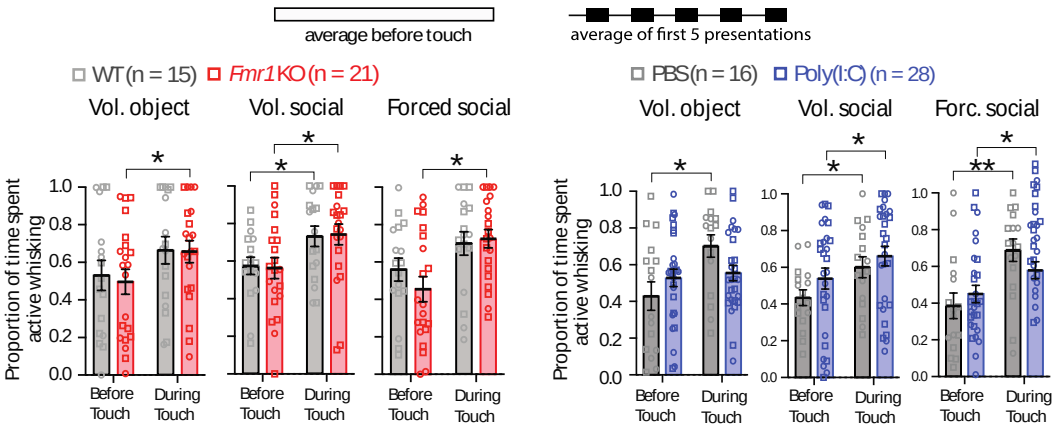

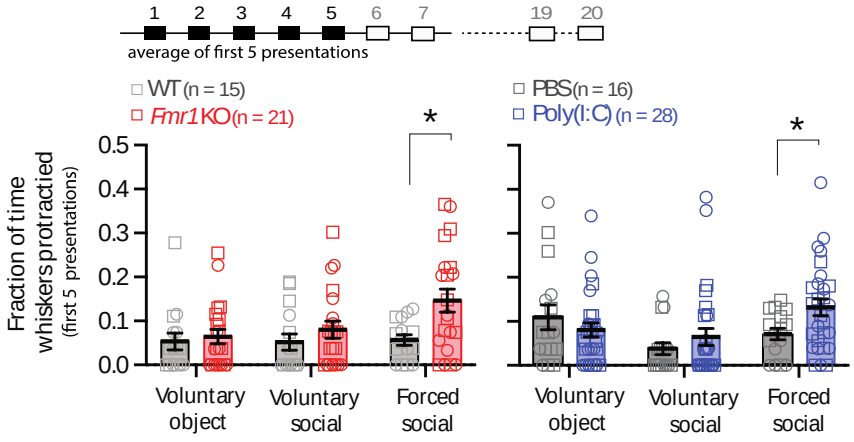

Fig. 2-5: Prolonged whisker protraction during forced social touch in ASD mice

a. Summary of analysis for calculating prolonged whisker protraction and active whisking. To quantify periods of active whisking, we used Facemap. We denoted the whisker pad as a region of interest (ROI) and tracked changes in pixel value within the ROI as the motion energy for whisking. We then used MATLAB's findpeaks function to identify peaks and their local minima in the motion energy signal. We identified periods of active whisking as timepoints that were between the local minima of a peak. Whisking protraction was determined by training a deep neural network (NN) in DeepLabCut to detect 6 whisker follicles from a set of training video frames (randomly chosen frames). After training the NN and evaluating its performance, we processed full videos, which generated the x position of each whisker follicle in pixel space. We then calculated the median change from all follicle positions relative to its resting position along the x-axis. Negative changes in follicle position at a given frame that were 1 standard deviation below mean resting position and lasted at least 2 seconds were denoted as periods of aversive whisker protraction.

b. Active whisking did not differ between *Fmr1* KO and MIA mice and their controls both before and during object and social touch. There was, however, a significant increase in mean whisking during the first 5 stimulations compared to before touch. Squares = males, circles = females. *p<0.05, **p<0.01 for two-way ANOVA with Bonferroni's. Vol = voluntary.

c. The fraction of time *Fmr1 KO* and MIA mice exhibited prolonged whisker protraction was higher during forced social touch than their controls but not significantly for voluntary object and social touch. Squares=males, circles=females. ***p<0.001 for two-way ANOVA with Bonferroni's. No mice were excluded according to ROUT's analysis.

Next, we determined whether mice show orbital tightening during social touch by estimating the area of the eye during the first 5 presentations of social touch. Again, we used *DeepLabCut* to train a neuronal network to estimate the area of the eye (**Fig. 2-6a)**. We found that orbital area (relative to the period before touch) was significantly smaller (i.e., more orbital tightening) in *Fmr1* KO mice, and to a lesser extent in MIA mice, during forced social touch, but not during voluntary object or voluntary social touch, and not at all in the WT or PBS controls (**Fig. 2-6b**, WT vs. *Fmr1* KO p=0.0065, PBS vs. MIA p=0.051). The total area of the eye (in pixels) was also significantly smaller in *Fmr1* KO mice than in WT controls during forced social touch compared to just before touch (**Fig. 2-6c**, WT $p > 0.05$ vs. *Fmr1* KO p=0.0021). In contrast, when we quantified the eye area before and during voluntary social touch, we found no significant differences in *Fmr1* KO mice (**Fig. 2-6c**, $p > 0.05$). In the MIA mice, there was a slight decrease in the area of the eye during forced social touch, but this did not reach significance (p=0.091). Interestingly, some control mice, especially the PBS controls, tended to open their eyes more during social touch (**Fig. 2-6c**, PBS p=0.047; WT $p < 0.05$), which could represent increased arousal towards the other mouse. These findings suggest that AFEs like sustained whisker protraction and forceful eye closure are uniquely triggered by forced social interactions in ASD mouse models, particularly in the FXS model.

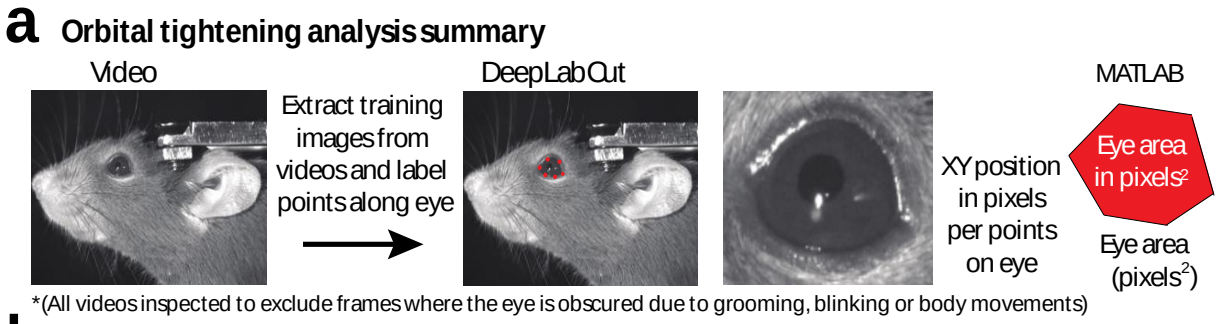
a
Orbital tightening analysis summary
Video
DeepLabCut
MATLAB
Extract training images from videos and label points along eye
XY position in pixels per points on eye
Eye area in pixels²
Eye area (pixels²)
*(All videos inspected to exclude frames where the eye is obscured due to grooming, blinking or body movements)

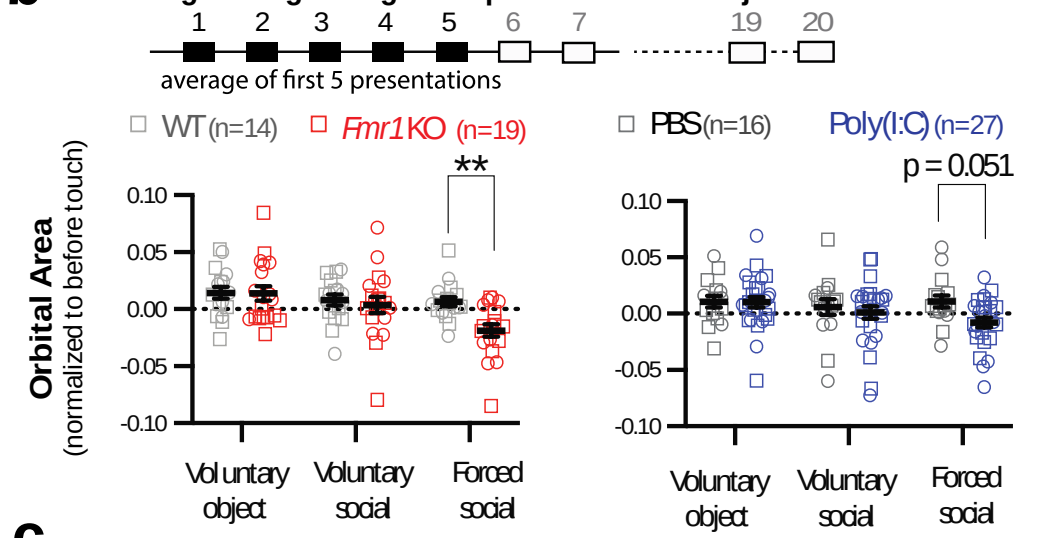
b
Orbital tightening during first 5 presentations of object/social touch
1 2 3 4 5 6 7 19 20
average of first 5 presentations
WT (n=14)
Fmr1 KO (n=19)
PBS (n=16)
Poly(I:C) (n=27)
**
p = 0.051
Orbital Area
(normalized to before touch)
0.10
0.05
0.00
-0.05
-0.10
Voluntary object
Voluntary social
Forced social

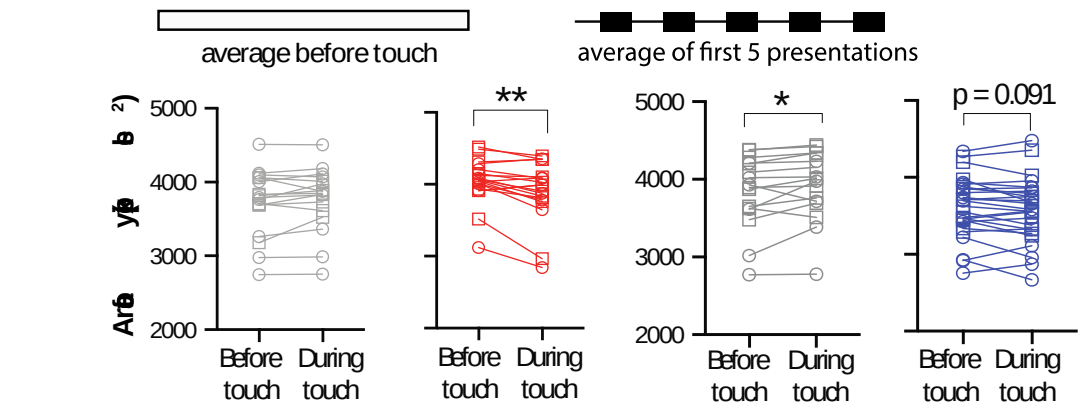
c
Orbital tightening before and during first 5 presentations of forced social touch
average before touch
average of first 5 presentations
**
*
p = 0.091
5000
4000
3000
2000
Before touch
During touch

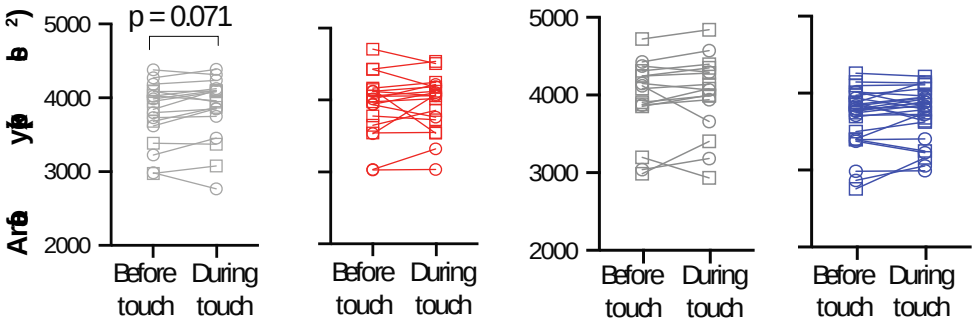
Orbital tightening before and during first 5 presentations of voluntary social touch
p = 0.071
5000
4000
3000
2000
Before touch
During touch

Fig. 2-6: Orbital tightening during forced social touch in ASD mice

a. Summary of analysis for calculating orbital tightening. Orbital tightening is determined by training a deep neural network (NN) in DeepLabCut to detect 6 points along the eye from a set of training images (frames randomly chosen from videos). After training the NN and evaluating its performance, we inputed videos into the Deep NN, which outputs the XY position of each point on the eye in pixel space. We then used MATLAB to generate a polygon connecting the six dots and calculated the area of that polygon as the orbital area. Orbital area in pixels was normalized to the orbital area before touch.

b. Orbital area during touch is normalized to area before touch (object or mouse visible but no touch in behavior rig). Orbital area is significantly lower (greater orbital tightening) during forced social touch in *Fmr1 KO* and MIA mice ($p=0.051$) compared to controls. 1 WT, 2 *Fmr1* KO & 1 MIA mice detected as outliers with ROUT's analysis in panel b were also excluded from analysis in panel c.

c. Orbital area is significantly smaller during forced social touch compared to the period before touch in *Fmr1 KO* mice, but not in MIA mice (there is also a slight but significant increase in orbital area in PBS controls during forced social touch). Orbital area is not significantly changed during voluntary social touch. Squares=males, circles=females. ***$p<0.001$, **$p<0.01$, *$p<0.05$, two-way ANOVA with Bonferroni's.

2.3.5: Fmr1 KO mice show greater avoidance and AFEs during forced interactions with stranger mice than WT controls (but similar maladaptive responses to forced object touch)

After completing this initial set of experiments, we considered the possibility that direct, forced contact with an inanimate object (particularly if it resembled a mouse) might elicit as much avoidance, hyperarousal, and increased AFEs in ASD mice as forced contact with a mouse (i.e., forced social touch). Indeed, people with ASD also exhibit tactile defensiveness to certain textures[16,20]. Because *Fmr1* KO mice had shown the largest differences with the social touch assay, we focused on this model for these additional control studies.

In an initial set of experiments, we tested how a new cohort of WT and *Fmr1* KO mice (n=12 and 10, respectively) responded to forced contact with the same novel object, a plastic 50 mL tube. In WT animals, forced touch with this object led to significantly greater running avoidance and whisker protraction than forced social touch, suggesting that social contact is better tolerated in WT animals (**Fig. 2-7b**, WT social vs. object, $p<0.001$ for avoidance and $p=0.009$ for whisker protraction). In contrast, in *Fmr1* KO mice, the difference between forced object touch and forced social touch was much smaller and did not reach significance for whisker protraction (**Fig. 2-7b**, *Fmr1* KO social vs. object, $p=0.025$, $p>0.05$, respectively). As a result, we found higher avoidance and whisker protraction in *Fmr1* KO compared to WT controls for forced social touch, but not for forced object touch (*Fmr1* KO vs. WT, $p=0.079$ for avoidance, $p=0.031$ for whisker protraction). Furthermore, we observed smaller orbital area in *Fmr1* KO mice than in WT controls during the last 5 presentations of forced social touch, but not with forced object touch (**Fig. 2-7b**, WT vs. *Fmr1* KO social $p=0.230$, object $p=0.382$). Note that orbital tightening in this new cohort of *Fmr1* KO mice was more prominent in the last 5 presentations, whereas it was present after only 5 presentations (and persisted) in the original cohort (**Fig. 2-6**). This likely reflects the smaller sample size and/or differences in behavioral habituation across batches of *Fmr1* KO mice (He et al., 2017).

Because the plastic tube is smooth, it may not be as aversive as the whiskers and fur of another mouse. Therefore, in a second set of control experiments with the same cohort of WT and *Fmr1* KO mice, we tested forced object touch using an inanimate plush toy mouse with fur and whiskers. Strikingly, we found that WT and *Fmr1* KO mice reacted very similarly to forced touch from the toy mouse as they did to the plastic tube, with greater avoidance and aversive whisking in WT mice to this object than to a forced social interaction with a stranger mouse (**Fig. 2-7c**, WT social vs. object, p=0.029 for running avoidance, p=0.001 for whisker protraction). Once again, *Fmr1* KO mice showed similar degrees of avoidance and whisker protraction to forced object and social touch (*Fmr1* KO social vs. object p>0.05 for both), but significantly more orbital tightening to only forced social interactions than WT mice (*Fmr1* KO vs. WT, p=0.031). Incidentally, when we compared the behavioral responses of WT and *Fmr1* KO mice to forced presentations of the 50 mL tube and the plush toy, we did not find significant differences in AFEs between these two objects (p=0.0674-0.999 for WT and p=0.395-0.415 for *Fmr1* KO), although *Fmr1* KO mice had slightly less running avoidance to the plush toy (p=0.029). Together, these results suggest that whereas forced touch from any object (smooth plastic tube or furry toy mouse) elicits similar maladaptive behaviors in WT and *Fmr1* KO mice, *Fmr1* KO mice are uniquely sensitive to forced social interactions with another live mouse.

a Experimental timeline for control experiments (Days 1-2)

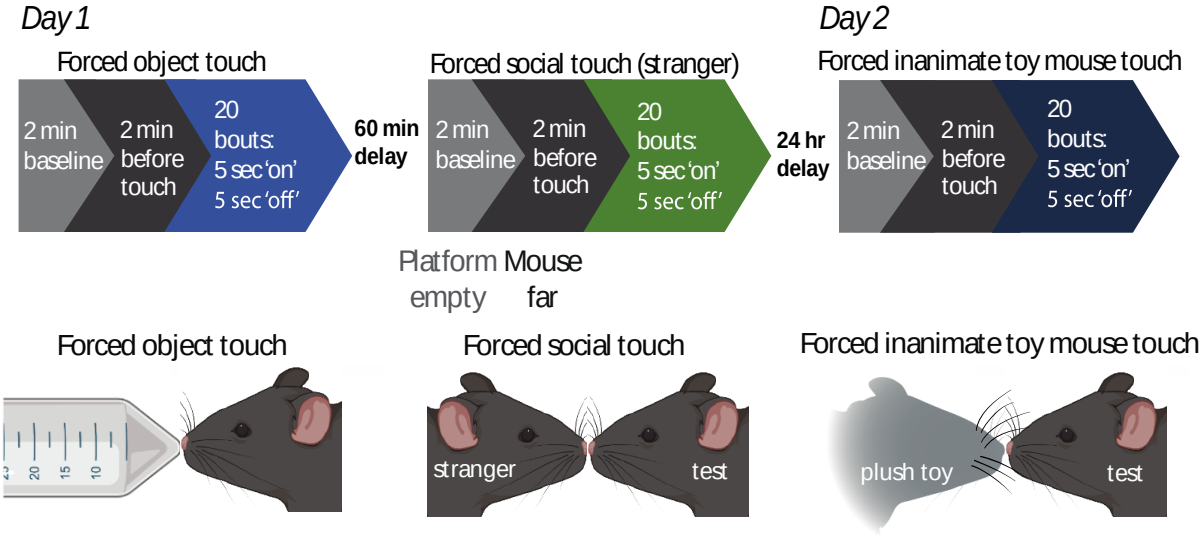

b Forced social vs forced object (50 mL conical tube)

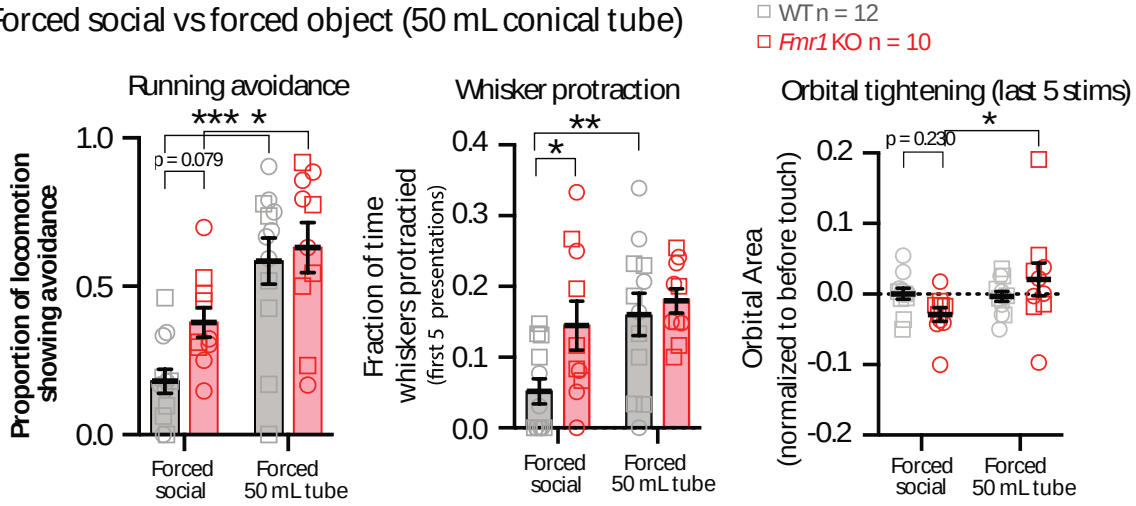

c Forced social vs forced inanimate toy mouse

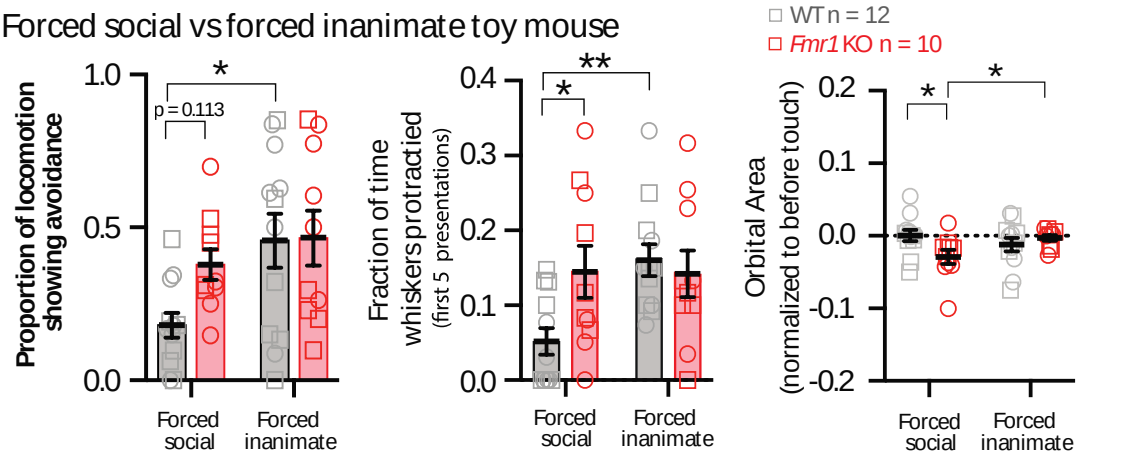

Fig. 2-7: *Fmr1* KO mice show greater avoidance and AFEs than WT controls during forced social interactions (but similar maladaptive responses to object touch)

a. Summary of the different types of object touch (50 mL conical tube and plush toy mouse) and social touch interactions and experimental timeline for control experiments.

b. Running avoidance, fraction of time spent showing whisker protraction and orbital area for WT and *Fmr1* KO in response to forced social touch with a stranger mouse vs. forced object touch with 50 mL conical tube. ***p<0.001, **p<0.01, *p<0.05, two-way ANOVA with Bonferroni's.

c. Same metrics as in panel *b* but using an inanimate toy mouse as the object. **p<0.01,*p<0.05, two-way ANOVA with Bonferroni's.

2.3.6: Fmr1 KO mice show less aversion to social touch with a mouse of the opposite sex, but whether the other mouse is familiar or a stranger matters less

Another important control related to social touch was to determine whether the sex of the visitor mouse influenced the degree of aversion it might elicit in ASD mice. For example, it is well-established that sensory inputs from mice of the same sex triggers aggression in males, whereas interactions with opposite sex animals leads to mating responses (Chen and Hong, 2018). Furthermore, female mice generally show more preference to males, though this tends to depend on receptivity[4]. Therefore, we sought to determine if the maladaptive behavioral responses to forced social touch are just as pronounced with a stranger mouse of the opposite sex (**Fig. 2-8a**). In general, WT mice showed similarly low levels of avoidance and AFEs when interacting with mice of either sex (**Fig. 2-8b**, $p>0.05$). In contrast, *Fmr1* KO mice showed more running avoidance and aversive whisking with a stranger mouse of the same sex than with opposite sex mice (**Fig. 2-8b**, $p=0.067$ for avoidance and $p=0.0213$ for whisker protraction). The magnitude of avoidance to stranger mice (this time of the opposite-sex) was significantly higher in *Fmr1* KO mice than in WT mice, further supporting our previous observations regarding social touch with same sex mice (**Fig. 2-8b**, WT vs. *Fmr1* KO $p=0.0374$). *Fmr1* KO mice also showed significantly more orbital tightening than WT controls during forced social interactions with mice of the same sex, but not with mice of the opposite sex ($p=0.035$ and $p>0.05$, respectively).

We next tested if aversion to forced social touch in *Fmr1* KO mice depended on whether the other mouse was familiar or a stranger. Some autistic individuals have difficulty recognizing and recalling faces of strangers[61,62]. Similarly, the Shank3B model of ASD shows deficits in discriminating between a novel and a familiar mouse [63]. In our social touch assay, we observed that *Fmr1* KO mice (n=8-10) exhibit similar levels of aversion to forced social touch with a familiar mouse and a stranger mouse (same-sex) (**Fig. 2-8c**, $p>0.05$ for avoidance and AFEs). Further confirming our previous results, this new cohort of *Fmr1* KO mice again showed significantly greater avoidance and whisker protraction to forced social touch with a familiar mouse than did

WT mice (n=11) (**Fig. 2-8c**, $p<0.001$ and $p=0.024$, respectively). Interestingly, WT mice showed a smaller orbital area during forced social touch with a familiar mouse relative to a stranger mouse (**Fig. 2-8c**, $p=0.012$). We surmised that repetitive presentations of social touch with the same animal over 2 d may elicit some anxiety in WT animals. Overall, these control experiments confirm that *Fmr1* KO mice show significantly more maladaptive responses to social touch than WT mice, and more avoidance/AFEs to opposite-sex mice than same-sex mice, but that it matters much less whether mice are familiar or stranger to them.

a

Experimental timeline for control experiments (Days 3-5)

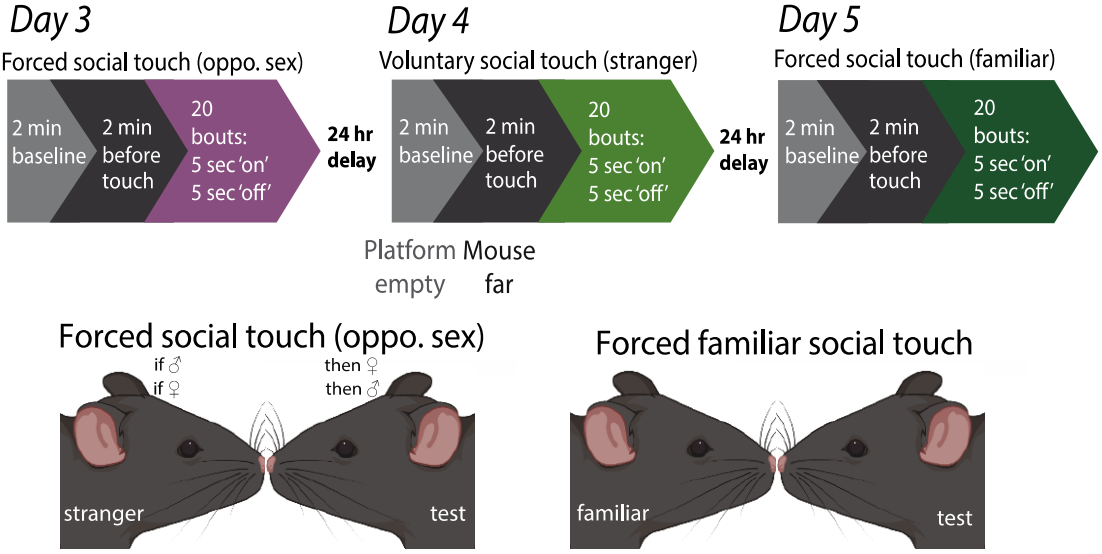

b

Forced social (same sex vs opposite sex)

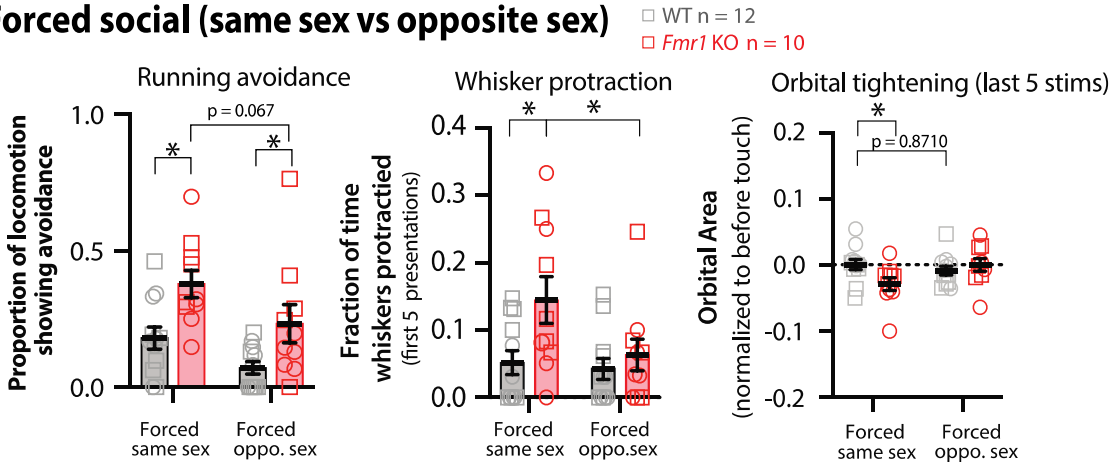

c

Forced social (stranger vs familiar)

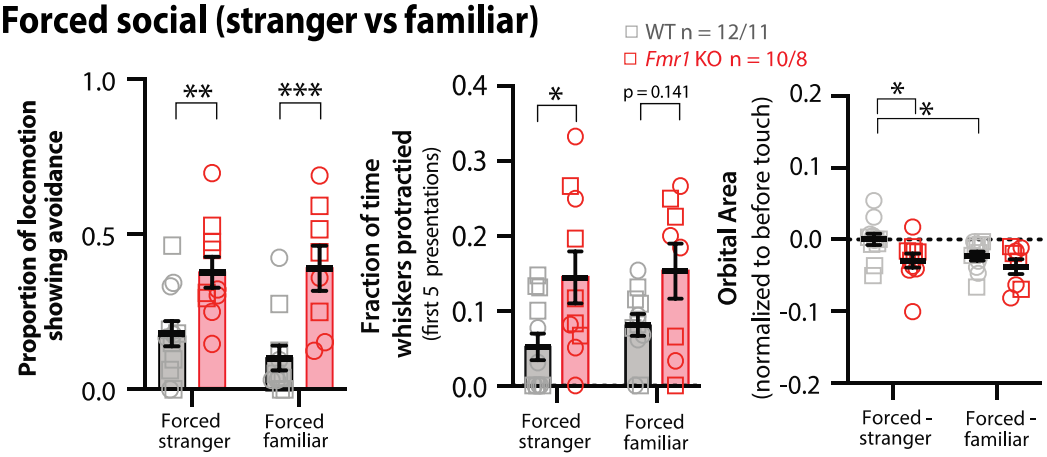

Fig. 2-8: *Fmr1* KO mice show less aversion to social touch with a mouse of the opposite sex (but whether the other mouse is familiar or a stranger does not matter)

a. Summary of the different types of social touch (same vs. opposite sex; stranger vs. familiar) and experimental timeline for forced social touch.

b. Running avoidance, fraction of time spent showing whisker protraction and orbital area for WT and *Fmr1* KO in response to forced social touch with same-sex stranger vs. opposite-sex stranger. **p<0.01, *p<0.05, two-way ANOVA with Bonferroni's.

c. Same metrics as in panel *b* but using stranger vs. familiar mouse (always same sex). ***p<0.001, **p<0.01, *p<0.05, two-way ANOVA with Bonferroni's.

2.4: Discussion

The main goal of this chapter was to implement a new behavioral paradigm that could be used to investigate social touch behaviors in rodents and the underlying circuits involved. Our findings can be summarized as follows: 1. Our new social touch assay can reliably distinguish behavioral responses of mice to social touch from their responses to object touch; 2. Relative to typically developing control mice, both *Fmr1* KO and MIA mice show increased avoidance running to both voluntary and forced social touch, but not to voluntary object touch; 3. Hyperarousal (as measured by pupil dilation) to social touch lasts longer in *Fmr1* KO mice but not MIA mice compared to their controls; 4. AFEs to social touch are more pronounced in ASD mice than in controls, especially during forced social touch; 5. *Fmr1* KO mice show similar aversion to forced object touch as WT controls but significantly greater aversion to forced social touch; and 6. Social touch from same-sex mice elicits greater avoidance and AFEs in *Fmr1* KO ASD mice, but whether the other mouse is familiar or a stranger does not matter.

2.4.1: A novel behavioral assay to quantify social touch aversion

A few prior studies had investigated social touch in freely moving rodents [5,7,8]. Despite their ingenuity, the assays relied on at least one animal initiating social touch, and they could not focus on any particular aspect of social touch (e.g., face-to-face contact) amongst the broad and complex behavioral repertoire (e.g., ano-genital sniffing, allo-grooming). Moreover, while naturalistic in their design, those assays were limited by the fact that individual social touch interactions varied in duration and frequency. We purposely designed a new assay for head-fixed rodents so the experimenter could control all aspects of the social touch interaction, from the duration and number of interactions to the context of the interaction (voluntary vs. forced, object vs. social). This allowed us to monitor various aversive behavioral responses of the animal to social touch, including body movements that indicated avoidance, facial expressions suggestive of aversion, and dilated pupils reflecting hyperarousal/anxiety. Importantly, our assay could easily

be combined with 2-photon calcium imaging and/or silicon probes to record neural activity during social interactions. Because the social touch presentations are highly stereotyped across large numbers of trials, the data from neural recordings would be highly reproducible, and one could quantify the degree to which neurons adapt their responses to repeated presentations. Thus, our assay should be of help to neuroscientists interested in investigating social behaviors in rodents and the circuits involved.

To validate this assay, we probed social touch within two different mouse models of ASD in which social deficits are observed. A major gap in our understanding of ASD, particularly when using mouse models, concerns the relationship between tactile hypersensitivity and social deficits[15,21,64]. Therefore, we used our social touch assay to characterize three maladaptive behavioral responses to social touch in well-established mouse models of ASD: avoidance running, hyperarousal, and AFEs.

2.4.2: Avoidance behaviors to social touch in ASD

We previously reported avoidance and defensive gestures to repetitive whisker stimulation in *Fmr1 KO* mice[16,65]. However, avoidance to social touch was not simply a manifestation of generalized sensory hypersensitivity (tactile defensiveness) because it occurred in the context of social touch and not voluntary object touch (**Fig. 2-3c**). Similar sensory avoidance is also observed in humans with ASD and FXS[18,41,45]. Escape or avoidance has been described in mice responding to threatening stimuli, or those causing discomfort, anxiety or pain[66-69]. It will be important to determine whether other avoidance behaviors, such as defensive grooming or gaze avoidance, can also be detected using our social touch assay[70,71].

2.4.3: Differences in social touch behaviors across ASD models

The maladaptive behaviors to social touch were not the same in both ASD models. For example, orbital tightening to forced social touch were more prominent in *Fmr1* KO mice than in

the MIA model (**Fig. 2-6b,c**), and only the *Fmr1* KO model exhibited sustained pupil dilation, particularly for forced social touch (**Fig. 2-4b, c**). Pupil size is commonly used as an indicator of arousal levels and autistic/FXS individuals show deficits in autonomic regulation, including hyper- and hypo- arousal[39,50,51,72,73]. Interestingly, some autistic individuals who do not exhibit hyperarousal fail to show sensory hypersensitivity[74], suggesting that the two phenomena may be strongly correlated. However, aside from pupil size, hyperarousal can manifest with other autonomic responses, such as changes in heart rate, perspiration, or breathing[49,72], which could also be monitored during social interactions with our assay.

2.4.4: Aversive behaviors in ASD mice are more prominent during forced touch

The observation that ASD mice exhibit more pronounced AFEs during forced social touch aligns well with previous findings concerning facial grimacing in mice[55,56,58,59]. Since the Mouse Grimace Scale (MGS) has been widely adopted to quantify responses to pain, it could also be combined with our assay. Autistic people are often unable to recognize or imitate facial expressions of others, which complicates their interactions in social settings[75]. We did not monitor the facial expressions of the stranger/familiar mice, but the camera setup could be modified to track this too.

Given that forced social touch elicited more pronounced behavioral deficits than voluntary social touch in ASD mice, it was critical to compare responses of *Fmr1* KO mice to forced social touch and forced object touch. Although both a Falcon tube and an inanimate toy mouse (similar shape and texture as a mouse) resulted in similar levels of avoidance and AFEs between WT and *Fmr1* KO mice, we repeatedly found that forced social interactions were only deemed aversive by the latter. A previous study found that social interaction was more preferable to WT mice than object interaction[32]. Thus, while forced interactions with any object are aversive to WT and *Fmr1* KO mice, only WT animals find forced social interactions more tolerable. Viewed differently, *Fmr1* KO mice exhibit a general hypersensitivity to all tactile stimuli, but they fail to down-modulate this

aversion in the context of social interactions the way WT controls can. This unique deficit in the social context of *Fmr1* KO mice deserves further investigation.

2.4.5: Social touch aversion varies under different social contexts

In general, mice tend to prefer social interactions with mice of the opposite sex[4]. Opposite-sex social interactions have not been studied extensively in ASD models, although one study found that 16p11.2 deletion mice exhibit fewer vocalizations in the presence of mice of the opposite sex[76]. We observed that *Fmr1* KO mice show milder impairments (less avoidance and no AFEs) during opposite-sex interactions (**Fig. 2-8b**). This would suggest that, even though ASD mice show maladaptive responses to opposite sex interactions relative to WT animals, they prefer it to same-sex interactions.

Finally, we observed ASD mice display similar levels of avoidance and AFEs in response to forced social touch from a familiar mouse relative to a stranger mouse. This finding was not unusual given that both ASD individuals and mouse models display deficits in social memory[61-63].

2.4.6: Limitations and future directions

We did not find significant sex differences in our assay. This was surprising given that the prevalence of ASD and the range of phenotypic behaviors are different in males and females[37]. It is possible that sex differences were not apparent in our head-fixed social touch paradigm because our sample size was not large enough, or because mice could not freely choose to engage in social investigation. However, our assay could easily be modified to allow the test mouse to exert control of the motorized stage.

We recognize that our social touch assay has some limitations. Compared to assays for freely moving mice, our assay is less naturalistic. In spontaneous social interactions, mice are free to decide when to approach another animal. They may choose to approach other mice from the rear, as opposed to face-to-face. Our head-fixed assay also prevents the mice from engaging

in other socially relevant behaviors that involve touch, such as allo-grooming, or fighting. Head-fixation also prevents head movements that may be important for mice to engage in social touch.

In summary, our novel head-fixed paradigm revealed that ASD mouse models manifest a shared repertoire of maladaptive responses to social touch and that these behavioral manifestations align well with symptoms and atypical behaviors observed in autistic humans. The fact that two rather distinct ASD models exhibited very similar behavioral phenotypes in avoidance, arousal and facial expressions suggests that our assay may uncover remarkable phenotypic convergence in social touch deficits in other ASD models (despite differences in arousal). Future studies could also explore social touch in other contexts, such as mother-to-pup interactions, or age dependent differences. Finally, one could utilize this assay in combination with in vivo 2-photon calcium imaging or silicon probes to explore changes in neural activity in relevant brain circuits in mouse models of neurodevelopmental conditions.

2.5: References

1. Dunbar, R.I. (2010). The social role of touch in humans and primates: behavioural function and neurobiological mechanisms. Neurosci Biobehav Rev *34*, 260-268. 10.1016/j.neubiorev.2008.07.001.

2. Adolphs, R. (2009). The social brain: neural basis of social knowledge. Annu Rev Psychol *60*, 693-716. 10.1146/annurev.psych.60.110707.163514.

3. Bales, K.L., Witczak, L.R., Simmons, T.C., Savidge, L.E., Rothwell, E.S., Rogers, F.D., Manning, R.A., Heise, M.J., Englund, M., and Arias Del Razo, R. (2018). Social touch during development: Long-term effects on brain and behavior. Neurosci Biobehav Rev *95*, 202-219. 10.1016/j.neubiorev.2018.09.019.

4. Chen, P., and Hong, W. (2018). Neural Circuit Mechanisms of Social Behavior. Neuron *98*, 16-30. 10.1016/j.neuron.2018.02.026.

5. Jennings, J.H., Kim, C.K., Marshel, J.H., Raffiee, M., Ye, L., Quirin, S., Pak, S., Ramakrishnan, C., and Deisseroth, K. (2019). Interacting neural ensembles in orbitofrontal cortex for social and feeding behaviour. Nature *565*, 645-649. 10.1038/s41586-018-0866-8.

6. Lenschow, C., and Brecht, M. (2015). Barrel cortex membrane potential dynamics in social touch. Neuron *85*, 718-725. 10.1016/j.neuron.2014.12.059.

7. Bobrov, E., Wolfe, J., Rao, R.P., and Brecht, M. (2014). The representation of social facial touch in rat barrel cortex. Curr Biol *24*, 109-115. 10.1016/j.cub.2013.11.049.

8. Yu, H., Miao, W., Ji, E., Huang, S., Jin, S., Zhu, X., Liu, M.Z., Sun, Y.G., Xu, F., and Yu, X. (2022). Social touch-like tactile stimulation activates a tachykinin 1-oxytocin pathway to promote social interactions. Neuron *110*, 1051-1067.e1057. 10.1016/j.neuron.2021.12.022.

9. Mosher, C.P., Zimmerman, P.E., Fuglevand, A.J., and Gothard, K.M. (2016). Tactile Stimulation of the Face and the Production of Facial Expressions Activate Neurons in the Primate Amygdala. eNeuro *3*. 10.1523/eneuro.0182-16.2016.

10. Resendez, S.L., Namboodiri, V.M.K., Otis, J.M., Eckman, L.E.H., Rodriguez-Romaguera, J., Ung, R.L., Basiri, M.L., Kosyk, O., Rossi, M.A., Dichter, G.S., and Stuber, G.D. (2020). Social Stimuli Induce Activation of Oxytocin Neurons Within the Paraventricular Nucleus of the Hypothalamus to Promote Social Behavior in Male Mice. J Neurosci *40*, 2282-2295. 10.1523/jneurosci.1515-18.2020.

11. Jeon, Y.S., Jeong, D., Kweon, H., Kim, J.H., Kim, C.Y., Oh, Y., Lee, Y.H., Kim, C.H., Kim, S.G., Jeong, J.W., et al. (2023). Adolescent Parvalbumin Expression in the Left Orbitofrontal Cortex Shapes Sociability in Female Mice. J Neurosci *43*, 1555-1571. 10.1523/jneurosci.0918-22.2023.

12. Willmore, L., Minerva, A.R., Engelhard, B., Murugan, M., McMannon, B., Oak, N., Thiberge, S.Y., Peña, C.J., and Witten, I.B. (2023). Overlapping representations of food and social stimuli in mouse VTA dopamine neurons. Neuron *111*, 3541-3553.e3548. 10.1016/j.neuron.2023.08.003.

13. Ebbesen, C.L., and Froemke, R.C. (2022). Automatic mapping of multiplexed social receptive fields by deep learning and GPU-accelerated 3D videography. Nat Commun *13*, 593. 10.1038/s41467-022-28153-7.

14. Bufo, M.R., Guidotti, M., Mofid, Y., Malvy, J., Bonnet-Brilhault, F., Aguillon-Hernandez, N., and Wardak, C. (2022). Atypical Response to Affective Touch in Children with Autism: Multi-Parametric Exploration of the Autonomic System. J Clin Med *11*. 10.3390/jcm11237146.

15. Lee Masson, H., Pillet, I., Amelynck, S., Van De Plas, S., Hendriks, M., Op de Beeck, H., and Boets, B. (2019). Intact neural representations of affective meaning of touch but lack of embodied resonance in autism: a multi-voxel pattern analysis study. Mol Autism *10*, 39. 10.1186/s13229-019-0294-0.

16. He, C.X., Cantu, D.A., Mantri, S.S., Zeiger, W.A., Goel, A., and Portera-Cailliau, C. (2017). Tactile Defensiveness and Impaired Adaptation of Neuronal Activity in the Fmr1 Knock-Out Mouse Model of Autism. J Neurosci *37*, 6475-6487. 10.1523/JNEUROSCI.0651-17.2017.

17. Cascio, C., McGlone, F., Folger, S., Tannan, V., Baranek, G., Pelphrey, K.A., and Essick, G. (2008). Tactile perception in adults with autism: a multidimensional psychophysical study. J Autism Dev Disord *38*, 127-137. 10.1007/s10803-007-0370-8.

18. Green, S.A., and Ben-Sasson, A. (2010). Anxiety disorders and sensory over-responsivity in children with autism spectrum disorders: is there a causal relationship? J Autism Dev Disord *40*, 1495-1504. 10.1007/s10803-010-1007-x.

19. Green, S.A., Hernandez, L., Tottenham, N., Krasileva, K., Bookheimer, S.Y., and Dapretto, M. (2015). Neurobiology of Sensory Overresponsivity in Youth With Autism Spectrum Disorders. JAMA Psychiatry *72*, 778-786. 10.1001/jamapsychiatry.2015.0737.

20. Green, S.A., Hernandez, L.M., Bowman, H.C., Bookheimer, S.Y., and Dapretto, M. (2018). Sensory over-responsivity and social cognition in ASD: Effects of aversive sensory stimuli and attentional modulation on neural responses to social cues. Dev Cogn Neurosci *29*, 127-139. 10.1016/j.dcn.2017.02.005.

21. Thye, M.D., Bednarz, H.M., Herringshaw, A.J., Sartin, E.B., and Kana, R.K. (2018). The impact of atypical sensory processing on social impairments in autism spectrum disorder. Dev Cogn Neurosci *29*, 151-167. 10.1016/j.dcn.2017.04.010.

22. Foss-Feig, J.H., Heacock, J.L., and Cascio, C.J. (2012). Tactile Responsiveness Patterns and Their Association with Core Features in Autism Spectrum Disorders. Res Autism Spectr Disord *6*, 337-344. 10.1016/j.rasd.2011.06.007.

23. Orefice, L.L., Zimmerman, A.L., Chirila, A.M., Sleboda, S.J., Head, J.P., and Ginty, D.D. (2016). Peripheral Mechanosensory Neuron Dysfunction Underlies Tactile and Behavioral Deficits in Mouse Models of ASDs. Cell *166*, 299-313. 10.1016/j.cell.2016.05.033.

24. Orefice, L.L., Mosko, J.R., Morency, D.T., Wells, M.F., Tasnim, A., Mozeika, S.M., Ye, M., Chirila, A.M., Emanuel, A.J., Rankin, G., et al. (2019). Targeting Peripheral Somatosensory Neurons to Improve Tactile-Related Phenotypes in ASD Models. Cell *178*, 867-886.e824. 10.1016/j.cell.2019.07.024.

25. Choi, G.B., Yim, Y.S., Wong, H., Kim, S., Kim, H., Kim, S.V., Hoeffer, C.A., Littman, D.R., and Huh, J.R. (2016). The maternal interleukin-17a pathway in mice promotes autism-like phenotypes in offspring. Science *351*, 933-939. 10.1126/science.aad0314.

26. Reed, M.D., Yim, Y.S., Wimmer, R.D., Kim, H., Ryu, C., Welch, G.M., Andina, M., King, H.O., Waisman, A., Halassa, M.M., et al. (2020). IL-17a promotes sociability in mouse models of neurodevelopmental disorders. Nature *577*, 249-253. 10.1038/s41586-019-1843-6.

27. Kentner, A.C., Bilbo, S.D., Brown, A.S., Hsiao, E.Y., McAllister, A.K., Meyer, U., Pearce, B.D., Pletnikov, M.V., Yolken, R.H., and Bauman, M.D. (2019). Maternal immune activation: reporting guidelines to improve the rigor, reproducibility, and transparency of the model. Neuropsychopharmacology *44*, 245-258. 10.1038/s41386-018-0185-7.

28. Dutch-Belgian Fragile X Consortium, T., Bakker, C.E., Verheij, C., Willemsen, R., van der Helm, R., Oerlemans, F., Vermey, M., Bygrave, A., Hoogeveen, A., Oostra, B.A., et al. (1994). Fmr1 knockout mice: A model to study fragile X mental retardation. Cell *78*, 23-33. https://doi.org/10.1016/0092-8674(94)90569-X.

29. Estes, M.L., and McAllister, A.K. (2016). Maternal immune activation: Implications for neuropsychiatric disorders. Science *353*, 772-777. 10.1126/science.aag3194.

30. Garay, P.A., Hsiao, E.Y., Patterson, P.H., and McAllister, A.K. (2013). Maternal immune activation causes age- and region-specific changes in brain cytokines in offspring throughout development. Brain Behav Immun *31*, 54-68. 10.1016/j.bbi.2012.07.008.

31. Shin Yim, Y., Park, A., Berrios, J., Lafourcade, M., Pascual, L.M., Soares, N., Yeon Kim, J., Kim, S., Kim, H., Waisman, A., et al. (2017). Reversing behavioural abnormalities in mice exposed to maternal inflammation. Nature *549*, 482-487. 10.1038/nature23909.

32. Yang, M., Silverman, J.L., and Crawley, J.N. (2011). Automated three-chambered social approach task for mice. Curr Protoc Neurosci *Chapter 8*, Unit 8.26. 10.1002/0471142301.ns0826s56.

33. Deacon, R.M. (2006). Digging and marble burying in mice: simple methods for in vivo identification of biological impacts. Nat Protoc *1*, 122-124. 10.1038/nprot.2006.20.

34. Stringer, C., Pachitariu, M., Steinmetz, N., Reddy, C.B., Carandini, M., and Harris, K.D. (2019). Spontaneous behaviors drive multidimensional, brainwide activity. Science *364*, 255. 10.1126/science.aav7893.

35. Nath, T., Mathis, A., Chen, A.C., Patel, A., Bethge, M., and Mathis, M.W. (2019). Using DeepLabCut for 3D markerless pose estimation across species and behaviors. Nat Protoc *14*, 2152-2176. 10.1038/s41596-019-0176-0.

36. Mathis, A., Mamidanna, P., Cury, K.M., Abe, T., Murthy, V.N., Mathis, M.W., and Bethge, M. (2018). DeepLabCut: markerless pose estimation of user-defined body parts with deep learning. Nat Neurosci *21*, 1281-1289. 10.1038/s41593-018-0209-y.

37. Werling, D.M., and Geschwind, D.H. (2013). Sex differences in autism spectrum disorders. Curr Opin Neurol *26*, 146-153. 10.1097/WCO.0b013e32835ee548.

38. Bartholomay, K.L., Lee, C.H., Bruno, J.L., Lightbody, A.A., and Reiss, A.L. (2019). Closing the Gender Gap in Fragile X Syndrome: Review on Females with FXS and Preliminary Research Findings. Brain Sci *9*. 10.3390/brainsci9010011.

39. Klusek, J., Martin, G.E., and Losh, M. (2013). Physiological arousal in autism and fragile X syndrome: group comparisons and links with pragmatic language. Am J Intellect Dev Disabil *118*, 475-495. 10.1352/1944.7558-118.6.475.

40. Zampella, C.J., Bennetto, L., and Herrington, J.D. (2020). Computer Vision Analysis of Reduced Interpersonal Affect Coordination in Youth With Autism Spectrum Disorder. Autism Res *13*, 2133-2142. 10.1002/aur.2334.

41. Mammen, M.A., Moore, G.A., Scaramella, L.V., Reiss, D., Ganiban, J.M., Shaw, D.S., Leve, L.D., and Neiderhiser, J.M. (2015). INFANT AVOIDANCE DURING A TACTILE TASK PREDICTS AUTISM SPECTRUM BEHAVIORS IN TODDLERHOOD. Infant Ment Health J *36*, 575-587. 10.1002/imhj.21539.

42. Robertson, C.E., and Baron-Cohen, S. (2017). Sensory perception in autism. Nat Rev Neurosci *18*, 671-684. 10.1038/nrn.2017.112.

43. Baranek, G.T., Foster, L.G., and Berkson, G. (1997). Tactile defensiveness and stereotyped behaviors. Am J Occup Ther *51*, 91-95. 10.5014/ajot.51.2.91.

44. Sinclair, D., Oranje, B., Razak, K.A., Siegel, S.J., and Schmid, S. (2017). Sensory processing in autism spectrum disorders and Fragile X syndrome-From the clinic to animal models. Neurosci Biobehav Rev *76*, 235-253. 10.1016/j.neubiorev.2016.05.029.

45. Rais, M., Binder, D.K., Razak, K.A., and Ethell, I.M. (2018). Sensory Processing Phenotypes in Fragile X Syndrome. ASN Neuro *10*, 1759091418801092. 10.1177/1759091418801092.

46. Goel, A., Cantu, D.A., Guilfoyle, J., Chaudhari, G.R., Newadkar, A., Todisco, B., de Alba, D., Kourdougli, N., Schmitt, L.M., Pedapati, E., et al. (2018). Impaired perceptual learning in a mouse model of Fragile X syndrome is mediated by parvalbumin neuron dysfunction and is reversible. Nat Neurosci *21*, 1404-1411. 10.1038/s41593-018-0231-0.

47. Fukuyama, H., Kumagaya, S.I., Asada, K., Ayaya, S., and Kato, M. (2017). Autonomic versus perceptual accounts for tactile hypersensitivity in autism spectrum disorder. Sci Rep *7*, 8259. 10.1038/s41598-017-08730-3.

48. McGlone, F., Wessberg, J., and Olausson, H. (2014). Discriminative and affective touch: sensing and feeling. Neuron *82*, 737-755. 10.1016/j.neuron.2014.05.001.

49. Heilman, K.J., Harden, E.R., Zageris, D.M., Berry-Kravis, E., and Porges, S.W. (2011). Autonomic regulation in fragile X syndrome. Dev Psychobiol *53*, 785-795. 10.1002/dev.20551.

50. Vinck, M., Batista-Brito, R., Knoblich, U., and Cardin, J.A. (2015). Arousal and locomotion make distinct contributions to cortical activity patterns and visual encoding. Neuron *86*, 740-754. 10.1016/j.neuron.2015.03.028.

51. Joshi, S., and Gold, J.I. (2020). Pupil Size as a Window on Neural Substrates of Cognition. Trends Cogn Sci *24*, 466-480. 10.1016/j.tics.2020.03.005.

52. Anderson, D.J., and Adolphs, R. (2014). A framework for studying emotions across species. Cell *157*, 187-200. 10.1016/j.cell.2014.03.003.

53. Kliemann, D., Dziobek, I., Hatri, A., Steimke, R., and Heekeren, H.R. (2010). Atypical reflexive gaze patterns on emotional faces in autism spectrum disorders. J Neurosci *30*, 12281-12287. 10.1523/jneurosci.0688-10.2010.

54. Schmitt, L.M., Cook, E.H., Sweeney, J.A., and Mosconi, M.W. (2014). Saccadic eye movement abnormalities in autism spectrum disorder indicate dysfunctions in cerebellum and brainstem. Mol Autism *5*, 47. 10.1186/2040-2392-5-47.

55. Langford, D.J., Bailey, A.L., Chanda, M.L., Clarke, S.E., Drummond, T.E., Echols, S., Glick, S., Ingrao, J., Klassen-Ross, T., Lacroix-Fralish, M.L., et al. (2010). Coding of facial expressions of pain in the laboratory mouse. Nat Methods *7*, 447-449. 10.1038/nmeth.1455.

56. Dolensek, N., Gehrlach, D.A., Klein, A.S., and Gogolla, N. (2020). Facial expressions of emotion states and their neuronal correlates in mice. Science *368*, 89-94. 10.1126/science.aaz9468.

57. Wolfe, J., Mende, C., and Brecht, M. (2011). Social facial touch in rats. Behav Neurosci *125*, 900-910. 10.1037/a0026165.

58. Ebbesen, C.L., and Froemke, R.C. (2021). Body language signals for rodent social communication. Curr Opin Neurobiol *68*, 91-106. 10.1016/j.conb.2021.01.008.

59. Defensor, E.B., Corley, M.J., Blanchard, R.J., and Blanchard, D.C. (2012). Facial expressions of mice in aggressive and fearful contexts. Physiol Behav *107*, 680-685. 10.1016/j.physbeh.2012.03.024.

60. Bush, N.E., Solla, S.A., and Hartmann, M.J. (2016). Whisking mechanics and active sensing. Curr Opin Neurobiol *40*, 178-188. 10.1016/j.conb.2016.08.001.

61. Williams, D.L., Goldstein, G., and Minshew, N.J. (2005). Impaired memory for faces and social scenes in autism: clinical implications of memory dysfunction. Arch Clin Neuropsychol *20*, 1-15. 10.1016/j.acn.2002.08.001.

62. Stantić, M., Ichijo, E., Catmur, C., and Bird, G. (2022). Face memory and face perception in autism. Autism *26*, 276-280. 10.1177/13623613211027685.

63. Cope, E.C., Wang, S.H., Waters, R.C., Gore, I.R., Vasquez, B., Laham, B.J., and Gould, E. (2023). Activation of the CA2-ventral CA1 pathway reverses social discrimination dysfunction in Shank3B knockout mice. Nat Commun *14*, 1750. 10.1038/s41467-023-37248-8.

64. Suvilehto, J.T., Glerean, E., Dunbar, R.I., Hari, R., and Nummenmaa, L. (2015). Topography of social touching depends on emotional bonds between humans. Proc Natl Acad Sci U S A *112*, 13811-13816. 10.1073/pnas.1519231112.

65. Kourdougli, N., Suresh, A., Liu, B., Juarez, P., Lin, A., Chung, D.T., Graven Sams, A., Gandal, M.J., Martinez-Cerdeno, V., Buonomano, D.V., et al. (2023). Improvement of sensory deficits in fragile X mice by increasing cortical interneuron activity after the critical period. Neuron. 10.1016/j.neuron.2023.06.009.

66. Yilmaz, M., and Meister, M. (2013). Rapid innate defensive responses of mice to looming visual stimuli. Curr Biol *23*, 2011-2015. 10.1016/j.cub.2013.08.015.

67. La-Vu, M., Tobias, B.C., Schuette, P.J., and Adhikari, A. (2020). To Approach or Avoid: An Introductory Overview of the Study of Anxiety Using Rodent Assays. Front Behav Neurosci *14*, 145. 10.3389/fnbeh.2020.00145.

68. Huang, T., Lin, S.H., Malewicz, N.M., Zhang, Y., Goulding, M., LaMotte, R.H., and Ma, Q. (2019). Identifying the pathways required for coping behaviours associated with sustained pain. Nature *565*, 86-90. 10.1038/s41586-018-0793-8.

69. Gehrlach, D.A., Dolensek, N., Klein, A.S., Roy Chowdhury, R., Matthys, A., Junghänel, M., Gaitanos, T.N., Podgornik, A., Black, T.D., Reddy Vaka, N., et al. (2019). Aversive state processing in the posterior insular cortex. Nat Neurosci *22*, 1424-1437. 10.1038/s41593-019-0469-1.

70. Stuart, N., Whitehouse, A., Palermo, R., Bothe, E., and Badcock, N. (2022). Eye Gaze in Autism Spectrum Disorder: A Review of Neural Evidence for the Eye Avoidance Hypothesis. J Autism Dev Disord. 10.1007/s10803-022-05443-z.

71. Kleberg, J.L., Högström, J., Nord, M., Bölte, S., Serlachius, E., and Falck-Ytter, T. (2017). Autistic Traits and Symptoms of Social Anxiety are Differentially Related to Attention to Others' Eyes in Social Anxiety Disorder. J Autism Dev Disord *47*, 3814-3821. 10.1007/s10803-016-2978-z.

72. Kushki, A., Brian, J., Dupuis, A., and Anagnostou, E. (2014). Functional autonomic nervous system profile in children with autism spectrum disorder. Mol Autism *5*, 39. 10.1186/2040-2392-5-39.

73. Cuve, H.C., Gao, Y., and Fuse, A. (2018). Is it avoidance or hypoarousal? A systematic review of emotion recognition, eye-tracking, and psychophysiological studies in young adults with autism spectrum conditions. Research in Autism Spectrum Disorders *55*, 1-13. https://doi.org/10.1016/j.rasd.2018.07.002.

74. Rogers, S.J., and Ozonoff, S. (2005). Annotation: what do we know about sensory dysfunction in autism? A critical review of the empirical evidence. J Child Psychol Psychiatry *46*, 1255-1268. 10.1111/j.1469-7610.2005.01431.x.

75. Drimalla, H., Baskow, I., Behnia, B., Roepke, S., and Dziobek, I. (2021). Imitation and recognition of facial emotions in autism: a computer vision approach. Mol Autism *12*, 27. 10.1186/s13229-021-00430-0.

76. Yang, M., Mahrt, E.J., Lewis, F., Foley, G., Portmann, T., Dolmetsch, R.E., Portfors, C.V., and Crawley, J.N. (2015). 16p11.2 Deletion Syndrome Mice Display Sensory and Ultrasonic Vocalization Deficits During Social Interactions. Autism Res *8*, 507-521. 10.1002/aur.1465.

CHAPTER 3: Encoding of Social Facial Touch in Cortical, Striatal and Amygdalar Circuits

3.1 Introduction

The sense of touch is a crucial sensory aspect of social communication and interaction, as manifested in humans by hugging, kissing, caressing, and even tickling. Through touch, animals within the same species offer comfort to one another, provide inference about their respective internal states, and build or modify new/existing social relationships[1-5]. It stands to reason that brain circuits would have evolved to tolerate and even seek social touch, over non-social tactile stimuli. On the other hand, social touch may be perceived as aversive when it is unwanted[6,7], and autistic individuals often demonstrate aversion to social touch, which can lead them to avoid social interactions[4,8-11].

The circuits involved in social touch are beginning to be elucidated[12-16]. As early as the somatosensory cortex and spinal cord within the tactile sensory pathway of humans and rodents, studies have shown that neural activity is driven by social touch and is also perceived differently from non-social touch[13,17-19]. Vibrissal somatosensory cortical (vS1) cells in rodents are also capable of distinguishing partner from stranger and sex[20]. Furthermore, brain regions within the amygdalar, mesolimbic and hypothalamic pathways have been strongly implicated in the encoding of social pleasurable touch[14-16].

While all these studies have transformed our understanding of how social touch is encoded in the brain, it is still unknown how social touch, typically perceived as pleasurable, can become aversive. The emotional valence of social touch may depend on the context of social touch in which an animal or person is given the flexibility to engage in social touch versus is forced to engage in social interaction.

In this chapter, we focused on the encoding of social touch in the brain of wild type (WT) animals. Since WTs displayed strong differences in aversion to social versus non-social touch in the head-fixed assay described in chapter 2, they provide a reference point to assess typical social touch encoding across different brain regions[10]. We chose to first address which brain regions are distinctly activated by social versus object touch using Targeted Recombination in

Active Populations (TRAP)[21]. We then chose to explore the neuronal responses to voluntary and forced social and object touch in three different brain regions relevant to distinct properties of the social stimulus and that we could record from simultaneously using Neuropixels silicon probes for in vivo electrophysiology[22]. The first brain region, vS1, would allow us to address the sensory properties of social touch and is important for encoding whisker-mediated touch[23]. Furthermore, it has previously been reported that vS1 encodes social touch in rats[13,19,20]. vS1 has also been implicated in tactile hypersensitivity and reduced adaptation to passive tactile stimuli in a mouse model of ASD[24]. The second brain region we chose to target was the basolateral amygdala (BLA) since this region is important for emotional processing, has been directly associated with the encoding of aversive and social stimuli and its activity is also dependent on the animal's behavioral state[25-30]. Finally, we chose to record from tail of the striatum (tS) since targeting vS1 and BLA simultaneously would allow us to also record from tS. The tS has been strongly implicated in the integration of salient sensory input with motor output[31,32]. Interestingly, the tS has also been associated in aversion to novelty in ASD mice[33].

We show that vS1, tS and BLA neurons show distinct temporal responses over the course of social versus object touch. vS1 is modulated more by social touch than object, whereas the differences in modulation by social versus object touch in tS and BLA depends on if the interaction if voluntary or forced. Furthermore, vS1, tS and BLA cells contain a subset of cells that prefer social over object touch and vice-versa, but the BLA neuronal population favors object over social touch. Lastly, we show that discrimination between social and object touch also occurs at the behavioral level and is dependent on whisker movements.

3.2 Materials & Methods

3.2.1: Animal details

Adult male and female C5BL/6 mice at postnatal day 60-90 were used for all experiments. A cohort of adult mice (9 males and 8 females) was used for TRAP labeling of neurons activated

by social/object touch. These so-called 'TRAP2' mice were obtained by crossing $Fos^{2A\text{-}iCreER/+}$ (TRAP2) (JAX line 021882) with $R26^{Ai14/+}$ (Ai14) (JAX line 030323).

A second cohort of WT mice (>20 g in weight, 6 males and 3 females) was used for electrophysiological recordings and were derived from the following line: wild type (WT) B6J (JAX line 000664).

All mice were group-housed with access to food and water (HydroGel, ClearH_2O) *ad libitum* under a 12:12 hour light-dark cycle in controlled temperature conditions. All experiments were done in the light cycle. Mice with Neuropixels implants were single housed during habituation and behavioral testing (~1-2 weeks) to avoid damage to the implant that could have occurred by other animals in group housing. We followed the U.S. National Institutes of Health guidelines for animal research under an animal use protocol (ARC #2007-035) approved by the Chancellor's Animal Research Committee and Office for Animal Research Oversight at the University of California, Los Angeles.

3.2.2: TRAP2 mice drug preparation

4-hydroxytamoxifen (4-OHT, Sigma-Aldrich #H6278) was dissolved in 20 mg/mL in 70% EtOH and was aliquoted and stored at -20°C for up to 4 weeks. On the day before behavioral testing, 4-OHT was redissolved in 70% EtOH by warming the aliquot at 37°C and vortexing vigorously for 1 min, 2-3 times. Corn oil (Sigma Aldrich, C8267) was added to each aliquot for a final concentration of 10 mg/mL of 4-OHT. The aliquots were vacuum centrifuged for 30 min until all EtOH had evaporated. 4-OHT was then stored at 4°C for next-day use.

3.2.3: Behavioral social/object touch experiments for TRAP labeling

To identify brain regions involved in social touch, we used the social touch behavioral assay described in chapter 2[10]. Adult TRAP2 mice (and the corresponding visitor mice in the social touch assay) were first surgically implanted with a titanium head bar. Briefly, mice were

anesthetized with isoflurane (5% induction, 1.5-2% maintenance via nose cone v/v) and secured on a motorized stereotaxic frame (Kopf; StereoDrive, Neurostar) via metal ear bars. The head of the animal was shaved with an electric razor and the skin overlying the skull was then sterilized with three alternating swabs of 70% EtOH and betadine. A 1 cm long midline scalp incision was made with a scalpel and the custom U-shaped head bar (3.15 mm wide x 10 mm long) was secured on the back of the skull first with Krazy Glue and then with a thin layer of C&B Metabond (Parkell) applied to the dry skull surface. The entire skull was then covered with acrylic dental cement (Lang Dental). This surgery lasted ~15-20 min and mice fully recovered within 30 min, after which they were returned to group-housed cages.

At least 48 h after head bar implantation, TRAP2 mice were habituated to head restraint, to running on an air-suspended 200 mm polystyrene ball, and to the movement of a motorized stage that was used for repeated presentations of an inanimate object or a stranger mouse. The stage consisted of an aluminum bread board (15 x 7.6 x 1 cm) attached to a translational motor (Zaber Technologies, X-LSM100A), the movement of which was fully controlled through MATLAB (Mathworks). All of this occurred in a custom-built, sound-attenuated behavioral rig (93 x 93 x 57 cm) that was dimly illuminated by two infrared lights (Bosch, 850 nm). For habituation of TRAP2 mice, test mice were placed on the ball for 20 min each day for 14 consecutive days before testing. In parallel, 'visitor' mice (stranger to the test mouse) were habituated to head-restraint in a plexiglass tube (diameter: 4 cm) on the motorized stage. The stage is always translated at a constant speed of 1.65 cm/s when moving during habituation and behavioral testing.

Following habituation, all TRAP2 test mice were single-housed the day before the social touch assay[10]. On the day of behavioral testing and 30 min prior to testing, TRAP2 mice were injected with 4-OHT (50 mg/kg, i.p.). TRAP2 test mice were tested under three different conditions: 1. no touch, in which the platform moved back and forth in repeated bouts but was empty (n=5 mice); 2. object touch, in which test mice experienced repeated bouts of forced interactions with a plastic 50 mL Falcon conical tube (n=6 mice); and 3. social touch, in which test

mice experienced repeated bouts of forced interactions with a visitor novel mouse (stranger to the test mouse) (n=6 mice). For the forced object/social interactions, the stage stopped at a position that brought the tip of the plastic tube or the snout of the visitor mouse in direct contact with the snout of the test mouse. These positions were calibrated before each experiment. For the condition where the platform was empty, the stage was moved to a set template position that was tested during calibration for forced interactions. Each bout lasted 5 s, with a 5 s interstimulus interval (ISI) during which the platform moved away by 1 cm and the object/mouse was out of reach of the test mouse's whiskers. The ISI included a 1.2 s period of back-and-forth travel time for the platform. Each session (no touch, social touch, object touch) lasted 30 min, which was equivalent to a total of 180 such presentations.

Following the assay, TRAP2 test mice were returned to their single cage housing until the end of the day (~6-8 h), at which point they were placed back in group housing, and then they were perfused at 72 h. For each session of tamoxifen preparation/injections and behavioral testing, at least 3 mice were used (at least one mouse each for no touch, object touch and social touch condition).

3.2.4: Histology and quantification of cFos expression in TRAP2 mice

72 h after 4-OHT induction (to allow *Cre* recombination to occur), TRAP2 mice were transcardially perfused with 4% PFA in cold PBS (0.1M) and their brains were harvested and left overnight in 4% PFA. Next, fixed brains were sliced coronally to obtain 60 μm sections. The coronal sections were mounted on VectaShield glass slides and stained with DAPI (Vector Laboratories). Sections were imaged on an Apotome2 microscope (Zeiss; 10x objective). Images were taken as a z-stack ranging from 30-50 μm (Zen2 software, Zeiss). ImageJ was used to quantify the density of cells expressing tdTomato (tdTom) in each brain region (cFos-tdTom$^+$cells/mm^2). Cell densities in each brain region from 'object touch' mice (TRAP2-OBJECT)

and ‘social touch’ mice (TRAP2-SOCIAL) were normalized to average cell density in each brain region from ‘no touch’ mice (TRAP2-CTRL) in the same session of behavioral testing to account for variability in tamoxifen preparation from one session to the next.

3.2.5: Surgical implantation of Neuropixels probes for chronic recordings

Each Neuropixels 1.0 probe (Imec, PRB_1_4_0480_1_C) was first connected to the acquisition hardware to confirm that the probe was functional using the SpikeGLX data acquisition software (see below) both prior to and after soldering a grounding wire (0.01 in, A.M. Systems) to the probe flex cable. The probe was inserted and screwed into a dovetail probe holder (Imec, HOLDER_1000_C) and set aside for surgical implantation. A custom-made external chassis cover (eventually used to protect the probe during implantation) was 3D-printed (Hubs) using standard black resin (Formlabs, RS-F2-GPBK-04). The CAD files for the 3D printed cover were acquired at https://github.com/Brody-Lab/chronic_neuropixels[34].

Adult mice were anaesthetized with isoflurane and placed on a motorized stereotaxic frame. Their head was shaved and the scalp sterilized as above. A 1 cm long midline scalp incision was made with a scalpel and a small craniotomy (0.5 mm diameter) was drilled over the cerebellum (1 mm posterior to Lambda) with a dental drill (Midwest Tradition) through which a ground screw (McMaster Carr) was loosely screwed. A second craniotomy (0.5 mm diameter) was drilled at the probe implantation site at coordinates -1.46 AP, 2.9 ML 3.75 DV (in mm). This allowed for targeting of vS1, tS and BLA simultaneously with a single Neuropixels probe. Saline soaked Surgifoam (Ethicon) was placed on both craniotomies while a thin layer of C&B Metabond (Parkell) was applied to the dry skull surface. A small well (0.75 cm diameter, 1 cm height) was built around the craniotomy site with self-adhesive resin cement (RelyX Unicem 2 Automix, 3M ESPE) and set with dental curing lamp (Sino Dental). Surgifoam was removed from the implantation craniotomy and saline was applied to maintain tissue hydration.

Before insertion, the probe holder (with the probe attached) was screwed and secured to a StereoDrive (Neurostar) instrument. The probe shank tip was dipped for 30 s in DiI (1-2 mg/mL in isopropyl alcohol, Sigma Aldrich, applied onto Parafilm, Bemis) by moving the holder with StereoDrive. DiI fluorescence enabled subsequent histological reconstruction of the probe tract in fixed tissue sections. The ground wire soldered to the probe was then wrapped around the ground screw, after which the ground screw was tightly screwed into the ground craniotomy. Conductive epoxy (8331, MG Chemical) was applied on the ground screw and wire. A titanium U-shaped head bar (3.15 x 10 mm) was affixed to the skull with Metabond caudal to the ground screw, to allow for head-restraint during recordings and behavioral testing. Next, the probe shank was lowered at a rate of 10 μm/s with StereoDrive through the implantation craniotomy. Saline in the cement well was then absorbed carefully with Surgifoam and replaced with Dura-Gel (Cambridge Neurotech). Additional resin cement was applied and cured to the cement well and onto the probe base (avoiding contact with the shank). An additional layer of Metabond was applied on the skull, including on the ground craniotomy site and along the outside of the resin cement well. The two parts of external case were then placed around the probe and cemented together and to the resin cement wall with acrylic (Lang Dental). This surgery lasts 3-4 h and hydration was provided by injecting saline every hour (0.1 mL, i.p.). Mice fully recovered within 1-2 h after surgery. Afterwards, implanted animals were single housed for habituation and behavioral testing. Mice were injected with carprofen (1mg/ml, i.p., Rimadyl) immediately after surgery and again at 24 h and 48 h post-op and given ad lib access to HydroGel (ClearH_2O) and food.

3.2.6: Social touch assay in mice with chronic Neuropixels implants

Following probe implantation, test mice were subjected to the social touch assay described above, but in addition to forced object/social touch we introduced additional interactions (see below). First, mice bearing Neuropixels implants were habituated to head restraint, to running

on the polystyrene ball, and to the behavioral apparatus (just as for the TRAP experiments above, but for only 7-9 d).

Following habituation, test mice were subjected to both voluntary and forced interactions with a visitor mouse or a novel inanimate object over the course of 2 d. On day 1, test mice were placed on the ball and recorded for a 2 min baseline period (the plexiglass tube on the moving stage was empty). Next, we inserted the plastic object (50 mL Falcon conical tube) into the plexiglass tube on the motorized stage. For this control interaction, the test mouse first experienced a 2 min period of no touch but was able to visualize the object in the neutral position (before touch, 6 cm away). Next, the motorized stage moved the object to within whisker reach of the test mouse for a total of 40 such presentations of either voluntary (whisker-to-object) or forced (snout-to-object) object touch. Each bout lasted 5 s, with a 5 s ISI during which the platform moved away by 1 cm and the object was out of reach of the test mouse. The ISI included the total travel time of the platform (1.2 s).

After this object touch session, the test mouse was returned to its cage to rest for at least 1 h before being head-restrained again to undergo either voluntary or forced social touch session (same type of touch as previous session for object touch) with a visitor mouse. A same-sex, same age (P60-90) novel WT mouse was head-restrained inside the plexiglass tube on the motorized stage. Following a 2 min period in the neutral position where the test mouse could see but not touch the stranger mouse, the motorized stage moved to the position for voluntary social touch (whisker-to-whisker) or forced social touch (snout-to-snout) for 40 bouts (also lasting 5 s with a 5 s ISI where the mouse on the platform moved out of reach of the test mouse). The test mouse was then returned to its cage for at least 24 h.

On day #2 of behavior testing, the mouse was placed back on the ball again for a 2 min baseline period followed by a 2 min period of no touch. Depending on what interaction the test mouse had received (voluntary or forced object and social touch) on testing day #1, the mouse

received 40 presentations of the alternate touch type with a novel object (50 ml Falcon tube with different color and conical shape) and another stranger mouse.

3.2.7: Social touch behavioral assay controls

We tested a subset of the Neuropixels-implanted mice (8 WT) on subsequent days to 40 presentations of forced touch from a novel inanimate furry/plush toy mouse (PennPlax) onto which we glued Nylon whiskers (1.5 cm length, 0.5 mm thickness) and a stranger mouse of the same sex injected with chlorprothixene (1 mg/ml, i.p.) 15 min prior to behavioral testing and lightly anaesthetized with isoflurane 30 s prior to testing. The test animal received forced inanimate toy touch followed by forced social touch with an anaesthetized mouse on the next 2 days (days 3 & 4).

3.2.8: Electrophysiological recordings

During the social touch behavioral assay, electrophysiological recordings were performed using Neuropixels 1.0 acquisition hardware (Imec). The acquisition hardware was used in combination with PCI eXtensions for Instrumentation (PXI) hardware (PXIe-1071 chassis, PXIe-8381 remote control module and PXIe-6341 I/O module for recording analog and digital inputs, National Instruments). SpikeGLX software was used to acquire data (https://github.com/billkarsh/SpikeGLX, HHMI/Janelia Research Campus). Recording channels acquired electrical signals from the most dorsal region of vS1 down to the most ventral region of the BLA using the deepest 964 electrode sites. Action potential spikes were sorted with Kilosort2.5 (https://github.com/MouseLand/Kilosort) using default parameters and then manually curated with Phy2 (https://github.com/cortex-lab/phy)[35,36]. Only single units were used for electrophysiological data analysis. Post-processing with the following quality metrics was used to isolate single units: ISI violation <10%, amplitude cutoff and median amplitude >50 μV, as previously described[37].

3.2.9: Removal of Neuropixels probes

Neuropixels probes were explanted for subsequent re-use. Mice implanted with Neuropixels were anesthetized with isoflurane and secured on a stereotaxic frame. The external case holder was removed with a dental drill, and any excess acrylic or resin cement around the probe dovetail was gently drilled off while avoiding direct contact with the probe. The dovetail holder was inserted and screwed into the probe and attached to the stereotaxic arm. Resin cement was carefully drilled around the circumference of the resin cement well to separate the skull from the probe. Once the skull and probe were separated, the probe was lifted using Stereodrive until the probe was completely outside the resin cement well. The probe was removed from the dovetail holder and forceps were used to gently remove any excess resin from the probe. After explantation, the probe shank was fully immersed in 1% tergazyme (Alconox) for 24-48 h, followed by a 1-2 h rinse in distilled water.

3.2.10: Histology and fluorescence imaging of probe location

Following probe removal, mice were anaesthetized with 5% isoflurane and transcardially perfused with 4% PFA and post-fixed overnight. The fixed brain was then rinsed with PBS and sliced coronally with a vibratome to generate 50 μm sections. The coronal sections were mounted on slides with VectaShield mounting medium (Vector Laboratories). DiI fluorescence in each section per brain was imaged on an Apotome2 microscope (Zeiss; 5x objective; 5x5 grid of images, Zen2 software). ImageJ was used to visualize each section image and reconstruct the entry point of the probe shank to the tip of the probe shank in the brain.

3.2.11: Electrophysiological data analysis

We first converted action potential spikes to firing rates (in Hz) for each single unit by binning spike counts in 50 ms bins. For the generation of peristimulus time histograms (PSTHs), firing rates were smoothed with a 250 ms moving window and taken as an average of all touch

presentations from 2 s before the platform stops to 2 s after the platform withdraws [-2 to +7s]. Units were assigned as belonging to vS1, tS or BLA based on the dynamics of their action potential spiking by depth and across time (**Supp. Fig. 3-3.1**). vS1 units were split as putative regular spiking (RS) or fast spiking (FS) according to their spike waveform peak to trough duration (in μs) (**Supp Fig. 3-3.7a**).

3.2.12: Unbiased clustering of single unit responses to social and object touch

Despite the heterogeneity of single unit responses to voluntary and forced touch, we sought to determine whether some units behaved similarly to others, i.e., whether there exist different functional groups of neurons in each brain region. We performed clustering of single units twice using PSTHs of all presentations (object and social) of (1) voluntary touch and (2) forced touch. Clustering of the PSTHs was also done separately for each brain region (vS1, tS and BLA), so the procedure was employed 6 times. By grouping units in this manner, we could compare how a unit assigned to a cluster by k-means responds differentially to voluntary object and social touch and responds differentially to forced object and social touch. The clustering procedure we used takes the z-scored, trial-averaged PSTH of each unit and combines all responses into a matrix (PSTH x unit). Units from WT and *Fmr1* KO mice were included together within the PSTH x unit matrix. Principal component analysis (PCA) was then performed on this matrix followed by k-means clustering of the top *k* components that explained >95% of the variance. The gap statistic criterion was used to estimate the ideal number of clusters for each clustering followed by visual inspection of temporal firing of units in each cluster (to confirm their different responses). We applied 1,000 iterations of k-means clustering for each clustering procedure performed. Clustering of single units was also performed on vS1, tS and BLA units separately for the recording session in which the test mouse received forced touch from an inanimate toy mouse and similarly for the session in which the test mouse received forced touch from an anaesthetized mouse.

3.2.13: Modulation of single units by social and object touch

To quantify differences in the mean firing rates of units in each cluster between voluntary or forced object and social touch, we calculated the z-score firing rate normalized to the average firing rate during the ISI period. To assess the modulation of units by social and object touch we grouped together neurons from clusters with similar temporal properties. Units in clusters that we moderately to strongly excited were grouped together ('excited' cells), as were moderately or strongly suppressed units ('suppressed' cells). A modulation index (*MI*) was used to calculate how much the firing rate (*FR*) of each unit changed during the stimulus period (*stim*) relative to the ISI period in each trial:

$$MI = \frac{FR^{stim} - FR^{ISI}}{FR^{stim} + FR^{ISI}}$$

The MI was calculated using three different time ranges for the stim and ISI period. For calculating the MI over the entire stimulation period (MI^{STIM}) we used the mean FR over 5 s during which the platform was stopped (touch) for FR^{stim} and the mean firing rate over the 5 s ISI for FR^{ISI}. For the MI of the first few seconds of the presentation period ($MI^{SHORTSTIM}$), we used the mean FR from the first 3 s of presentation for FR^{stim} and the mean FR for the 3 s prior to the presentation onset for FR^{ISI}. For the MI during the period that the platform moves ($MI^{PLATFORM}$), with the platform as the stim, we used the mean FR from [-1 1] s with time 0 as the presentation onset for FR^{stim} and the mean FR from [-3 -1] s for FR^{ISI}. MI^{STIM} was used to compare modulation of vS1 suppressed and excited cells, tS excited cells and BLA excited cells. We also assessed MI of units in each cluster. For assessing modulation by cluster, $MI^{PLATFORM}$ was used for units in clusters that showed the largest change in FR during the period the platform moves, MI^{STIM} was used for units in clusters that showed a sustained change in FR during the period of touch and $MI^{SHORTSTIM}$ was used for units in clusters that showed a larger change in FR during the initial onset of touch as well as a sustained change in FR during touch.

3.2.14: Single neuron coding of stimulus preference and behavior

To determine which units show clear preference for object vs. social touch, we used receiver operating characteristic (ROC) analysis, which was applied to the firing rate (Hz) during the presentation period [0, 5s], as previously described[38-40]. Each unit's preference was calculated based on the firing rate response to each trial relative to the mean PSTHs for object touch and social touch trials. Each trial was assigned a decision variable (DV) score and the DV for social touch and object touch trials was calculated as follows:

$$DV^{social} = t_i(\ \llbracket meanSocial \rrbracket\_(k \neq i) - meanObject)$$

$$DV^{object} = t_i(meanSocial - \llbracket meanObject \rrbracket\_(k \neq i))$$

where t_i is the firing rate for the current (i^{th} trial) and *meanSocial* and *meanObject* correspond to the mean social and object touch PSTHs. An ROC curve was obtained by varying the criterion value for the DV and the area under ROC (auROC) was calculated from the ROC curve using the MATLAB function *trapz.* The auROC value was considered significant by bootstrapping 1,000 times with a threshold probability of 0.05. Single units that were excited by touch and showed significant auROC values >0.5 were deemed to show preference for social touch (social cells) and those with significant values <0.5 showed preference for object touch (object cells). For suppressed units, those with significant auROC values <0.5 were social cells, and those with significant values >0.5 show were object cells. Units with non-significant auROC values were considered as showing no preference.

ROC analysis was similarly used to determine a unit's preference for firing during bouts of running avoidance, whisker protraction or orbital tightening (as opposed to times when the animal did not exhibit these behaviors) by comparing their firing during the behavioral bout relative to firing before the behavioral bout[41].

3.2.15: Decoding touch context from neuronal activity and behavior

We used support vector machine (SVM) linear classifiers to determine how well all neurons, or neurons within a particular cluster, could decode the presentation type (object vs. social) under voluntary or forced conditions. We used activity from 80% of ramdomly-chosen trials (64/80 of both object and social touch trials) as the training dataset. The remaining 20% (26/80) was used for testing the classifier's accuracy. Firing rates, either as an average of the stimulus period (0-5 s) or binned as 50 ms across the stimulus period (-2-7 s), were used as the feature space of the SVM. 100 iterations of the decoding analysis were performed in which the neurons of a cluster and trials were randomly chosen for the training and test data set. The mean decoding accuracy was calculated based on the average performance of all 100 iterations. In addition, we separately trained the decoder on neural data in which the trial labels were randomly shuffled for the test dataset ("Shuffled"). Decoding was performed with neurons within each cluster by brain region. A different population size of neurons ranging from 1 neuron to the 20 neurons was used for decoding context from averaged activity during the stimulus period and 20 neurons were used for decoding context across time. For decoding context from behavior across time, we binned each behavioral measure in 100 ms bins. For decoding context from facial motion, a total 23 DeepLabCut (DLC) labels were used. Aversive behaviors (running avoidance, aversive whisker protraction, eye area and saccade direction – see behavior analysis below) were used to decode context in a separate classifier.

3.2.16: Data analysis of behavioral data

During the social touch behavioral assay, high-resolution videos (.avi files) were recorded of the test mouse's eye, face, and body using three cameras (Teledyne Flir, Blackfly S USB3) at 120 FPS for behavioral analyses. Locomotion and running direction, facial expressions (including aversive facial expressions; AFEs), and pupil saccades were analyzed from these videos of the eye, face, and body. Locomotion, running direction and AFEs (whisker protraction & orbital tightening) were quantified as described previously (Chari et al., 2023) using MATLAB, FaceMap

and DLC[10,42,43]. For analysis of pupil saccades and facial motion, a DLC neural network was trained on images from the face videos to identify markers on the mouse's pupil, eye, 6 whisker follicles, mouth and nose. The markers on the animal's face were used to quantify the following metrics: motion of each marker (change in marker position every 2 frames), saccades along temporal-nasal plane (displacement of pupil on x-axis), and eye area (pixel area of eye markers)[44]. For analysis of pupil saccades and facial motion and expressions (including AFEs), we excluded video frames when the animal was blinking, grooming, or other movements obscured the animal's face.

3.2.16: Statistical analyses

Statistical tests were performed in Prism software (GraphPad). Statistical analyses of normality (Lilliefors and Shapiro Wilk tests) were performed on each data set; if data deviated from normality ($p<0.05$) or not ($p>0.05$), appropriate non-parametric and parametric tests were performed. For parametric two-group comparisons, a Student's t-test (paired or unpaired) was used. For non-parametric tests, we used Mann-Whitney test (two groups) and the Kruskal-Wallis test (repeated measures). Multiple comparisons across touch conditions and genotypes/groups were analyzed using two-way ANOVA with post-hoc Bonferroni's test. If data was non-normal, we applied a logarithmic transformation on the data and compared the two-way ANOVA with and without the transformation. Since the statistical output of the two-way ANOVA was similar for the transformed and the non-transformed (non-normal data), we used the latter. All experiments were conducted in animals from at least two different litters for each genotype/group. For the graph in Fig. 3-1g, we used the number of images as the sample size with 6 images taken for each brain region from each mouse. Graphs in Fig. 3-3e & Supp. Fig. 3-3.4-6,7b show statistics using the number of single units or cells as the sample size, but all the rest of the figure panels the statistics were done using individual mice as the sample size (averaged over cells for different mice)

superimposed on individual data points. In all figures, the error bars denote standard error of mean (s.e.m.).

3.3: Results

3.3.1: WT mice show avoidance and aversive facial expressions to object touch but not to social touch

In this chapter, we investigate the brain circuits that underlie social touch using chronically implanted Neuropixels probes in WT mice. We first wanted to confirm that these head implants did not affect how these mice respond to social or object touch. We used the same social touch assay used in chapter 2 in which a head-fixed test mouse that can run on a polystyrene ball is exposed to repeated presentations of either an inanimate object (50 mL plastic tube) or a stranger mouse using a motorized platform (5 s presentations, with 5 s ISI during which platform moved away and toward the test mouse; **Fig. 3-1a**; see Materials & Methods)[10]. Using high-resolution videos, we used DLC, together with custom code in MATLAB, to quantify changes in aversive facial expressions (AFEs; aversive whisker protraction, orbital tightening) and in running direction (see Methods). Chapter 2 describes that WT mice (without Neuropixels implants) show running avoidance and aversive facial expressions (AFEs) to forced object touch, but not nearly as much to forced social touch. We once again observed that WT mice (n=9) exhibit significantly more avoidance running to object touch than to social touch even after being implanted with Neuropixels probes (**Fig. 3-1b**; p=0.006 voluntary, p=0.023). Additionally, WT mice displayed significantly higher rates of aversive whisker protraction with object touch compared to social touch (voluntary p=0.020, forced p=0.013). A different AFE, orbital tightening, was also more prominent for voluntary object touch, though the difference was not significant in this smaller cohort of mice (**Fig. 3-1c-d**; voluntary p=0.105). We also quantified the total number of bouts that mice exhibited each of these avoidance/defensive behaviors. We found that object touch led to a significantly greater number of bouts of AFEs than social touch, and this was particularly true for

forced touch (**Fig. 3-1e**; whisker protraction p=0.025 voluntary, p=0.010 forced, orbital tightening p=0.467 voluntary, p=0.087 forced). We did not observe sex differences (**Supp. Fig. 3-1.1**).

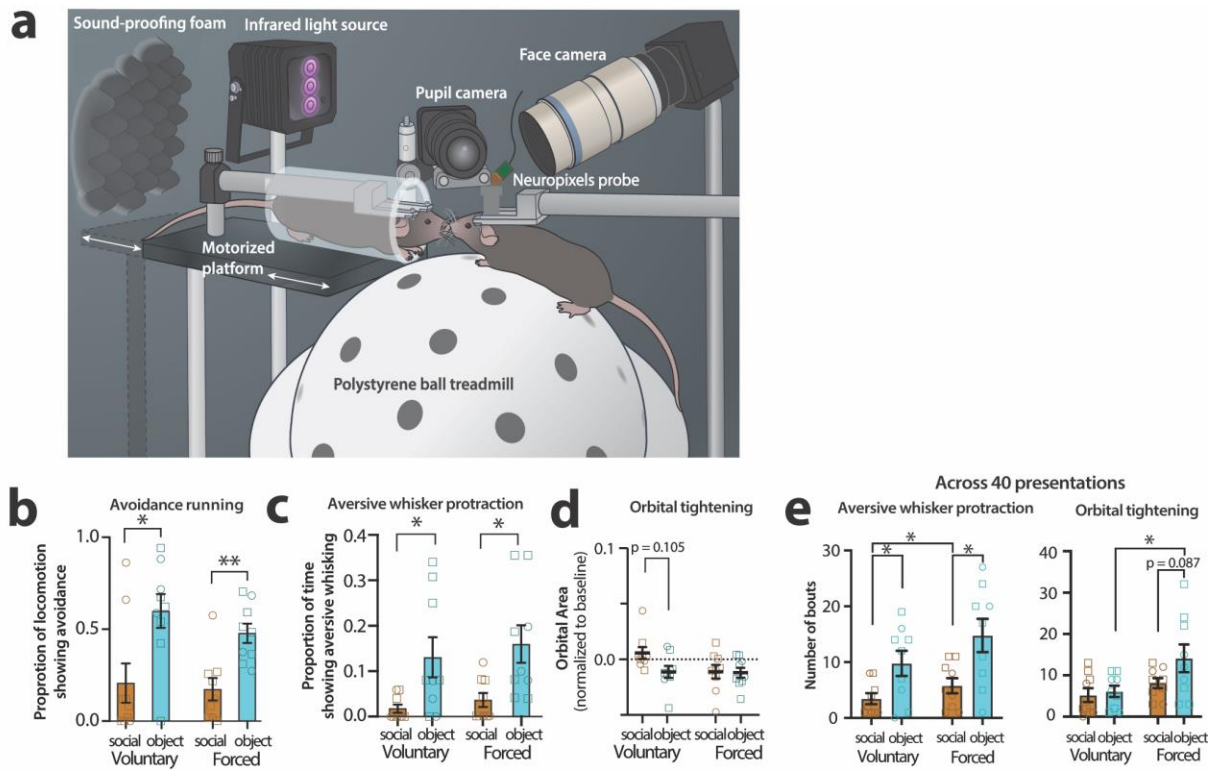
a
Sound-proofing foam
Infrared light source
Face camera
Pupil camera
Neuropixels probe
Motorized platform
Polystyrene ball treadmill
b
Avoidance running
Proprotion of locomotion showing avoidance
1.0
0.5
0.0
*
**
social object social object
Voluntary Forced
c
Aversive whisker protraction
Proportion of time showing aversive whisking
0.4
0.3
0.2
0.1
0.0
*
*
social object social object
Voluntary Forced
d
Orbital tightening
Orbital Area (normalized to baseline)
0.1
0.0
p = 0.105
social object social object
Voluntary Forced
e
Across 40 presentations
Aversive whisker protraction
Orbital tightening
Number of bouts
30
20
10
0
40
30
20
10
0
*
*
*
*
p = 0.087
social object social object
Voluntary Forced
social object social object
Voluntary Forced

Fig. 3-1: WT mice show differences in avoidance and aversive facial expressions.

a. Overview of head-fixed setup for the social touch behavioral assay. A head-fixed test mouse, chronically implanted with a Neuropixels 1.0 probe, runs on an air-suspended polystyrene ball while interacting with a stranger mouse restrained in a plexiglass tube secured to a motorized platform. The system is fully automated to move the stranger mouse to different distances away from the test mouse. Two cameras focus on the face and the eye/pupil, respectively, while a third camera that tracks the mouse and ball motion is overhead (not shown). An infrared light source provides light for tracking behavioral responses. Acoustic foam is used for sound insulation.

b. Running avoidance (backwards to left or right) is higher in WT mice for voluntary and forced object touch than social touch. Squares=males, circles females. **$p<0.01$, *$p<0.05$, two-way ANOVA with Bonferroni's. No outliers were detected with ROUT's analysis.

c. The fraction of time WT mice exhibited prolonged whisker protraction was higher during voluntary and forced object touch than voluntary and forced social touch, respectively. Squares=males, circles=females. *$p<0.05$ for two-way ANOVA with Bonferroni's. No mice were excluded according to ROUT's analysis.

d. Orbital area during touch is normalized to area before touch (object or mouse visible but no touch). Orbital area is not significantly different between voluntary and forced object and social touch. Squares=males, circles=females. $p>0.05$ for two-way ANOVA with Bonferroni's. No mice were excluded according to ROUT's analysis.

e. Number of bouts of aversive whisker protraction behavior was higher in object than social touch and slightly higher in forced than voluntary touch. Number of bouts of orbital tightening are higher during forced touch and slightly higher in forced object than social touch. Number of bouts were taken across 40 presentations of voluntary, or forced, social or object touch. Squares=males, circles=females. *$p<0.05$ for two-way ANOVA with Bonferroni's. No mice were excluded according to ROUT's analysis.

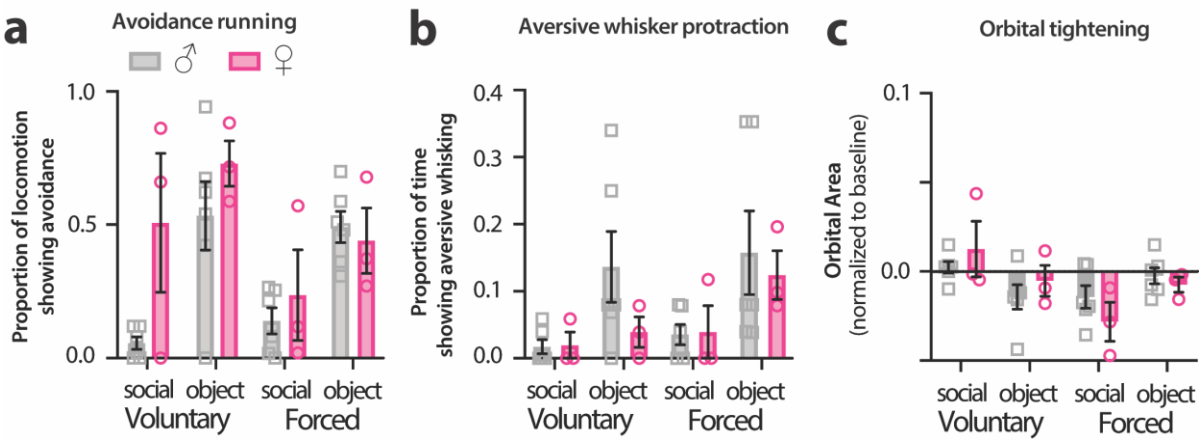
a
Avoidance running
♂
♀
Proportion of locomotion showing avoidance
1.0
0.5
0.0
social
object
social
object
Voluntary
Forced
b
Aversive whisker protraction
Proportion of time showing aversive whisking
0.4
0.3
0.2
0.1
0.0
social
object
social
object
Voluntary
Forced
c
Orbital tightening
Orbital Area
(normalized to baseline)
0.1
0.0
social
object
social
object
Voluntary
Forced

Supplementary Fig. 3-1.1: Male and female WT mice show similar avoidance and AFEs to voluntary and forced object and social touch

a. Running avoidance (backwards to left or right) is similar between WT male and female mice for voluntary and forced object touch than social touch. Squares=males, circles females. $p>0.05$ for two-way ANOVA with Bonferroni's. No mice were excluded according to ROUT's analysis.

b. The fraction of time WT mice exhibited prolonged whisker protraction was similar during voluntary and forced object touch and voluntary and forced social touch for males and females. Squares=males, circles=females. $p>0.05$ for two-way ANOVA with Bonferroni's. No outliers were detected with ROUT's analysis.

c. Orbital area during touch is normalized to area before touch (object or mouse visible but no touch). Orbital area is not significantly different during voluntary and forced object and social touch between males and females. Squares=males, circles=females. $p>0.05$ for two-way ANOVA with Bonferroni's. No mice were excluded according to ROUT's analysis.

3.3.2: Differential cFos expression to social vs. object touch across brain regions

To guide our electrophysiological recordings, we first surveyed which brain regions might be differentially engaged by social vs. object touch. We used transgenic TRAP2 mice in which the expression of tdTom is driven by Cre-recombinase in an activity-dependent manner via the cFos promoter (cFos-CreER^{T2} x Ai14)[21,45]. TRAP2 mice received repetitive presentations of either forced social (n=6) or object touch (n=6) (5 s duration with 5 s ISI) for 30 min following induction with 4-hydroxytamoxifen (4-OHT); the mice were perfused 72 h later and tdTom expression was quantified throughout the brain (**Fig. 3-2a-b**; see Methods). A separate cohort of TRAP2 mice (TRAP2-CTRL; n=5) that was induced with 4-OHT in a no-touch condition (the moving platform was empty) was used as a control.

Forced social and object touch induced cFos expression across many regions throughout the brain. As expected, we identified cFos induction in vS1, which processes whisker inputs (**Fig. 3-2b-c**). Additionally, we observed high expression of tdTom in regions including the NAc, the MeA and BLA, the paraventricular nucleus of the thalamus (PVT), the periaqueductal gray (PAG), and InsCx. Importantly, tdTom expression was significantly higher after social touch than after object touch in layer 2/3 (L2/3) of vS1, in the tS, in ACCx, as well as in InsCx, BLA, MeA, the central amygdala (CeA), PVT and the paraventricular nucleus of the hypothalamus (PvtH) (**Fig. 3-2c**; L2/3 p=0.002, L4 p=0.156, L5/6 p=0.286, tS p=0.006, ACCx p<0.001, NAc p=0.051, InsCx p=0.008, BLA p=0.005, MeA p=0.03, CeA p=0.002, PVT p=0.002, PvtH p=0.055). These cortical and subcortical brain regions are all known to be involved in social behavior and aversive processing[16,27,30,32,33,41,46-50]. In contrast, we did not observe significant differences between social and object touch in the density of tdTom^{+} cells in the PAG, primary motor cortex (MC), or visual cortex (V1) (**Fig. 3-2c**).

Thus, social touch engages these circuits differently from object touch across many (but not all) brain regions. We chose to implant single Neuropixels probes in such a way that their trajectory would allow us to record simultaneously from vS1, tS, and BLA. In this way, we could

investigate how social facial touch is represented within sensory (vS1)[13,19,20] and emotional-related brain areas (BLA)[26-28,30,46], as well as within a sensorimotor-related brain region (tS)[31-33]. Furthermore, these brains regions have been shown to be involved during social and aversive behaviors and implicated in autism based on research findings described in chapter 1.

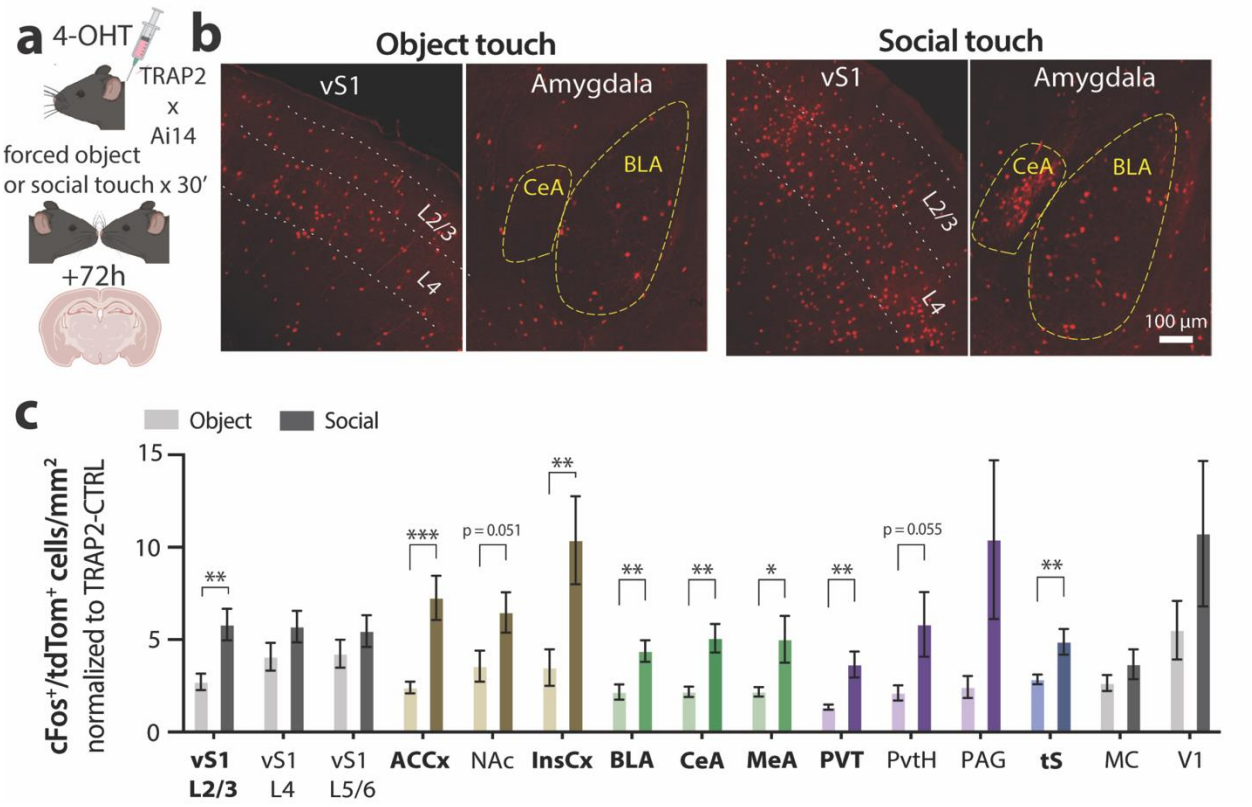
a
4-OHT
TRAP2
x
Ai14
forced object
or social touch x 30'
+72h
b
Object touch
Social touch
vS1
Amygdala
L2/3
L4
CeA
BLA
100 µm
c
Object
Social
cFos+/tdTom+ cells/mm2
normalized to TRAP2-CTRL
15
10
5
0
**
***
p = 0.051
p = 0.055
*
vS1 L2/3
vS1 L4
vS1 L5/6
ACCx
NAc
InsCx
BLA
CeA
MeA
PVT
PvtH
PAG
tS
MC
V1

Fig. 3-2: cFos$^+$ expression varies across brain regions in response to object versus social touch.

a. Experimental protocol for TRAP2 behavioral experiments. TRAP2 WT mice are injected with 4-OHT 30 min prior to behavior testing. These test mice then undergo either repetitive bouts of social or object touch (5 s stim, 5 s ISI) lasting 30 minutes. A subset of mice undergo repetitive bouts of the same duration with the platform moving but without an object or mouse present (TRAP2-CTRL). Following behavioral testing, mice are perfused 72 h later for histology.

b. Example images of cFos$^+$ expression from vibrissal somatosensory cortex (vS1) and central (CeA) and basolateral amygdala (BLA) during object and social touch in two mice (scale bar = 100 µm).

c. Cell density of cFos$^+$/tdTom$^+$ cells per mm for mice that received forced object and social touch normalized to cell density of TRAP2-CTRL mice for each brain region. *$p<0.05$, normality was tested with D'Agostino & Pearson test followed by unpaired nonparametric Mann-Whitney or parametric t-test for each brain region. Each data point is a single image and 6 images were derived from a single mouse for each brain region. 5-6 mice were imaged from for each brain region and for object and social touch separately. Brain regions were grouped together based on color (gray – sensory/motor cortices, brown – prefrontal/ventral areas, green – amygdalar nuclei, purple – thalamic/hypothalamic-associated areas, blue – dorsal striatal regions). vS1 layer 2/3-L2/3, layer 4-L4, layer 5/6-L5/6, anterior cingulate cortex-ACCx, nucleus accumbens-NAc, insular cortex-InsCx, medial amygdala-MeA, paraventricular nucleus of the thalamus-PVT, paraventricular nucleus of the hypothalamus-PvtH, periaqueductal grey-PAG, tail of the striatum-tS, motor cortex-MC, primary visual cortex-V1.

3.3.3: vS1, tS and BLA neurons are differentially modulated by object vs. social touch

We chronically implanted single-shank Neuropixels 1.0 silicon probes in 9 WT mice and confirmed targeting through histological reconstruction of the probe tract (**Supp. Fig. 3-3.1a-b**). We also used the trajectories of the probes and the characteristics of action potential spiking across time and depth (or the lack of activity in white matter bundles) to infer which units putatively belonged to vS1, tS, or BLA (see Materials & Methods). For example, within vS1, we could distinguish L2/3, L4 and L5/6 based on the dense spiking of L4 neurons to object and social touch (**Supp. Fig. 3-3.1c**).

We recorded the activity of single units across these three regions as mice were presented with 40 bouts of voluntary or forced social and object touch (5 s duration, 5 s ISI; see Materials & Methods). Some neurons increased their firing in response to different presentations of touch, whereas others suppressed their firing (**Fig. 3-3a**). We first considered the mean activity of all neurons, regardless of whether they were excited or suppressed by facial touch (**Fig. 3-3a**), although we analyzed separately fast-spiking and regular spiking neurons in vS1. On average, neurons across all three regions showed increased firing to both social and object touch, and this was apparent even before the platform stopped, because mice could initiate contact with their whiskers as the platform approached (**Fig. 3-3b**). Overall, forced touch trials (when the object or visitor mouse are placed in direct contact with the snout of the test mouse) elicited much higher z-score firing than voluntary touch trials (when test mice contact the object or visitor mouse with their whiskers; **Fig. 3-3b**). Neurons in vS1 showed greater firing to social touch under both voluntary and forced conditions (**Fig. 3-3b**). In contrast, tS and BLA neurons did not show an obvious preference for social touch in the voluntary condition but showed greater firing for object touch in the forced condition (**Fig. 3-3b**).

Using support vector machine (SVM) linear classifiers, we found that, overall, all three brain regions performed very well at decoding touch context (social vs. object) for both voluntary and forced conditions, based on the activity of 1-20 neurons per area (**Fig. 3-3c, Supp Fig. 3-**

3.2a). When estimating decoding accuracy across time, performance was always > 60% but increased sharply for vS1 and tS on contact, ~0.5 s before the platform stopped (**Fig. 3-3c, Supp. Fig. 3-3.2a**).

Based on the peak activity raster of all neurons in each region, we observed diverse response behaviors: some neurons were suppressed by touch, some were excited only briefly upon contact, others exhibited sustained firing during touch, and still others were barely modulated by touch (**Fig. 3-3a**). To compare the activity of neurons with such different behaviors, we performed principal component analysis on trial-averaged z-scored PSTH, followed by k-means clustering of the top PCA components (see Materials & Methods). We examined how single units in WT mice differentially respond to object vs. social touch under voluntary and forced conditions. This approach identified 5 significantly distinct clusters of single units in vS1, 6 clusters in tS and 4 clusters in BLA for voluntary for forced touch (**Fig. 3-3d**). The proportion of neurons in each cluster (Cl.) varied across brain regions. Neurons that were least modulated by social/object touch (Cl. 1, Cl. 6, Cl. 12) tended to be the most abundant in all regions (**Supp**. **Fig. 3-3.3a**). Surprisingly, neurons that were suppressed by social/object touch (Cl. 1-2, 6-7, 12-13) tended to represent a substantial proportion of the entire population (e.g., 47%, 36% and 66% in vS1, tS, BLA, respectively, for voluntary touch; **Supp. Fig. 3-3.3a)**.

SVM classifiers applied to these clusters showed that clusters that are strongly excited or suppressed by touch tended to perform better at decoding touch context than those that are mildly or moderately excited across all regions (**Supp. Fig. 3-3.2b-c**). The best decoding was obtained from clusters in tS and vS1. Based on similarities in SVM performance and in neural responses to facial touch, we combined clusters that were strongly excited by touch within each region (Cl. 3-5 in vS1, Cl. 9-11 in tS, and Cl. 14 & 15 in BLA) and focused on these for subsequent analyses. We compared differences in the modulation of their firing as an average of all 40 stimulations of social and object touch (**Fig 3-3e**).

In vS1, we found that both excited and suppressed cells (Cl. 2) were significantly more modulated by social than by object touch, regardless of whether the interaction was voluntary or forced (**Fig. 3-3e**; p-value range: 0.07 to <0.001). In tS, excited cells also showed greater modulation by social than object touch (**Fig. 3-3e**; p=0.004), but only during voluntary interactions. Indeed, the opposite occurred during forced interactions, when excited cells in tS were more modulated by object touch (p=0.012). In the BLA, we observed no significant differences in modulation of excited cells by voluntary social vs. object touch (p=0.181), but under forced conditions the same cells showed a tendency toward greater activity to object touch (p=0.066). We also examined suppressed cells in tS and BLA but found no significant differences in modulation between social vs. object touch (**Supp. Fig. 3-3.4 & 3-3.5**).

These results show that: 1. vS1 neurons are uniquely and strongly modulated by social touch under both voluntary and forced conditions; 2. tS neurons are preferentially modulated by social stimuli under voluntary conditions, but under forced touch conditions, they switch to being more strongly modulated by object touch (which is more aversive to the animal); and 3. BLA neurons are not differentially modulated by social vs. object touch, except perhaps during the most aversive experience (forced object touch). The same conclusions were reached when inspecting the modulation of individuals clusters (**Supp. Figs. 3-3.4 & 3-3.5**). For example, Cl. 14 in the BLA was significantly more modulated by forced object touch (**Supp. Fig 3-3.5c**).

It is possible that differences in the responses of neurons to social vs. object touch simply reflected differences in texture between the plastic object and the visitor mouse, especially for vS1 neurons. To address this, we performed some control experiments with the same test mice. First, we recorded neural responses in vS1, tS and BLA to repeated forced presentations of an inanimate plush toy mouse (with furry hair and whiskers; see Materials & Methods). Although this recording session was performed on a different day, we compared the mean responses of excited/suppressed neurons in each region to contact with this toy mouse with neural responses to the plastic 50 mL tube (even if the units in each cluster were perhaps not the same). After

clustering, we found that excited cells in vS1 showed greater modulation to the toy mouse compared to a falcon tube (**Supp. Fig. 3-3.6a**; $p<0.001$), suggesting that texture plays a role. In contrast, however, neither suppressed neurons in vS1, nor excited neurons in the tS or the BLA showed any difference in modulation between these two objects (**Supp. Fig. 3-3.6a**; $p>0.05$). These findings suggest that the differences in modulation by object vs. social touch that we observed for suppressed cells in vS1 and excited cells in tS and BLA, cannot be explained by differences in texture alone.

In a separate control experiment, we tested whether reciprocal whisking from the visitor mouse contributed to the difference in modulation of neural activity between social and object touch by examining forced interactions with a lightly anaesthetized mouse. Interestingly, we observed no differences in modulation between awake vs. anaesthetized forced social touch in any brain region (with the exception of Cl. 4 in vS1 which showed greater modulation by the live mouse) (**Supp. Fig. 3-3.6b**). Thus, the changes in modulation we observed between social vs. object touch are largely independent of reciprocal whisking by the stranger mouse.

Our recordings also allowed us to differentiate between regular spiking cells (putative excitatory neurons) and fast-spiking (FS) units (presumed inhibitory neurons) based on peak-to-trough duration of the spike waveform (**Supp. Fig. 3-3.7a**). When examining FS units in vS1, we found that excited FS cells, like their RS counterparts, showed greater modulation by social touch under both voluntary and forced conditions, whereas the relatively small number of suppressed FS cells showed no difference between social vs. object (**Supp. Fig. 3-3.7b**).

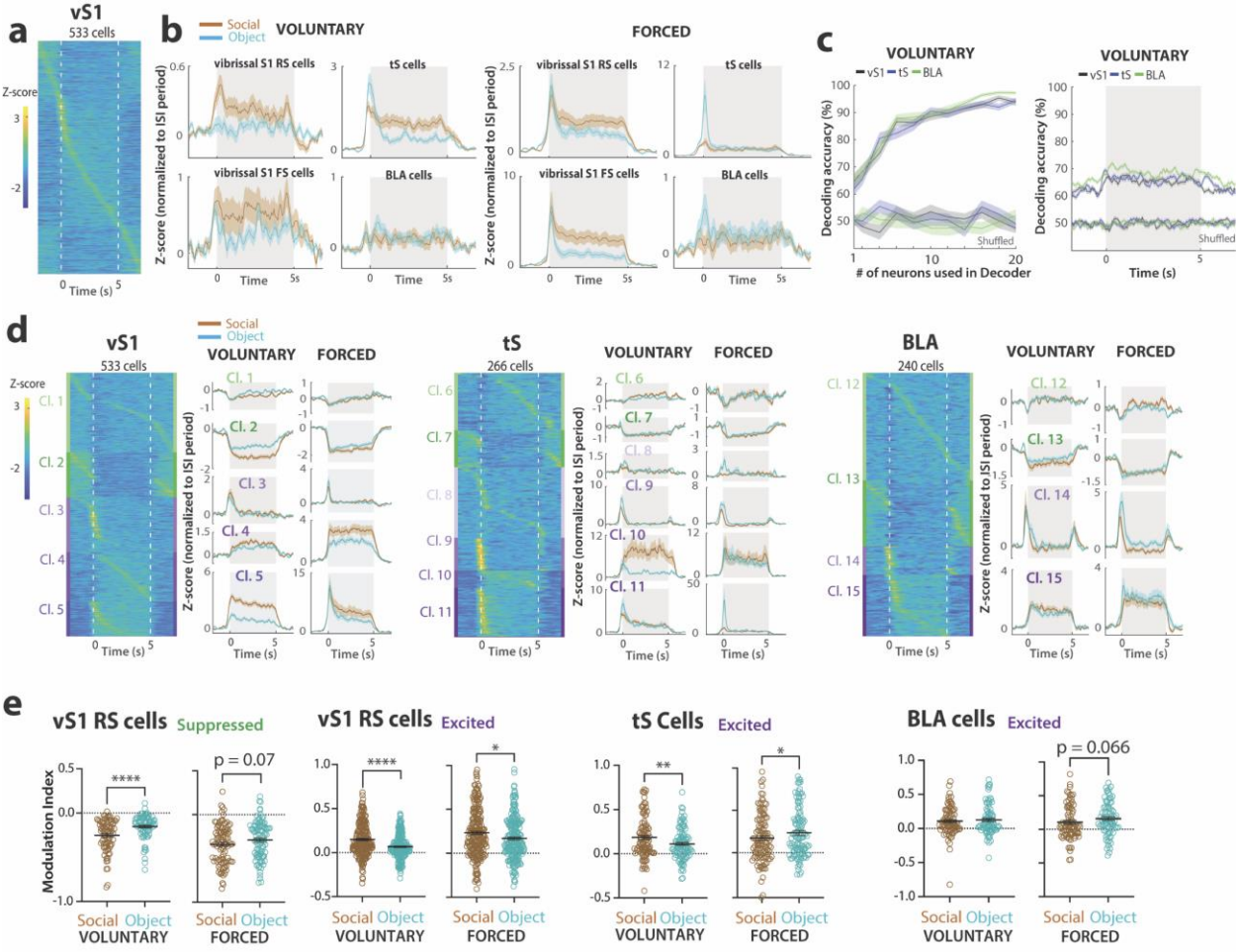
a
vS1
533 cells
Z-score
Time (s)
b
Social
Object
VOLUNTARY
FORCED
vibrissal S1 RS cells
tS cells
vibrissal S1 FS cells
BLA cells
Z-score (normalized to ISI period)
Time
c
VOLUNTARY
vS1 tS BLA
Decoding accuracy (%)
Shuffled
# of neurons used in Decoder
Time (s)
d
vS1
533 cells
tS
266 cells
BLA
240 cells
Cl. 1
Cl. 2
Cl. 3
Cl. 4
Cl. 5
Cl. 6
Cl. 7
Cl. 8
Cl. 9
Cl. 10
Cl. 11
Cl. 12
Cl. 13
Cl. 14
Cl. 15
e
vS1 RS cells Suppressed
vS1 RS cells Excited
tS Cells Excited
BLA cells Excited
Modulation Index
p = 0.07
p = 0.066
****
**
*
Social Object
VOLUNTARY
FORCED

Fig. 3-3: vS1, tS and BLA respond differently across time and show differential modulation by social and object touch.

a. Example heatmap of all vS1 cells sorted by peak of trial-averaged, z-scored PSTHs.

b. Trial-averaged z-scoring firing normalized to the period before touch (ISI) for all vS1 regular-spiking (RS) and fast-spiking (FS), tS and BLA cells from 9 WT mice during voluntary and forced social and object touch. Z-score firing is shown from 2 seconds before onset of touch to 2 seconds after end of touch period (-2, 7 s).

c. Decoding accuracy for touch context based on activity of vS1, tS and BLA cells during stimulation period of voluntary touch (0, 5s) and the number of neurons (n = 1-20) randomly chosen from each brain region to be used in the SVM classifier. Decoding accuracy is also shown based on the activity of neurons in each region when context identity is shuffled in the 80% of object and social touch stimulations (64 stimulations total) used for the training data set. Decoding accuracy for touch context based on activity of 20 randomly selected cells in vS1, tS and BLA for every 50 ms during the stimulation period of voluntary touch (-2, 7s). Decoding accuracy from shuffled neural data is also plotted for each brain region every 50 ms.

d. Heatmap of the trial-averaged PSTHs for voluntary touch (taken as an average of all object and social touch stims) for all vS1, tS and BLA cells splits by clusters derived from PCA-k-means clustering and sorted by peak firing in time within each cluster. Z-score firing of clusters derived from PCA-k-means clustering in vS1 during voluntary and forced social versus object touch. Clusters are sorted by suppressed (green) to excited (purple) and by mildly (light shaded) to strongly (dark shaded) suppressed/excited. Time 0 s denotes onset of touch.

e. Modulation index of vS1 RS excited and suppressed, tS excited and BLA excited cells to voluntary and forced social versus object touch as an average of all 40 stimulations of touch. ****$p<0.001$, **$p<0.01$, *$p<0.05$ for paired parametric t-test. Each marker represents a single cell taken from across 9 WT mice.

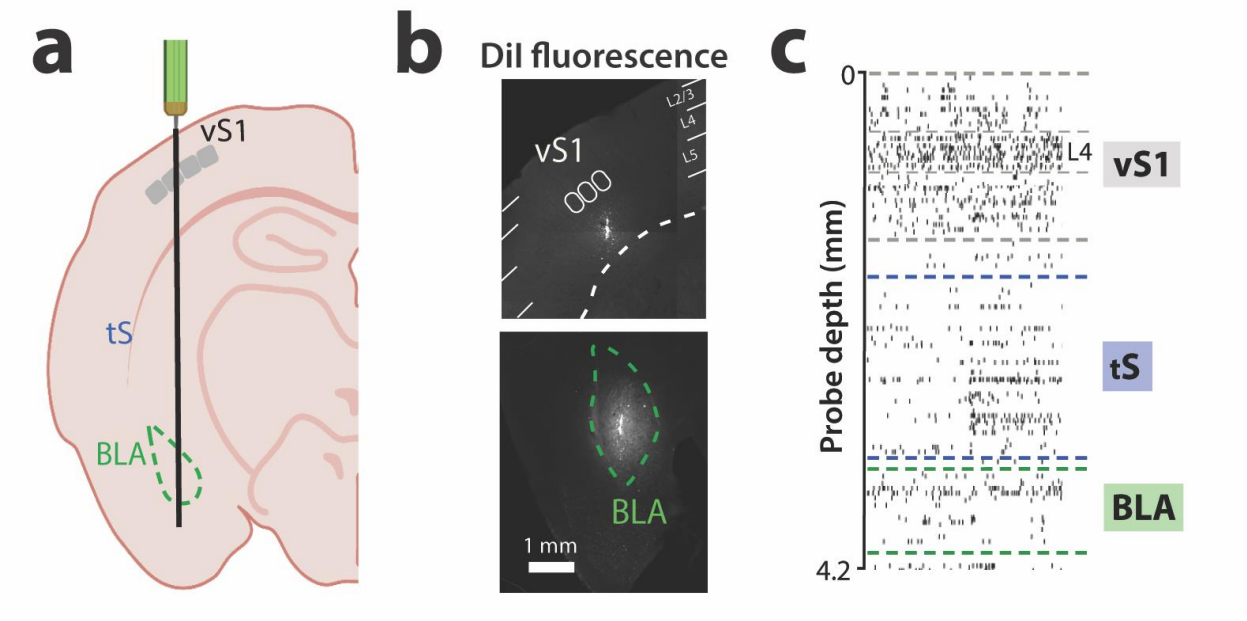
a
vS1
tS
BLA
b
Dil fluorescence
vS1
L2/3
L4
L5
BLA
1 mm
c
0
4.2
Probe depth (mm)
L4
vS1
tS
BLA

Supplementary Fig. 3-3.1: Histological reconstruction of probe trajectory and differences in firing by depth and time across vS1, tS & BLA.

a. Neuropixels probe was implanted at 0° angle at mouse brain coordinates -1.46 AP, 2.9 ML 3.75 DV to target vS1, tS and BLA simultaneously.

b. DiI fluorescence was used to confirm probe targeting in respective brain regions. Scale denotes 1 mm.

c. Action potential spiking differs across time and by depth (in mm) and can be used to allocate units recorded from Neuropixels towards vS1, tS and BLA.

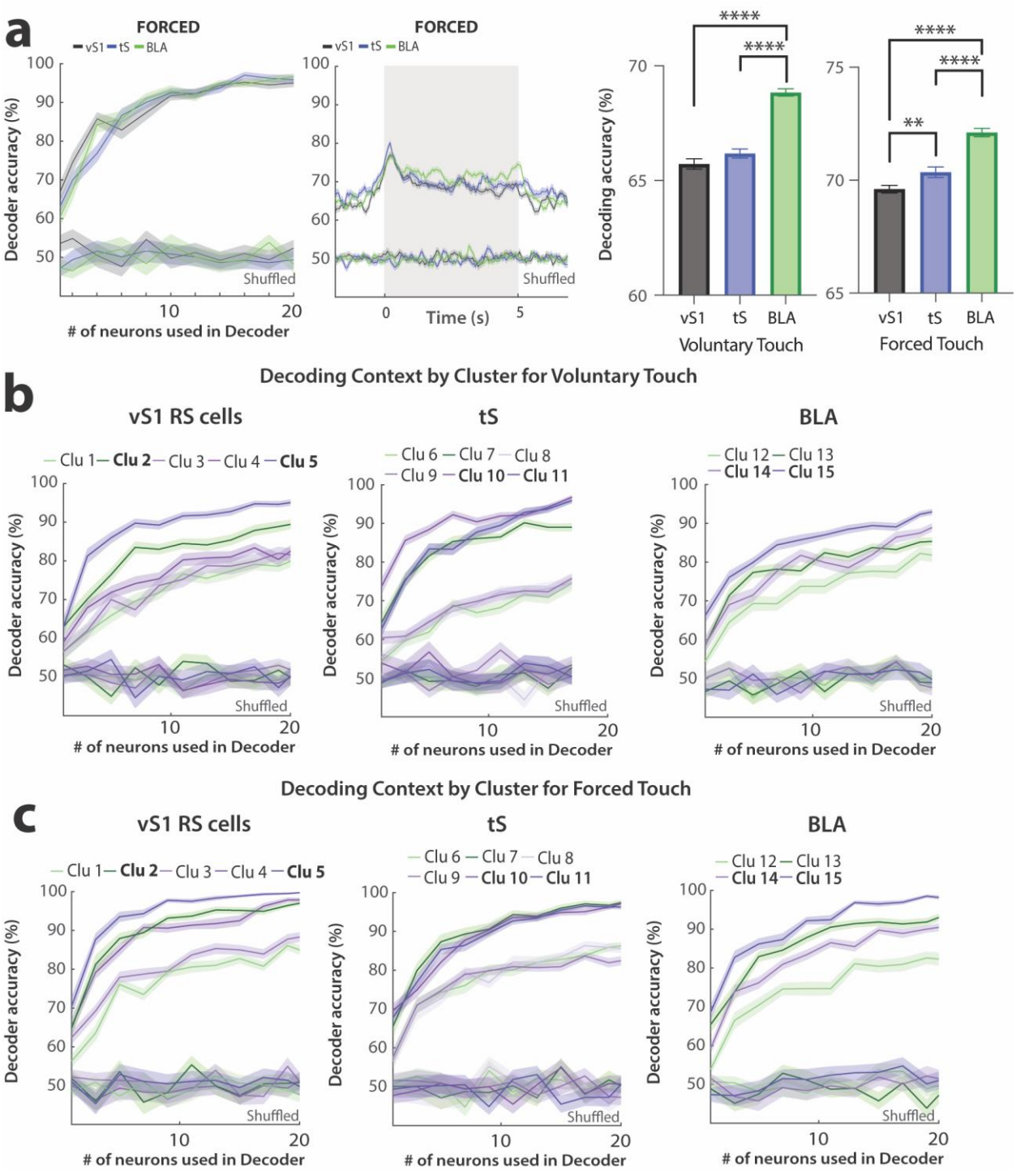
a
FORCED
vS1 tS BLA
Decoder accuracy (%)
Shuffled
# of neurons used in Decoder
Time (s)
Decoding accuracy (%)
****
**
vS1 tS BLA
Voluntary Touch
Forced Touch
b
Decoding Context by Cluster for Voluntary Touch
vS1 RS cells
tS
BLA
Clu 1 Clu 2 Clu 3 Clu 4 Clu 5
Clu 6 Clu 7 Clu 8
Clu 9 Clu 10 Clu 11
Clu 12 Clu 13
Clu 14 Clu 15
c
Decoding Context by Cluster for Forced Touch

Supplementary Fig. 3-3.2: Decoding context from average activity during stimulation period for each cluster in vS1, tS and BLA for voluntary and forced touch.

a. Accuracy for touch context based on activity of vS1, tS and BLA cells during stimulation period of forced touch (0, 5s) and the number of neurons (n = 1-20) randomly chosen from each brain region to be used in the SVM classifier. Decoding accuracy is also shown based on the activity of neurons in each region when context identity is shuffled in the 80% of object and social touch stimulations (64 stimulations total) used for the training data set. Decoding accuracy for touch context based on activity of 20 randomly selected cells in vS1, tS and BLA for every 50 ms during the stimulation period of forced touch (-2, 7s). Decoding accuracy is also plotted from shuffled neural data for each brain region every 50 ms. Decoding accuracy was averaged from all 50 ms bins during the 5 s of the stimulation period and averaged across all SVM iterations for each brain region in voluntary and forced touch. ****$p<0.001$, **$p<0.01$.

b. Decoding accuracy for touch context based on activity of vS1 RS, tS and BLA clusters during stimulation period of voluntary touch (0, 5s) and the number of neurons (n=1-20) used in the SVM classifier. Decoding accuracy is also shown based on the activity of each cluster when context identity is shuffled in the 80% of object and social touch stimulations (64 stims) used for the training data set.

c. Decoding accuracy for touch context based on activity of vS1 RS, tS and BLA clusters during stimulation period of forced touch (0, 5s) and the number of neurons (n=1-20) used in the SVM classifier. Decoding accuracy is also shown based on the activity of each cluster when context identity is shuffled in the 80% of object and social touch stimulations (64 stims) used for the training data set.

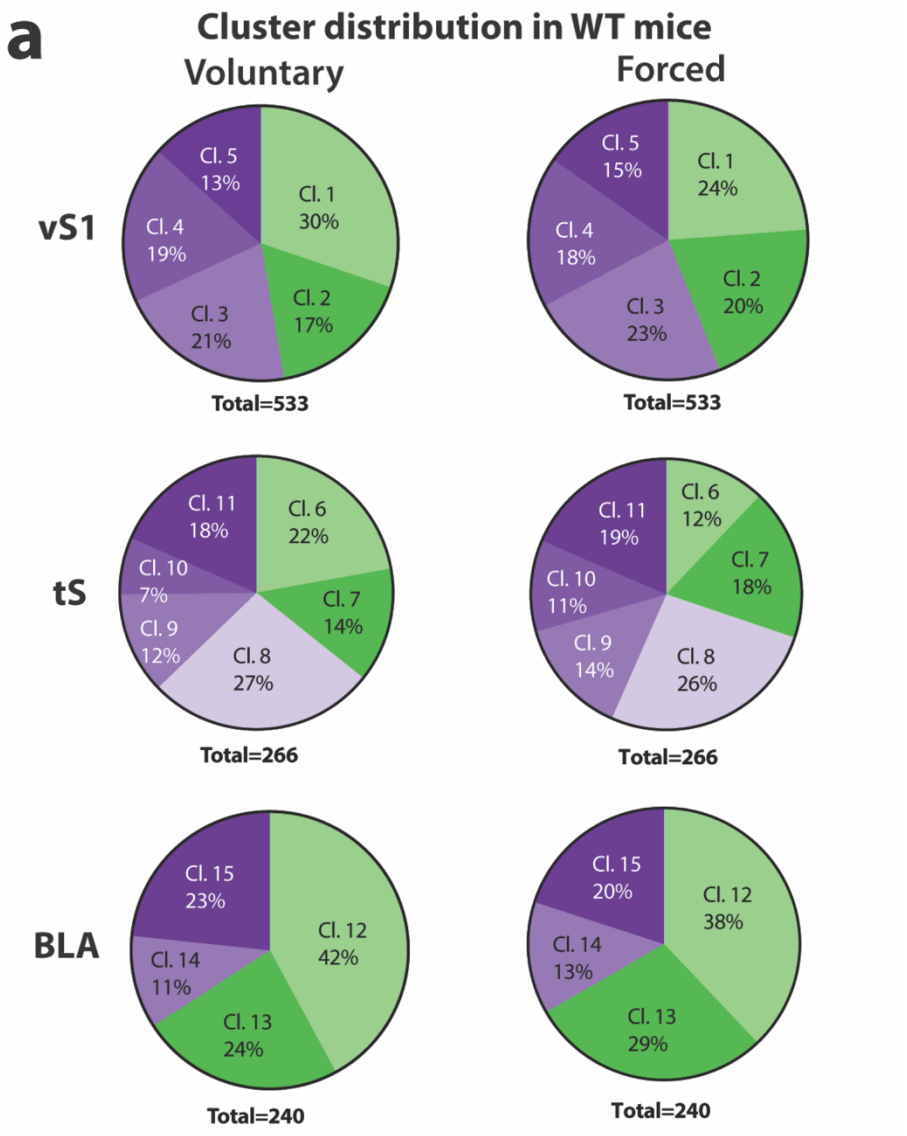
a
Cluster distribution in WT mice
Voluntary
Forced
vS1
Cl. 5 13%
Cl. 1 30%
Cl. 4 19%
Cl. 2 17%
Cl. 3 21%
Total=533
Cl. 5 15%
Cl. 1 24%
Cl. 4 18%
Cl. 2 20%
Cl. 3 23%
Total=533
tS
Cl. 11 18%
Cl. 6 22%
Cl. 10 7%
Cl. 7 14%
Cl. 9 12%
Cl. 8 27%
Total=266
Cl. 11 19%
Cl. 6 12%
Cl. 7 18%
Cl. 10 11%
Cl. 9 14%
Cl. 8 26%
Total=266
BLA
Cl. 15 23%
Cl. 12 42%
Cl. 14 11%
Cl. 13 24%
Total=240
Cl. 15 20%
Cl. 12 38%
Cl. 14 13%
Cl. 13 29%
Total=240

Supplementary Fig. 3-3.3: Proportion of total cells in each cluster differs within WT mice.

a. Number of cells in each cluster as a proportion of total cells for vS1, tS and BLA from all WT for voluntary touch (left). Number of cells in each cluster as a proportion of total cells for vS1, tS and BLA from all WT mice for forced touch (right).

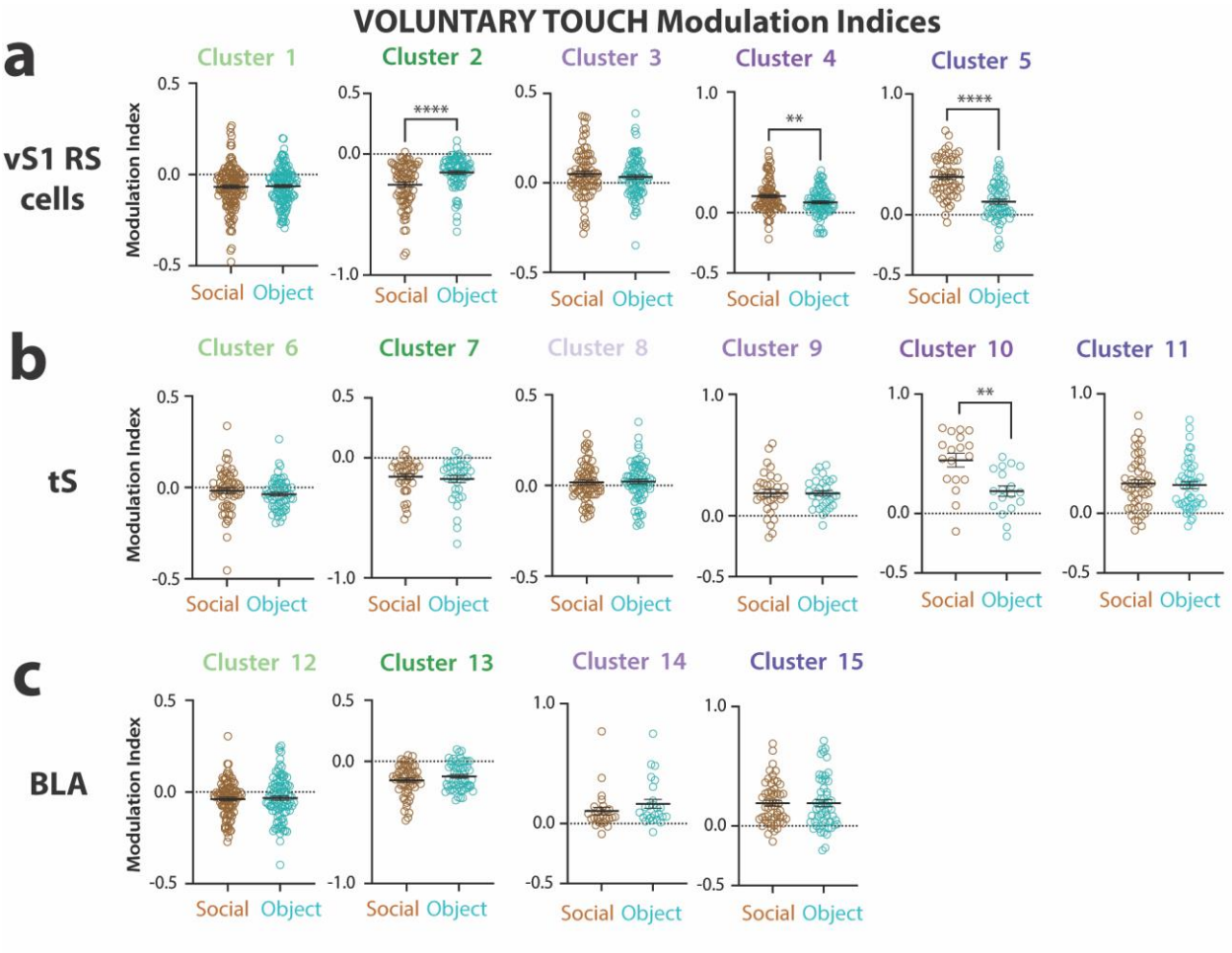
VOLUNTARY TOUCH Modulation Indices
a
vS1 RS cells
b
tS
c
BLA
Cluster 1
Cluster 2
Cluster 3
Cluster 4
Cluster 5
Cluster 6
Cluster 7
Cluster 8
Cluster 9
Cluster 10
Cluster 11
Cluster 12
Cluster 13
Cluster 14
Cluster 15
Modulation Index
Social
Object
****
**

Supplementary Fig. 3-3.4: Clusters in vS1, tS and BLA are modulated differently by voluntary social and object touch.

a. Modulation index of vS1 RS cells in each cluster to voluntary social versus object touch as an average of all 40 stimulations of touch. ****p<0.001, **p<0.01 for paired parametric t-test. Each marker represents a single cell taken from across 9 WT mice.

b. Modulation index of tS cells in each cluster to voluntary social versus object touch as an average of all 40 stimulations of touch. **p<0.01 for paired parametric t-test. Each marker represents a single cell taken from across 9 WT mice.

c. Modulation index of BLA cells in each cluster to voluntary social versus object touch as an average of all 40 stimulations of touch. p>0.05 for paired parametric t-test. Each marker represents a single cell taken from across 9 WT mice.

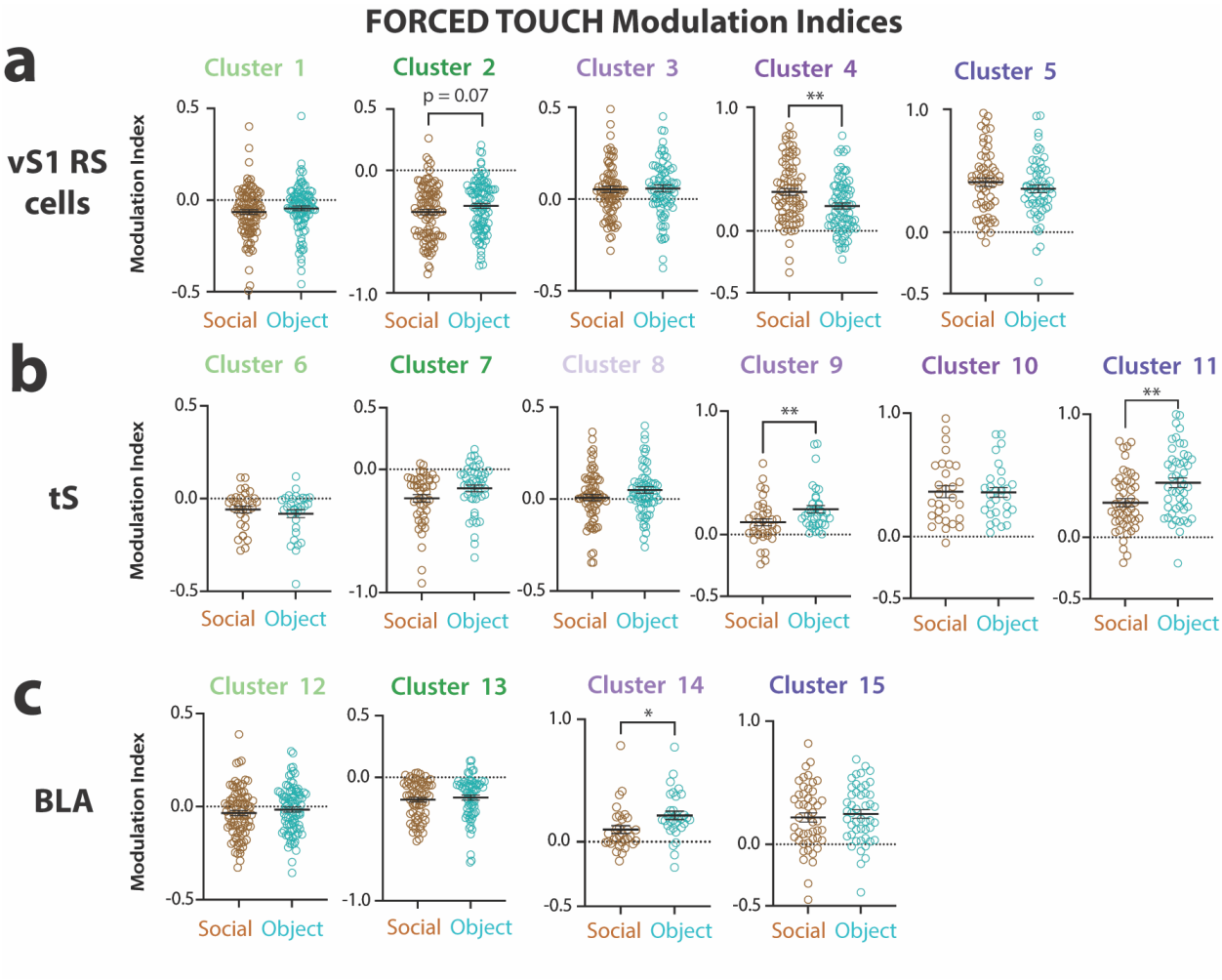
FORCED TOUCH Modulation Indices
a
vS1 RS cells
b
tS
c
BLA
Modulation Index
Cluster 1
Cluster 2
Cluster 3
Cluster 4
Cluster 5
Cluster 6
Cluster 7
Cluster 8
Cluster 9
Cluster 10
Cluster 11
Cluster 12
Cluster 13
Cluster 14
Cluster 15
p = 0.07
**
*
Social
Object

Supplementary Fig. 3-3.5: Clusters in vS1, tS and BLA are modulated differently by forced social and object touch.

a. Modulation index of vS1 RS cells in each cluster to forced social versus object touch as an average of all 40 stimulations of touch. **p<0.01 for paired parametric t-test. Each marker represents a single cell taken from across 9 WT mice.

b. Modulation index of tS cells in each cluster to forced social versus object touch as an average of all 40 stimulations of touch. **p<0.01 for paired parametric t-test. Each marker represents a single cell taken from across 9 WT mice.

c. Modulation index of BLA cells in each cluster to forced social versus object touch as an average of all 40 stimulations of touch. *p<0.05 for paired parametric t-test. Each marker represents a single cell taken from across 9 WT mice.

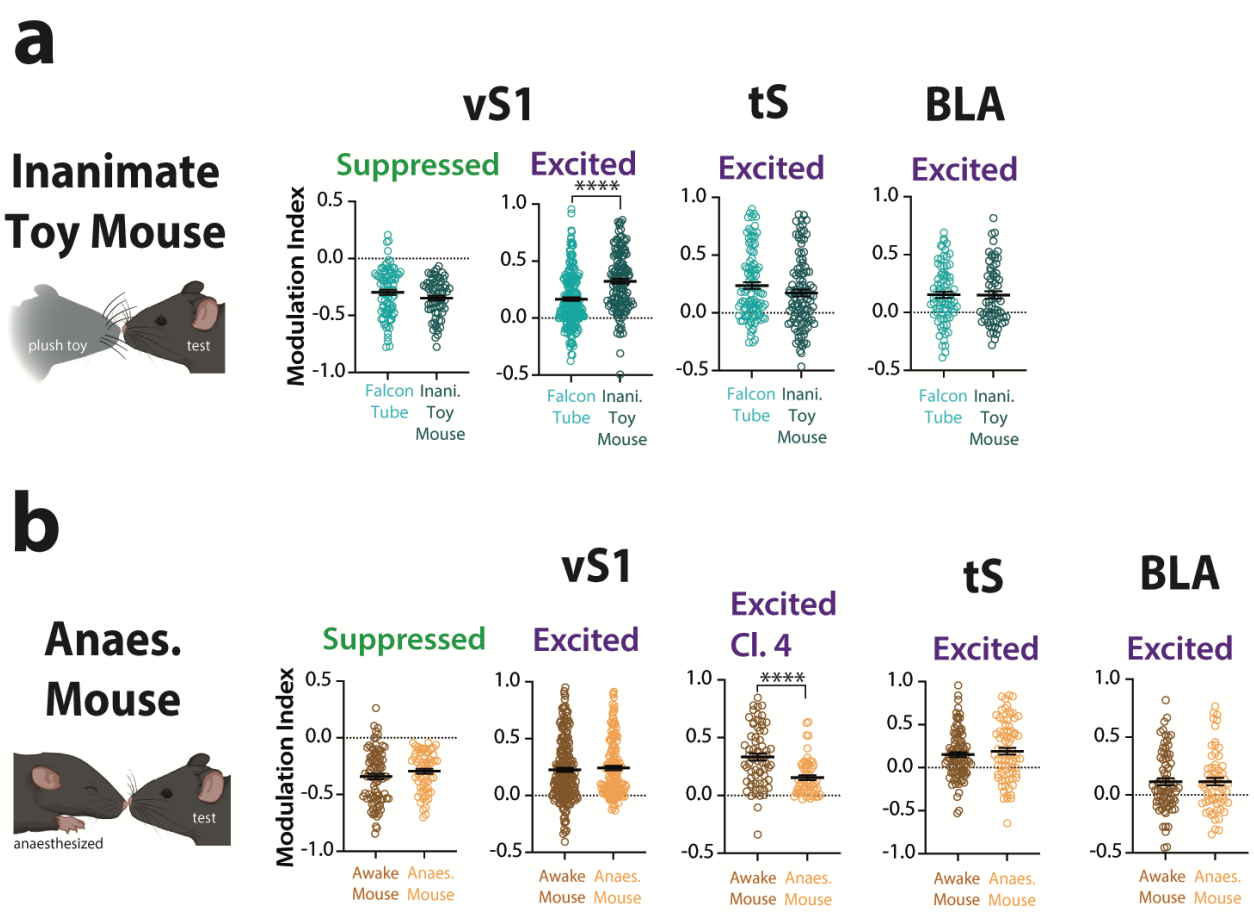
a
Inanimate Toy Mouse
plush toy
test
vS1
tS
BLA
Suppressed
Excited
Excited
Excited
Modulation Index
****
Falcon Tube
Inani. Toy Mouse
b
Anaes. Mouse
test
anaesthesized
vS1
tS
BLA
Suppressed
Excited
Excited Cl. 4
Excited
Excited
Modulation Index
****
Awake Mouse
Anaes. Mouse

Supplementary Fig. 3-3.6: vS1, tS and BLA cells show differences in modulation to forced touch with an inanimate toy mouse and with a stranger, anaesthetized mouse.

a. Modulation index of vS1 RS excited and suppressed, tS excited and BLA excited cells to forced object touch from a Falcon tube versus an inanimate toy mouse as an average of all 40 stimulations of touch. ****p<0.0001 for unpaired parametric t-test. Each marker represents a single cell taken from across 9 WT mice.

b. Modulation index of vS1 RS excited and suppressed (including Cl. 4 cells only), tS excited and BLA excited cells to forced social touch with a stranger awake mouse versus a stranger anaesthetized mouse as an average of all 40 stimulations of touch. ****p<0.0001 for unpaired parametric t-test. Each marker represents a single cell taken from across 9 WT mice.

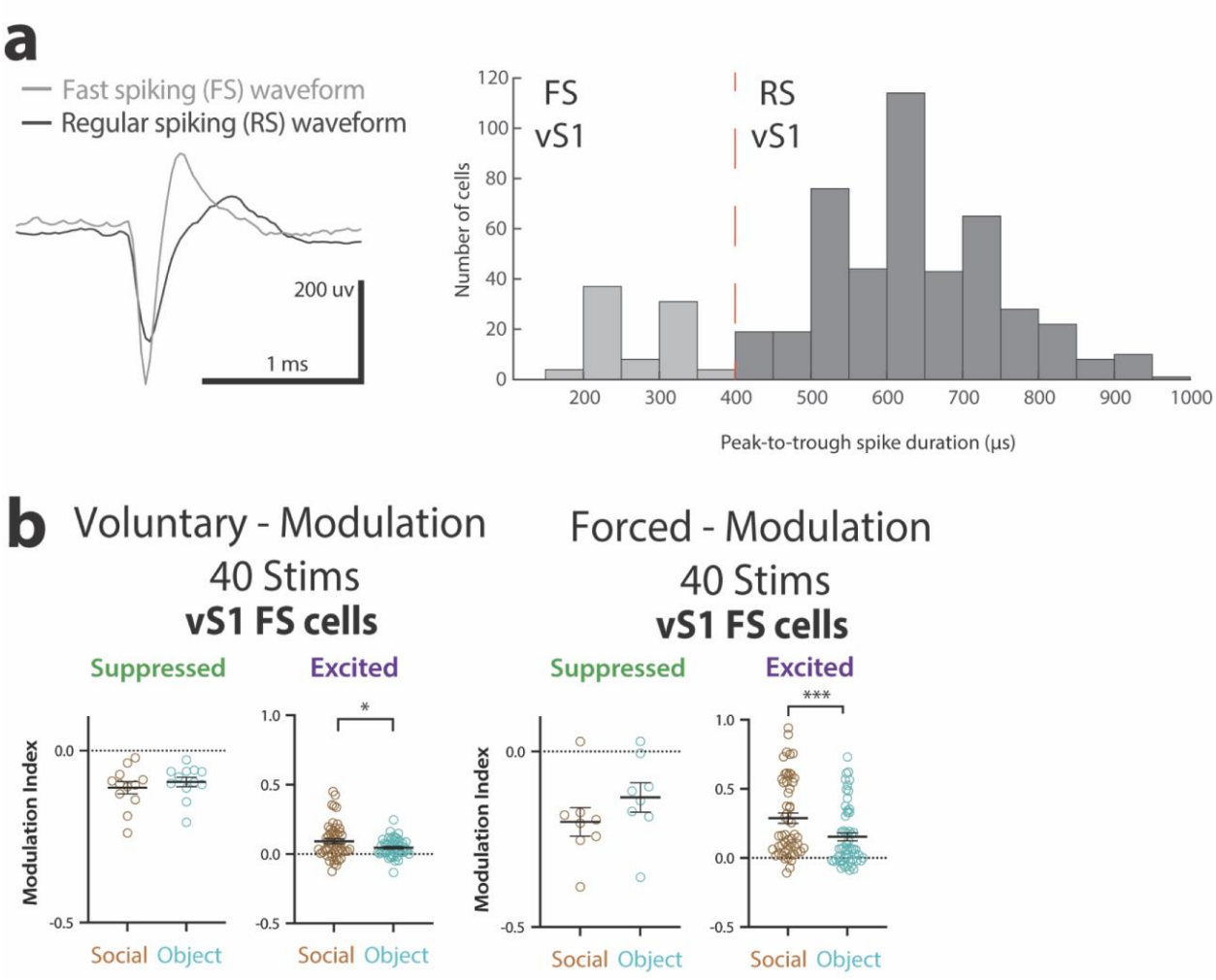
a
Fast spiking (FS) waveform
Regular spiking (RS) waveform
200 uv
1 ms
FS
vS1
RS
vS1
Number of cells
Peak-to-trough spike duration (µs)
b
Voluntary - Modulation
40 Stims
vS1 FS cells
Forced - Modulation
40 Stims
vS1 FS cells
Suppressed
Excited
Modulation Index
Social
Object
*
***

Supplementary Fig. 3-3.7: vS1 FS suppressed and excited cells show differences in modulation to voluntary and forced object touch in WT mice.

a. Categorization of RS and FS vS1 cells based on peak-to-trough spike duration of spike waveforms. Single units with peak-to-trough durations above 400 µs are considered RS cells and below 400 µs are considered FS cells.

b. Modulation index of vS1 FS excited and suppressed cells to voluntary and forced social versus object touch as an average of all 40 stimulations of touch. **p<0.01, ***p<0.001 for paired parametric t-test. Each marker represents a single cell taken from across 9 WT mice.

3.3.4: The relative abundance of neurons that exhibit preference for either social or object touch is different across brain regions

The fact that neural activity in vS1, tS, and BLA showed differential modulation by social vs. object touch raises the possibility that certain neurons may exhibit a true preference to either object or social touch. Whether vS1 contains neurons that are selectively, or even exclusively, tuned to social facial touch (as opposed to object touch) is not known. We utilized receiver operating characteristic (ROC) analysis to categorize object-preferring cells and social-preferring cells amongst excited units across brain regions (**Fig. 3-4a-c**; see Materials & Methods). When looking at all cells excited by touch, we found that at least 10% of units showed a clear preference for social touch, irrespective of the brain region (**Fig. 3-4d)**. In vS1, there is a similar proportion of object- and social-preferring units regardless of whether interactions were voluntary or forced (17-23%; **Fig. 3-4d, e**). In the tS, there were more social-preferring cells during voluntary interactions, but the opposite was true during forced interactions, with a higher proportion of object-preferring cells (**Fig. 3-4e**; p=0.055). In the BLA, we found the highest proportion of object-preferring units during forced interactions (nearly one-third of all touch-excited neurons in the BLA; **Fig. 3-4d**), which was significantly more than the proportion of social-preferring cells (**Fig. 3-4e**; p=0.003). We also looked at vS1 neurons that were suppressed by touch and found a lower proportion of object-preferring cells during forced interactions (**Supp. Fig. 3-4.1**; p=0.052).

Altogether, these findings imply that forced object touch presentations, which trigger avoidance and AFEs in test mice, selectively engage neurons in the tS and BLA, and uniquely recruit object-preferring cells. In contrast, vS1 neurons are preferentially engaged by social touch, which triggers no avoidance/AFEs, and the proportion of object- vs. social-preferring cells is unaffected by whether the stimulus is well tolerated or not.

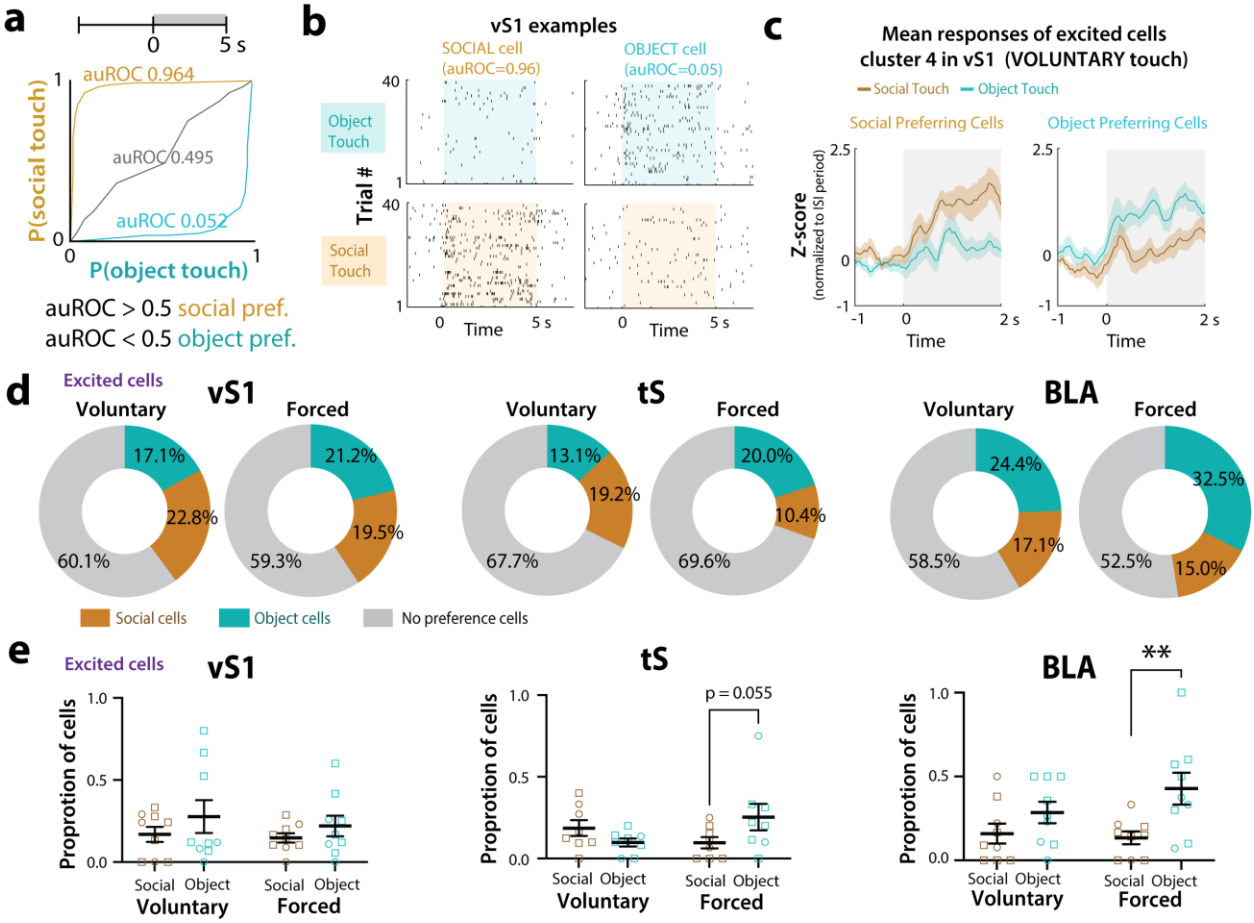
a
0
5 s
auROC 0.964
auROC 0.495
auROC 0.052
P(social touch)
P(object touch)
auROC > 0.5 social pref.
auROC < 0.5 object pref.
b
vS1 examples
SOCIAL cell
(auROC=0.96)
OBJECT cell
(auROC=0.05)
Object Touch
Social Touch
Trial #
Time
c
Mean responses of excited cells
cluster 4 in vS1 (VOLUNTARY touch)
Social Touch
Object Touch
Social Preferring Cells
Object Preferring Cells
Z-score
(normalized to ISI period)
Time
d
Excited cells
vS1
tS
BLA
Voluntary
Forced
17.1%
22.8%
60.1%
21.2%
19.5%
59.3%
13.1%
19.2%
67.7%
20.0%
10.4%
69.6%
24.4%
17.1%
58.5%
32.5%
15.0%
52.5%
Social cells
Object cells
No preference cells
e
Excited cells
vS1
tS
BLA
Proprotion of cells
Social
Object
Voluntary
Forced
p = 0.055
**

Fig. 3-4: Preference of vS1, tS and BLA cells towards object and social touch.

a. ROC criterion for a significant social preferring and object preferring vS1 excited cells and example ROC curves for a social preferring, object preferring and non-preferential cell in vS1.

b. Spike rasters across each stimulation of social and object touch for each example social and object preferring cell (vS1 cells excited by touch).

c. Example averaged z-score firing rate of social and object preferring cells in vS1 Cl. 4 during voluntary object and social touch. Social preferring cells show more firing to social than object touch and vice-versa for object preferring cells.

d. Proportion of object and social preferring cells in vS1, tS and BLA excited cells for voluntary and forced touch as total of all cells.

e. Proportion of object and social preferring cells in vS1, tS and BLA excited cells for voluntary and forced touch as total of all cells per mouse. **$p<0.01$ for two-way ANOVA with Bonferroni's. Squares=males, circles=females. 1 mouse was excluded according to ROUT's analysis for tS.

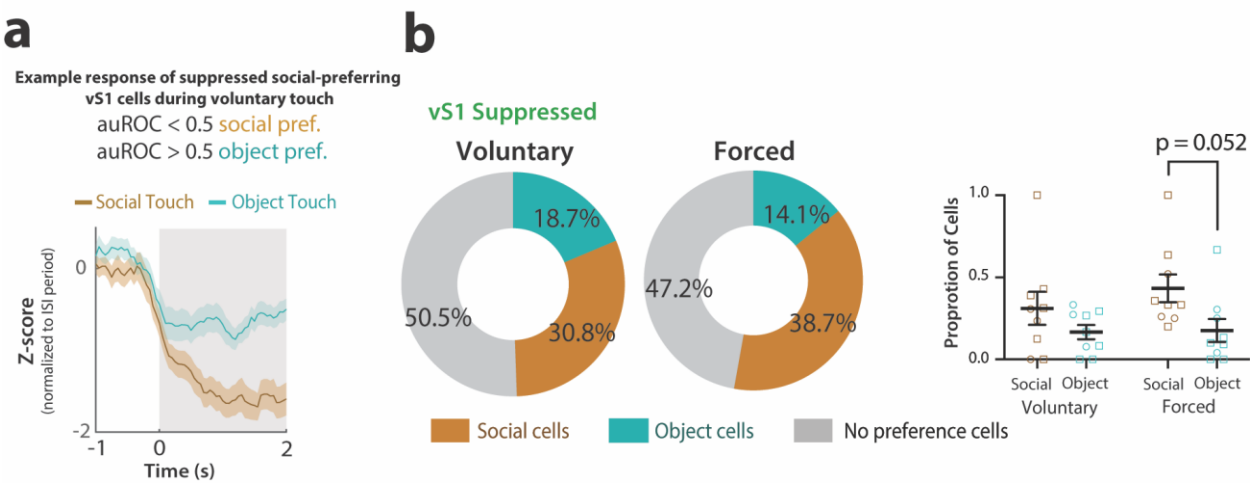
a
Example response of suppressed social-preferring vS1 cells during voluntary touch
auROC < 0.5 social pref.
auROC > 0.5 object pref.
Social Touch
Object Touch
Z-score
(normalized to ISI period)
0
-2
-1
0
2
Time (s)
b
vS1 Suppressed
Voluntary
Forced
18.7%
30.8%
50.5%
14.1%
38.7%
47.2%
Social cells
Object cells
No preference cells
p = 0.052
Proprotion of Cells
1.0
0.5
0.0
Social
Object
Voluntary
Social
Object
Forced

Supplementary Fig. 3-4.1: Preference of vS1 suppressed cells towards object and social touch.

a. ROC criterion for a significant social preferring and object preferring vS1 suppressed cells. Z-score firing rate of example social preferring cells in vS1 Cl. 2 during voluntary object and social touch. Social preferring cells show more firing to social than object touch.

b. Proportion of social and object preferring cells in vS1 suppressed cells for voluntary and forced touch as total of all cells (left). Proportion of social and object preferring cells in vS1 suppressed cells for voluntary and forced touch as total of all cells per mouse (right). $p>0.05$ for two-way ANOVA with Bonferroni's. Squares=males, circles=females. No mice were excluded according to ROUT's analysis.

3.3.5: WT mice can discriminate between social and object touch at the behavioral level and is largely dependent on whisker movements

Finally, based on the behavioral results and the Neuropixels data described above, we hypothesized that a classifier trained on WT behaviors would be able to accurately distinguish between social versus object touch bouts. Hence, we trained the SVM classifier on orofacial movements (agnostic to whether they represented AFEs or not), since these movements reflect how mice engage with their environment, particularly in an assay that involves facial touch[43,51,52]. First, we trained DeepLabCut (DLC) to track 23 labels positioned on the animal's whiskers, eye, pupil, nose and mouth across all voluntary and forced presentations of object and social touch (**Fig. 3-5a**). We also trained 5 separate decoders using DLC labels corresponding to the whiskers, eye, pupil, nose and mouth. The whiskers contributed most to decoding accuracy of touch context, such that the performance of the whisker-based decoder was the only one that was indistinguishable from that of the all-label decoder (**Fig. 3-5b**, $p>0.05$).

Together, these results suggest that WT are also able to distinguish between object and social touch based on the way in which they engage, primarily via their whiskers, with either type of tactile stimuli.

Decoding Touch Type Based on Motion of DLC Face Labels

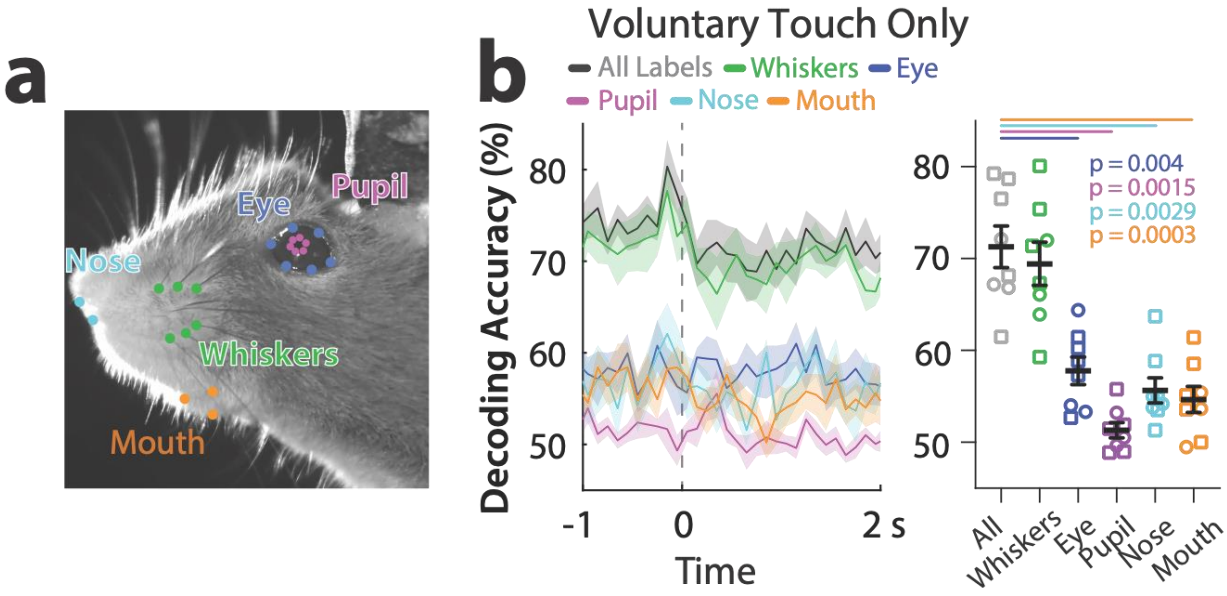

Fig. 3-5: Orofacial movements, primarily from whiskers, decode context of facial touch in WT mice.

a. Motion of features on the mouse's face can be acquired by using DLC to label individual points and then using MATLAB to determine how these labels change their position over time.

b. Motion of DLC labels can decode object from social voluntary touch across 100 ms time bins from 1 s before the onset of touch to 2 s after the onset of touch in WT mice via a SVM linear classifier. Motion energy of DLC whisker labels contribute the most to decoding context relative to other facial features (eye, pupil, nose, mouth). $p<0.01$, $p<0.001$ for nonparametric Kruskal-Wallis test. Squares=males, circles=females. No mice were excluded according to ROUT's analysis.

3.4: Discussion

The main goal in this chapter was to investigate how neuronal responses in vS1, tS and BLA are shaped by social facial touch and which brain regions may contribute to the emergence of avoidance and aversive behaviors to object and/or social touch. Our findings can be summarized as follows: 1. Specific sensory, emotional and movement related brains regions show differences in cFos expression to forced social versus object touch, including whisker input-mediated vS1, tS and BLA; 2. vS1, tS and BLA show diverse responses across time to both voluntary and forced social touch; 3. vS1, tS and BLA cells that are excited or suppressed by touch are differentially modulated by social and object touch and this also depends on if touch is voluntary or forced; 4. vS1, tS and BLA cells show preference to social over object touch and vice-versa; 5. WT mice differentiate between social and object touch at a behavioral level.

3.4.1: Neural coding of social facial touch

Recent studies have investigated the neural coding of social touch, an important sensory cue required for shaping social interaction and communication across animal species and humans[4,53]. Neurons in the vS1 (or barrel cortex) are known to respond to social facial touch, including affiliative touch, as do some cells in the basal ganglia and limbic regions[6,12,14,16,19,54]. However, it is not known whether these brain regions can distinguish social from non-social tactile inputs and whether this is dependent on an animal ability's to voluntarily engage in touch. Furthermore, it is not known how social touch may translate into an aversive response, particularly in individuals with autism that avoid social touch, and which regions contribute to social touch aversion[4,10].

Unexpectedly, while we saw increases in c-Fos expression in vS1 more so to social touch, this was layer-dependent and only occurred in L2/3. This would suggest that somatosensory cortical layers may process the context of tactile input differently[55]. Additionally, we also saw more c-Fos expression in the tS and BLA for social than object touch, though not surprising given the

role of tS in novelty and reward coding of sensory, including social, stimuli and BLA in encoding social stimuli[26,30,31,33,56].

Next, we found that vS1 RS cells showed a greater difference in modulation between object and social touch for voluntary than forced touch, though they still showed a larger response for social touch. These findings suggest under the forced condition, in which the animal has less control of engaging in touch, there is still greater modulation of vS1 activity by social tactile input. On the other hand, while tS cells show a larger response to voluntary social than object touch, there is a shift in firing more so towards object touch when touch is forced. BLA cells also show a similar but milder difference in modulation than tS cells between forced social and object touch.

These findings would suggest that vS1 RS cells are likely responding to a difference in texture (a plastic tube vs. a mouse). Indeed, vS1 excited cells are also differentially modulated by an inanimate furry toy mouse compared to a Falcon tube. vS1 cells may also by modulated more by social touch due to reciprocal whisking with another animal, which is reduced when the stranger mouse is lightly anaesthetized. vS1 FS cells, typically inhibitory interneurons, also showed more modulation by social over object touch (both voluntary and forced) but only in excited cells. Together, overall vS1 cortical circuit activity is driven more by the texture of social than object touch. However, previous studies have found that vS1 can be driven behaviorally by locomotion, including whisker-guided locomotion, which warrants further exploration of the influence of whisker-kinematics observed during social and object touch on vS1 activity[55,57].

3.4.2: The role of tS and BLA in the perception of social touch

Our data suggests that the activity of tS cells is driven by the salience of touch. Under voluntary conditions, social touch is expected to be more salient than object touch. Moreover, the modulation of neuronal activity in certain brain regions should be dependent on the animal's motivation to engage with the stimulus (e.g., how much it whisks). In contrast, during forced interactions, object and social stimuli likely have similar salience (or perhaps the object is even

more unpleasant, as evidenced by increased avoidance and AFEs to forced object touch in WT mice). This was an unexpected finding given that activity in vS1 and striatal areas is highly correlated; thus, we expected the tS to show greater modulation by social touch for both voluntary and forced touch [58,59]. Activity within tS may alone contribute to this shift in preference for object touch in the forced condition, but tS also receives inputs from amygdalar nuclei and prefrontal cortical areas[32,33]. It is clear from our findings and previous research that the tS has a unique role in selecting for highly salient rewarding or aversive sensory stimuli that also distinguishes it from other dorsal striatal areas[32].

Surprisingly, we did not see profound differences in modulation of BLA excited cells (or BLA cells by cluster) between voluntary and forced social and object touch. We did find a larger proportion of BLA excited cells with a preference towards forced object over social touch, which could link the recruitment of more BLA object-preferring cells to increased avoidance & aversive behaviors during object touch. BLA does receive projections from the ACCx and has been associated with the learning of aversive sensory stimuli[27,30]. Furthermore, the BLA has been shown to encode exploratory and aversive behavioral states[25].

3.4.3: Touch discrimination at the behavioral level

Given the strong differences in the responses of WT vS1, tS and BLA to social versus object touch in both the voluntary and forced condition, we posited that the overall behavior may relate to the discriminability of these two types of touch and would also suggest a strong link between neuronal responses in these regions and behavior. We focused on the orofacial movements of the animal since these movements contribute to the animal's engagement with the environment[43,51]. Orofacial movements contribute strongly to discriminating context even before the onset of touch and there is a slight decrease in decoding context following the onset of touch (**Fig 3-4b**). This may reflect minor similarities in the way the animal engages with different tactile stimuli upon initial contact. The decoder performance in discriminating touch context from

orofacial movements is largely dependent on the whiskers of the mouse, suggesting that mice display different whisking kinematics for object and social touch and this may explain differences in activity at the sensory cortical level.

3.4.4: Limitations and future directions

We did not address if there were significant sex differences in the vS1, tS and BLA neuronal responses to social touch, in part due to the small number of mice per sex that we were able to record from. Although we did not see any sex differences in behavior, it is worth investigating sex differences in neuronal dynamics to social touch given clear sex differences in social behaviors in mice[60].

Furthermore, our TRAP experiments revealed that the activity of certain brain regions, particularly prefrontal and insular cortices, are driven more by social touch relative to vS1, tS and BLA. Recordings from these brain regions would further expand our understanding of how social facial touch is represented across the brain. With the advent of novel recording techniques that would allow multiple Neuropixels probes to be implanted simultaneously within a single mouse, functional connectivity between multiple brain regions during social touch can be explored[61,62].

Finally, as our assay is not naturalistic, we could employ a modified version of the assay (also described in chapter 2), in which the test mouse has control over the motorized platform via a lever press, to investigate the motivational drive of mice to engage in social touch.

In summary, we find that social touch is encoded differently from object touch in vS1, tS and BLA. Cells in the brain regions show both increased or suppressed firing during social and object touch with different temporal profiles. vS1 is important for differentiating the texture of social and object touch while tS activity may reflect touch salience. The ability to discriminate between social and object touch also occurs at the behavioral level is largely dependent on whisker movements and links behavior to sensory cortical, striatal and amygdalar activity.

3.5: References

1. de Waal, F.B.M., and Preston, S.D. (2017). Mammalian empathy: behavioural manifestations and neural basis. Nat Rev Neurosci *18*, 498-509. 10.1038/nrn.2017.72.

2. Adolphs, R. (2009). The social brain: neural basis of social knowledge. Annu Rev Psychol *60*, 693-716. 10.1146/annurev.psych.60.110707.163514.

3. Jablonski, N.G. (2021). Social and affective touch in primates and its role in the evolution of social cohesion. Neuroscience *464*, 117-125. 10.1016/j.neuroscience.2020.11.024.

4. Cascio, C.J., Moore, D., and McGlone, F. (2019). Social touch and human development. Dev Cogn Neurosci *35*, 5-11. 10.1016/j.dcn.2018.04.009.

5. Keysers, C., Kaas, J.H., and Gazzola, V. (2010). Somatosensation in social perception. Nat Rev Neurosci *11*, 417-428. 10.1038/nrn2833.

6. Elias, L.J., and Abdus-Saboor, I. (2022). Bridging skin, brain, and behavior to understand pleasurable social touch. Curr Opin Neurobiol *73*, 102527. 10.1016/j.conb.2022.102527.

7. Li, L., Durand-de Cuttoli, R., Aubry, A.V., Burnett, C.J., Cathomas, F., Parise, L.F., Chan, K.L., Morel, C., Yuan, C., Shimo, Y., et al. (2023). Social trauma engages lateral septum circuitry to occlude social reward. Nature *613*, 696-703. 10.1038/s41586-022-05484-5.

8. Green, S.A., Hernandez, L.M., Bowman, H.C., Bookheimer, S.Y., and Dapretto, M. (2018). Sensory over-responsivity and social cognition in ASD: Effects of aversive sensory stimuli and attentional modulation on neural responses to social cues. Dev Cogn Neurosci *29*, 127-139. 10.1016/j.dcn.2017.02.005.

9. Robertson, C.E., and Baron-Cohen, S. (2017). Sensory perception in autism. Nat Rev Neurosci *18*, 671-684. 10.1038/nrn.2017.112.

10. Chari, T., Hernandez, A., and Portera-Cailliau, C. (2023). A novel head-fixed assay for social touch in mice uncovers aversive responses in two autism models. J Neurosci *43*, 7158-7174. 10.1523/JNEUROSCI.0226-23.2023.

11. Orefice, L.L., Zimmerman, A.L., Chirila, A.M., Sleboda, S.J., Head, J.P., and Ginty, D.D. (2016). Peripheral Mechanosensory Neuron Dysfunction Underlies Tactile and Behavioral Deficits in Mouse Models of ASDs. Cell *166*, 299-313. 10.1016/j.cell.2016.05.033.

12. Lenschow, C., and Brecht, M. (2015). Barrel cortex membrane potential dynamics in social touch. Neuron *85*, 718-725. 10.1016/j.neuron.2014.12.059.

13. Bobrov, E., Wolfe, J., Rao, R.P., and Brecht, M. (2014). The representation of social facial touch in rat barrel cortex. Curr Biol *24*, 109-115. 10.1016/j.cub.2013.11.049.

14. Elias, L.J., Succi, I.K., Schaffler, M.D., Foster, W., Gradwell, M.A., Bohic, M., Fushiki, A., Upadhyay, A., Ejoh, L.L., Schwark, R., et al. (2023). Touch neurons underlying dopaminergic pleasurable touch and sexual receptivity. Cell *186*, 577-590.e516. 10.1016/j.cell.2022.12.034.

15. Yu, H., Miao, W., Ji, E., Huang, S., Jin, S., Zhu, X., Liu, M.Z., Sun, Y.G., Xu, F., and Yu, X. (2022). Social touch-like tactile stimulation activates a tachykinin 1-oxytocin pathway to promote social interactions. Neuron *110*, 1051-1067.e1057. 10.1016/j.neuron.2021.12.022.

16. Wu, Y.E., Dang, J., Kingsbury, L., Zhang, M., Sun, F., Hu, R.K., and Hong, W. (2021). Neural control of affiliative touch in prosocial interaction. Nature *599*, 262-267. 10.1038/s41586-021-03962-w.

17. Lee Masson, H., Pillet, I., Boets, B., and Op de Beeck, H. (2020). Task-dependent changes in functional connectivity during the observation of social and non-social touch interaction. Cortex *125*, 73-89. 10.1016/j.cortex.2019.12.011.

18. Gazzola, V., Spezio, M.L., Etzel, J.A., Castelli, F., Adolphs, R., and Keysers, C. (2012). Primary somatosensory cortex discriminates affective significance in social touch. Proc Natl Acad Sci U S A *109*, E1657-1666. 10.1073/pnas.1113211109.

19. Wolfe, J., Mende, C., and Brecht, M. (2011). Social facial touch in rats. Behav Neurosci *125*, 900-910. 10.1037/a0026165.

20. Ebbesen, C.L., Bobrov, E., Rao, R.P., and Brecht, M. (2019). Highly structured, partner-sex- and subject-sex-dependent cortical responses during social facial touch. Nat Commun *10*, 4634. 10.1038/s41467-019-12511-z.

21. DeNardo, L.A., Liu, C.D., Allen, W.E., Adams, E.L., Friedmann, D., Fu, L., Guenthner, C.J., Tessier-Lavigne, M., and Luo, L. (2019). Temporal evolution of cortical ensembles promoting remote memory retrieval. Nat Neurosci *22*, 460-469. 10.1038/s41593-018-0318-7.

22. Jun, J.J., Steinmetz, N.A., Siegle, J.H., Denman, D.J., Bauza, M., Barbarits, B., Lee, A.K., Anastassiou, C.A., Andrei, A., Aydın, Ç., et al. (2017). Fully integrated silicon probes for high-density recording of neural activity. Nature *551*, 232-236. 10.1038/nature24636.

23. Petersen, C.C. (2007). The functional organization of the barrel cortex. Neuron *56*, 339-355. S0896-6273(07)00715-5 [pii]
10.1016/j.neuron.2007.09.017.

24. He, C.X., Cantu, D.A., Mantri, S.S., Zeiger, W.A., Goel, A., and Portera-Cailliau, C. (2017). Tactile Defensiveness and Impaired Adaptation of Neuronal Activity in the Fmr1 Knock-Out Mouse Model of Autism. J Neurosci *37*, 6475-6487. 10.1523/JNEUROSCI.0651-17.2017.

25. Gründemann, J., Bitterman, Y., Lu, T., Krabbe, S., Grewe, B.F., Schnitzer, M.J., and Lüthi, A. (2019). Amygdala ensembles encode behavioral states. Science *364*. 10.1126/science.aav8736.

26. Fustiñana, M.S., Eichlisberger, T., Bouwmeester, T., Bitterman, Y., and Lüthi, A. (2021). State-dependent encoding of exploratory behaviour in the amygdala. Nature. 10.1038/s41586-021-03301-z.

27. Corder, G., Ahanonu, B., Grewe, B.F., Wang, D., Schnitzer, M.J., and Scherrer, G. (2019). An amygdalar neural ensemble that encodes the unpleasantness of pain. Science *363*, 276-281. 10.1126/science.aap8586.

28. Tye, K.M. (2018). Neural Circuit Motifs in Valence Processing. Neuron *100*, 436-452. 10.1016/j.neuron.2018.10.001.

29. Beyeler, A., Chang, C.J., Silvestre, M., Leveque, C., Namburi, P., Wildes, C.P., and Tye, K.M. (2018). Organization of Valence-Encoding and Projection-Defined Neurons in the Basolateral Amygdala. Cell Rep *22*, 905-918. 10.1016/j.celrep.2017.12.097.

30. Allsop, S.A., Wichmann, R., Mills, F., Burgos-Robles, A., Chang, C.J., Felix-Ortiz, A.C., Vienne, A., Beyeler, A., Izadmehr, E.M., Glober, G., et al. (2018). Corticoamygdala Transfer of Socially Derived Information Gates Observational Learning. Cell *173*, 1329-1342.e1318. 10.1016/j.cell.2018.04.004.

31. Akiti, K., Tsutsui-Kimura, I., Xie, Y., Mathis, A., Markowitz, J.E., Anyoha, R., Datta, S.R., Mathis, M.W., Uchida, N., and Watabe-Uchida, M. (2022). Striatal dopamine explains novelty-induced behavioral dynamics and individual variability in threat prediction. Neuron *110*, 3789-3804.e3789. 10.1016/j.neuron.2022.08.022.

32. Valjent, E., and Gangarossa, G. (2021). The Tail of the Striatum: From Anatomy to Connectivity and Function. Trends Neurosci *44*, 203-214. 10.1016/j.tins.2020.10.016.

33. Krüttner, S., Falasconi, A., Valbuena, S., Galimberti, I., Bouwmeester, T., Arber, S., and Caroni, P. (2022). Absence of familiarity triggers hallmarks of autism in mouse model through aberrant tail-of-striatum and prelimbic cortex signaling. Neuron *110*, 1468-1482.e1465. 10.1016/j.neuron.2022.02.001.

34. Luo, T.Z., Bondy, A.G., Gupta, D., Elliott, V.A., Kopec, C.D., and Brody, C.D. (2020). An approach for long-term, multi-probe Neuropixels recordings in unrestrained rats. Elife *9*. 10.7554/eLife.59716.

35. Pachitariu M, S.N., Kadir S, Carandini M, Harris K. (2016). Kilosort: realtime spike-sorting for extracellular electrophysiology with hundreds of channels. bioRxiv.

36. Hill, D.N., Mehta, S.B., and Kleinfeld, D. (2011). Quality metrics to accompany spike sorting of extracellular signals. J Neurosci *31*, 8699-8705. 10.1523/jneurosci.0971-11.2011.

37. O'Connor, D.H., Peron, S.P., Huber, D., and Svoboda, K. (2010). Neural activity in barrel cortex underlying vibrissa-based object localization in mice. Neuron *67*, 1048-1061. 10.1016/j.neuron.2010.08.026.

38. Minamisawa, G., Kwon, S.E., Chevée, M., Brown, S.P., and O'Connor, D.H. (2018). A Non-canonical Feedback Circuit for Rapid Interactions between Somatosensory Cortices. Cell Rep *23*, 2718-2731.e2716. 10.1016/j.celrep.2018.04.115.

39. Rahmatullah, N., Schmitt, L.M., De Stefano, L., Post, S., Robledo, J., Chaudhari, G., Pedapati, E., Erickson, C., Portera-Cailliau, C., and Goel, A. (2023). Hypersensitivity to Distractors in Fragile X Syndrome from Loss of Modulation of Cortical VIP Interneurons. J Neurosci *43*, 8172-8188. 10.1523/jneurosci.0571-23.2023.

40. Li, Y., Mathis, A., Grewe, B.F., Osterhout, J.A., Ahanonu, B., Schnitzer, M.J., Murthy, V.N., and Dulac, C. (2017). Neuronal Representation of Social Information in the Medial Amygdala of Awake Behaving Mice. Cell *171*, 1176-1190.e1117. 10.1016/j.cell.2017.10.015.

41. Mathis, A., Mamidanna, P., Cury, K.M., Abe, T., Murthy, V.N., Mathis, M.W., and Bethge, M. (2018). DeepLabCut: markerless pose estimation of user-defined body parts with deep learning. Nat Neurosci *21*, 1281-1289. 10.1038/s41593-018-0209-y.

42. Syeda, A., Zhong, L., Tung, R., Long, W., Pachitariu, M., and Stringer, C. (2023). FaceMap: a framework for modeling neural activity based on orofacial tracking. Nat Neurosci. 10.1038/s41593-023-01490-6.

43. Miura, S.K., and Scanziani, M. (2022). Distinguishing externally from saccade-induced motion in visual cortex. Nature *610*, 135-142. 10.1038/s41586-022-05196-w.

44. Guenthner, C.J., Miyamichi, K., Yang, H.H., Heller, H.C., and Luo, L. (2013). Permanent genetic access to transiently active neurons via TRAP: targeted recombination in active populations. Neuron *78*, 773-784. 10.1016/j.neuron.2013.03.025.

45. Terburg, D., Scheggia, D., Triana Del Rio, R., Klumpers, F., Ciobanu, A.C., Morgan, B., Montoya, E.R., Bos, P.A., Giobellina, G., van den Burg, E.H., et al. (2018). The Basolateral

Amygdala Is Essential for Rapid Escape: A Human and Rodent Study. Cell *175*, 723-735.e716. 10.1016/j.cell.2018.09.028.

46. Sengupta, A., Yau, J.O.Y., Jean-Richard-Dit-Bressel, P., Liu, Y., Millan, E.Z., Power, J.M., and McNally, G.P. (2018). Basolateral Amygdala Neurons Maintain Aversive Emotional Salience. J Neurosci *38*, 3001-3012. 10.1523/jneurosci.2460-17.2017.

47. Gao, C., Leng, Y., Ma, J., Rooke, V., Rodriguez-Gonzalez, S., Ramakrishnan, C., Deisseroth, K., and Penzo, M.A. (2020). Two genetically, anatomically and functionally distinct cell types segregate across anteroposterior axis of paraventricular thalamus. Nat Neurosci *23*, 217-228. 10.1038/s41593-019-0572-3.

48. Gehrlach, D.A., Dolensek, N., Klein, A.S., Roy Chowdhury, R., Matthys, A., Junghänel, M., Gaitanos, T.N., Podgornik, A., Black, T.D., Reddy Vaka, N., et al. (2019). Aversive state processing in the posterior insular cortex. Nat Neurosci *22*, 1424-1437. 10.1038/s41593-019-0469-1.

49. de Kloet, S.F., Bruinsma, B., Terra, H., Heistek, T.S., Passchier, E.M.J., van den Berg, A.R., Luchicchi, A., Min, R., Pattij, T., and Mansvelder, H.D. (2021). Bi-directional regulation of cognitive control by distinct prefrontal cortical output neurons to thalamus and striatum. Nat Commun *12*, 1994. 10.1038/s41467-021-22260-7.

50. Li, W.R., Nakano, T., Mizutani, K., Matsubara, T., Kawatani, M., Mukai, Y., Danjo, T., Ito, H., Aizawa, H., Yamanaka, A., et al. (2023). Neural mechanisms underlying uninstructed orofacial movements during reward-based learning behaviors. Curr Biol *33*, 3436-3451.e3437. 10.1016/j.cub.2023.07.013.

51. Ebbesen, C.L., and Froemke, R.C. (2021). Body language signals for rodent social communication. Curr Opin Neurobiol *68*, 91-106. 10.1016/j.conb.2021.01.008.

52. Lim, K.Y., and Hong, W. (2023). Neural mechanisms of comforting: Prosocial touch and stress buffering. Horm Behav *153*, 105391. 10.1016/j.yhbeh.2023.105391.

53. Gothard, K.M., and Fuglevand, A.J. (2022). The role of the amygdala in processing social and affective touch. Curr Opin Behav Sci *43*, 46-53. 10.1016/j.cobeha.2021.08.004.

54. Ayaz, A., Stäuble, A., Hamada, M., Wulf, M.A., Saleem, A.B., and Helmchen, F. (2019). Layer-specific integration of locomotion and sensory information in mouse barrel cortex. Nat Commun *10*, 2585. 10.1038/s41467-019-10564-8.

55. Gangarossa, G., Castell, L., Castro, L., Tarot, P., Veyrunes, F., Vincent, P., Bertaso, F., and Valjent, E. (2019). Contrasting patterns of ERK activation in the tail of the striatum in response to aversive and rewarding signals. J Neurochem *151*, 204-226. 10.1111/jnc.14804.

56. de Kock, C.P., and Sakmann, B. (2009). Spiking in primary somatosensory cortex during natural whisking in awake head-restrained rats is cell-type specific. Proc Natl Acad Sci U S A *106*, 16446-16450. 10.1073/pnas.0904143106.

57. Peters, A.J., Fabre, J.M.J., Steinmetz, N.A., Harris, K.D., and Carandini, M. (2021). Striatal activity topographically reflects cortical activity. Nature *591*, 420-425. 10.1038/s41586-020-03166-8.

58. Pidoux, M., Mahon, S., Deniau, J.M., and Charpier, S. (2011). Integration and propagation of somatosensory responses in the corticostriatal pathway: an intracellular study in vivo. J Physiol *589*, 263-281. 10.1113/jphysiol.2010.199646.

59. Chen, P., and Hong, W. (2018). Neural Circuit Mechanisms of Social Behavior. Neuron *98*, 16-30. 10.1016/j.neuron.2018.02.026.

60. Melin, M.D., Churchland, A.K., and Couto, J. (2023). Large scale, simultaneous chronic neural recordings from multiple brain areas. bioRxiv. 10.1101/2023.12.22.572441.

61. Jia, X., Siegle, J.H., Durand, S., Heller, G., Ramirez, T.K., Koch, C., and Olsen, S.R. (2022). Multi-regional module-based signal transmission in mouse visual cortex. Neuron *110*, 1585-1598.e1589. 10.1016/j.neuron.2022.01.027.

CHAPTER 4: Differential Representation of Social Touch in Cortical, Striatal and Amygdalar Circuits of an Autism Model

4.1 Introduction

Individuals with ASD often demonstrate aversion to social touch which can lead them to avoid social touch interactions[1-5]. Given that the previous chapter showed that somatosensory cortical, striatal and amygdalar regions encode social facial touch, and with varying degrees, ASD rodent models may demonstrate changes in the neuronal dynamics of these circuits that could explain their increased aversion to social touch[4]. Furthermore, it is not known if in ASD whether these relevant brains regions perceive social touch as aversive even when there is flexibility to engage in social touch (voluntary touch).

In this chapter, we replicated the in vivo electrophysiological recordings described in chapter 3 with the Fragile X Syndrome (FXS) mouse model of autism (*Fmr1* KO) to determine how social touch is differentially represented in vS1, tS and BLA and how these regions contribute to stronger aversion of social touch in this model. We find that *Fmr1* KO mice show similar neuronal responses of vS1, tS and BLA cells between social and object touch contrary to our observations in WT mice. Furthermore, we find that the inability to distinguish between social and object touch also occurs at both the circuit and behavioral level in *Fmr1* KO mice. Finally, we show that *Fmr1* KO mice show a similar proportion of cells relevant for aversive behaviors in social and object touch. This is different from WT mice that show a larger proportion of behaviorally relevant cells for object than social touch.

4.2 Materials & Methods

4.2.1: Experimental model and animal details

A cohort of *Fmr1* KO mice (>20 g in weight, 5 males and 5 females) was used for electrophysiological recordings and were derived from the following line: *Fmr1* KO (JAX line 003025)[6,7].

All *Fmr1* KO mice were group-housed with access to food and water (HydroGel, ClearH_2O) *ad libitum* under a 12:12 hour light-dark cycle in controlled temperature conditions. All experiments were done in the light cycle. *Fmr1* KO mice with Neuropixels implants were single housed during habituation and behavioral testing (~2 weeks) to avoid damage to the implant that could have occurred by other animals in group housing. We followed the U.S. National Institutes of Health guidelines for animal research under an animal use protocol (ARC #2007-035) approved by the Chancellor's Animal Research Committee and Office for Animal Research Oversight at the University of California, Los Angeles.

4.2.2: Surgical implantation of Neuropixels probes for chronic recordings

Fmr1 KO mice were surgically implanted with Neuropixels probes for chronic recordings in a similar manner to the Neuropixels chronic implantations of WT mice described in chapter 3.

4.2.3: Social touch assay in Fmr1 KO mice with chronic Neuropixels implants

Following probe implantation, *Fmr1* KO test mice were subjected to the social touch assay. *Fmr1* KO mice with Neuropixels implants were habituated to head restraint, to running on the polystyrene ball, and to the behavioral apparatus for 7-9 d.

After habituation, *Fmr1* KO test mice were subjected to both voluntary and forced interactions with a visitor mouse or a novel inanimate object over the course of 2 d similar to the way WT mice underwent the assay in chapter 3.

4.2.4: Electrophysiological recordings

Data acquisition from electrophysiological recordings was done in a similar manner for *Fmr1* KO mice as described in chapter 3 such that electrical signals could be acquired from vS1 and BLA simultaneously, as well as tS. Only single units were used for electrophysiological data

analysis and the same post-processing quality metrics used on WT electrophysiological data was used on *Fmr1* KO data.

4.2.5: Removal of Neuropixels probes

Neuropixels probes were also explanted (see chapter 3 Materials & Methods) from *Fmr1* KO mice for re-use. After explantation, the probe shank was fully immersed in 1% tergazyme (Alconox) for 24-48 h, followed by a 1-2 h rinse in distilled water.

4.2.6: Histology and fluorescence imaging of probe location

Following probe removal, *Fmr1* KO mice were anaesthetized with 5% isoflurane and transcardially perfused with 4% PFA and post-fixed overnight. Histology and fluorescent imaging were done post-fixation to visualize DiI fluorescence of the probe tract similar to WT mice in chapter 3.

4.2.7: Electrophysiological data analysis

All analysis used for electrophysiological data of WT mice in chapter 3 was applied similarly to electrophysiological data of *Fmr1* KO mice. This includes generation of PSTHs, unbiased clustering of single unit responses, modulation indices, ROC for stimulus preference and behavior and decoding with SVMs.

4.2.8: Data analysis of behavioral data

Videos of the test *Fmr1* KO mice's eye, face and body were also recorded using the same cameras as WT mice. All the following behaviors were analyzed from the videos of *Fmr1* KO mice as described for the WT mice in chapter 3: running direction, pupil saccades, AFEs and facial motion.

4.2.9: Statistical analyses

Behavioral and electrophysiological data acquired from WT mice in chapter 3 were used for statistical comparisons with behavioral and electrophysiological data recorded from the *Fmr1* KO mice. Statistical tests were performed in Prism software (GraphPad). Statistical analyses of normality (Lilliefors and Shapiro Wilk tests) were performed on each data set. Multiple comparisons of neural or behavioral data across touch conditions and genotypes were analyzed using two-way ANOVA with post-hoc Bonferroni's test. If data deviated from normality ($p<0.05$) or not ($p>0.05$), we applied a logarithmic transformation on the data and compared the two-way ANOVA with and without the transformation. Since the statistical output of the two-way ANOVA was similar for the transformed and the non-transformed, non-normal data, we used the statistical output from the latter. Graphs in Figs. 4-1b-h and Supp Fig. 4-1.2 show statistics using the number of single units or cells as the sample size, but all the rest of the figure panels the statistics were done using individual mice as the sample size (averaged over cells for different mice) superimposed on individual data points. Because there are important sex differences in both the prevalence and symptoms of ASD[8,9], we also distinguished males from females across all figures.

4.3: Results

4.3.1: Fmr1 KO mice exhibit similar avoidance/AFEs to social and object touch (greater avoidance and AFEs to social touch than WT mice)

Chapter 2 showed that the *Fmr1* KO mice, a model of Fragile X syndrome that is widely used to study behavioral and circuit changes in autism, manifest more avoidance and AFEs to social touch than WT mice. In fact, *Fmr1* KO mice displayed similar negative reactions to both object and social stimuli and demonstrated noticeable AFEs (whisker protraction and orbital tightening) to unwanted facial touch during forced interactions. Thus, we felt that *Fmr1* KO mice could be useful to understand the circuits underlying behavioral responses to aversive social facial touch.

Fmr1 KO mice implanted with Neuropixels probes (n=10 mice) displayed similar avoidance/AFE responses to social touch as those we had previously reported (during the first 5 presentations). *Fmr1* KO mice showed no difference in running avoidance or whisker protraction between social and object touch during voluntary interactions (**Fig. 4-1a**; p>0.999 and p=0.542, respectively). However, they did show slightly more aversive whisker protraction to object touch during forced interactions (**Fig. 4-1a**; p=0.010). Orbital area was smaller (squinting) during forced social touch compared to voluntary social touch in *Fmr1 KO* (**Fig. 4-1a**; p=0.061), suggesting that voluntary touch was somewhat better tolerated than forced touch in this cohort.

When comparing the two genotypes, we once again observed significant differences in the responses to social touch that matched our previous results, with *Fmr1* KO mice showing greater avoidance and aversive whisker protraction to social facial touch that WT controls (**Fig. 4-1a**).

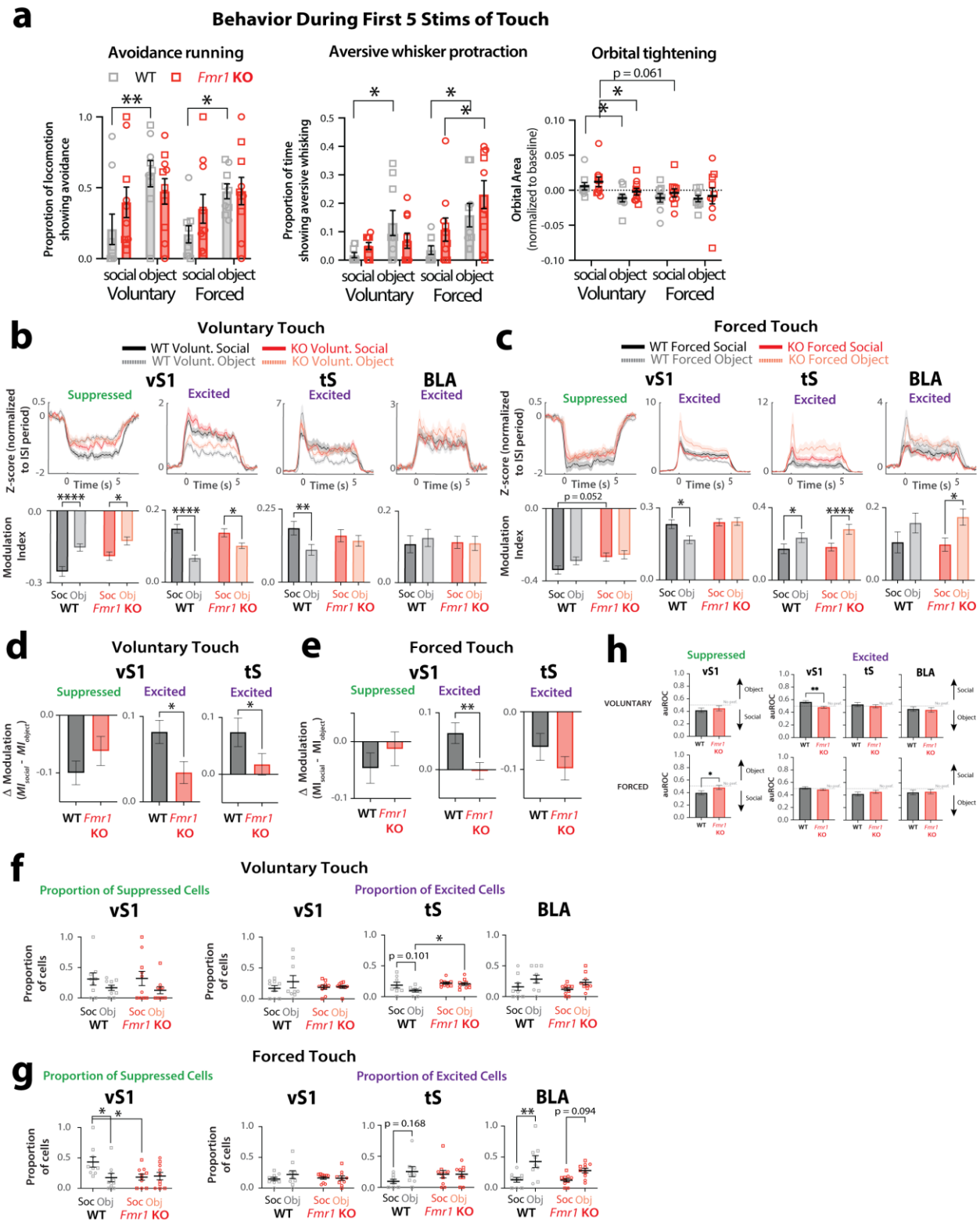
a
Behavior During First 5 Stims of Touch
Avoidance running
WT
Fmr1 KO
Proprotion of locomotion showing avoidance
social object social object
Voluntary Forced
Aversive whisker protraction
Proportion of time showing aversive whisking
Orbital tightening
p = 0.061
Orbital Area (normalized to baseline)
b
Voluntary Touch
WT Volunt. Social
KO Volunt. Social
WT Volunt. Object
KO Volunt. Object
vS1
tS
BLA
Suppressed
Excited
Z-score (normalized to ISI period)
Time (s)
Modulation Index
Soc Obj
WT
Fmr1 KO
c
Forced Touch
WT Forced Social
KO Forced Social
WT Forced Object
KO Forced Object
p = 0.052
d
Voluntary Touch
Δ Modulation (MI social - MI object)
e
Forced Touch
h
VOLUNTARY
FORCED
auROC
Object
Social
f
Voluntary Touch
Proportion of Suppressed Cells
Proportion of Excited Cells
Proportion of cells
p = 0.101
g
Forced Touch
p = 0.168
p = 0.094

Fig. 4-1: *Fmr1* KO mice show differences in avoidance behaviors and aversive facial expressions and neuronal responses to voluntary and forced social and object touch relative to WT mice.

a. Running avoidance (backwards to left or right) is higher in wild type mice for voluntary and forced object touch than social touch, but not *Fmr1* KO mice for first 5 stimulations of touch. The fraction of time *Fmr1* KO mice exhibited prolonged whisker protraction was similar between voluntary social and object touch but higher in forced object than social touch. Orbital area during touch is normalized to area before touch (object or mouse visible but no touch). Orbital area is not significantly different between forced object and social touch in both WT and *Fmr1* KO mice in the first 5 stimulations, but is higher in voluntary social than object touch. Squares=males, circles=females. **p<0.01, *p<0.05 for two-way ANOVA with Bonferroni's. No mice were excluded according to ROUT's analysis.

b. Z-score firing of vS1 suppressed and excited, tS excited and BLA excited cells during voluntary social versus object touch. Modulation index of vS1 RS excited and suppressed, tS excited and BLA excited cells to voluntary social versus object touch as an average of all 40 stimulations. ****p<0.001, **p<0.01, *p<0.05 for two-way ANOVA with Bonferroni's. Each marker represents a single cell taken from across 9 WT mice or 10 *Fmr1* KO mice.

c. Z-score firing of vS1 suppressed and excited, tS excited and BLA excited cells during forced social versus object touch. Modulation index of vS1 RS excited and suppressed, tS excited and BLA excited cells to forced social versus object touch as an average of all 40 stimulations of touch. ****p<0.001, *p<0.05 for two-way ANOVA with Bonferroni's. Each marker represents a single cell taken from across 9 WT mice or 10 *Fmr1* KO mice.

d. Δ modulation ($MI_{social} - MI_{object}$) of voluntary touch for vS1 suppressed and excited and tS excited cells between WT and *Fmr1* KO mice. *p<0.05 for unpaired nonparametric or parametric t-test.

e. Δ modulation ($MI_{social} - MI_{object}$) of forced touch for vS1 suppressed and excited and tS excited cells between WT and *Fmr1* KO mice. *p<0.05 for unpaired nonparametric or parametric t-test.

f. Number of object and social preferring cells in vS1, tS and BLA excited and vS1 suppressed cells for voluntary touch as a proportion of total cells in each brain region per mouse for WT versus *Fmr1* KO mice. *p<0.05 for two-way ANOVA with Bonferroni's. Squares=males, circles=females. **g.** Number of object and social preferring cells in vS1, tS and BLA excited and vS1 suppressed cells for forced touch as a proportion of total cells in each brain region per mouse for WT versus *Fmr1* KO mice. **p<0.01 for two-way ANOVA with Bonferroni's. Squares=males, circles=females. **h.** auROC values for excited vS1, tS and BLA and suppressed vS1 cells. auROC value above 0.5 for excited cells corresponds to social touch preference and below 0.5 to object touch preference. auROC value below 0.5 for suppressed cells corresponds to social touch preference and above 0.5 to object touch preference. auROC value at 0.5 corresponds to no preference for object versus social touch. All auROC values regardless of if they were statistically significant were included. **p<0.01, *p<0.05 for unpaired parametric t-test.

vS1, tS and BLA neurons in *Fmr1* KO mice are not differentially modulated by social vs. object touch, unlike WT controls

Just as for WT mice, we used Neuropixels to record from units in vS1, tS and BLA of *Fmr1* KO mice and used the same clustering approach, once again combining neurons that were strongly suppressed or excited by touch for each brain region. The proportion of units in various clusters differed in *Fmr1* KO mice compared to WT mice (**Supp. Fig. 4-1.1a**). For example, in vS1 there were significantly fewer cells in Cl. 2 and more in Cl. 5 in *Fmr1* KO mice, which are the clusters that in WT mice are the most modulated by social touch (**Supp. Fig. 4-1.1b;** $p<0.05$). When comparing how excited neurons were modulated by social vs. object touch across the three brain regions, we found that, in general, neurons in *Fmr1* KO mice responded more similarly to both types of touch than those in WT mice (**Fig. 4-1b-c**; voluntary: vS1 suppressed WT $p<0.001$, *Fmr1* KO $p=0.014$, vS1 excited WT $p<0.001$, *Fmr1* KO $p=0.013$, tS excited WT $p=0.007$, *Fmr1* KO $p=0.583$; forced: vS1 excited WT $p=0.020$, *Fmr1* KO $p=0.989$). The only exception was found in the tS and BLA under forced touch conditions, where neurons excited by touch were more strongly modulated by object touch in *Fmr1* KO mice (**Fig. 4-1c**; forced: tS excited WT $p=0.036$, *Fmr1* KO $p=0.001$, BLA excited WT $p=0.246$, *Fmr1* KO $p=0.015$). Indeed, when comparing the difference in modulation (Δ modulation) between social and object touch across brain regions, we found that *Fmr1* KO mice uniformly had significantly smaller magnitudes of difference (**Fig. 4-1d-e**; voluntary: vS1 excited $p=0.013$, tS excited $p=0.038$; forced: vS1 excited $p=0.005$). On the other hand, BLA cells of *Fmr1* KO mice did not show differences in the change in modulation compared to WT mice ($p>0.05$, not shown).

Next, we compared the responses of FS units between WT and *Fmr1* KO mice because previous studies have shown parvalbumin inhibitory interneurons in vS1 and V1 are hypoactive in the model of FXS and that boosting PV cell firing can ameliorate sensory processing in these regions[10,11]. Because of the small number of cells in tS and BLA relative to vS1 across mice, we focused on just vS1 FS cells. Just like for RS cells, FS units in vS1 of *Fmr1* KO mice showed

similar modulation by social and object touch, in contrast to those of WT mice (**Supp. Fig. 4-1.2a**; voluntary: WT p=0.038, *Fmr1* KO p=0.616; forced: WT p<0.001, *Fmr1* KO p=0.909). Under forced conditions, FS neurons were much less modulated by social touch in *Fmr1* KO mice than in WT controls (**Supp. Fig. 4-1.2a**; p=0.017). Similar loss of modulation of inhibitory interneurons by sensory stimuli has been described in *Fmr1* KO mice[10,12].

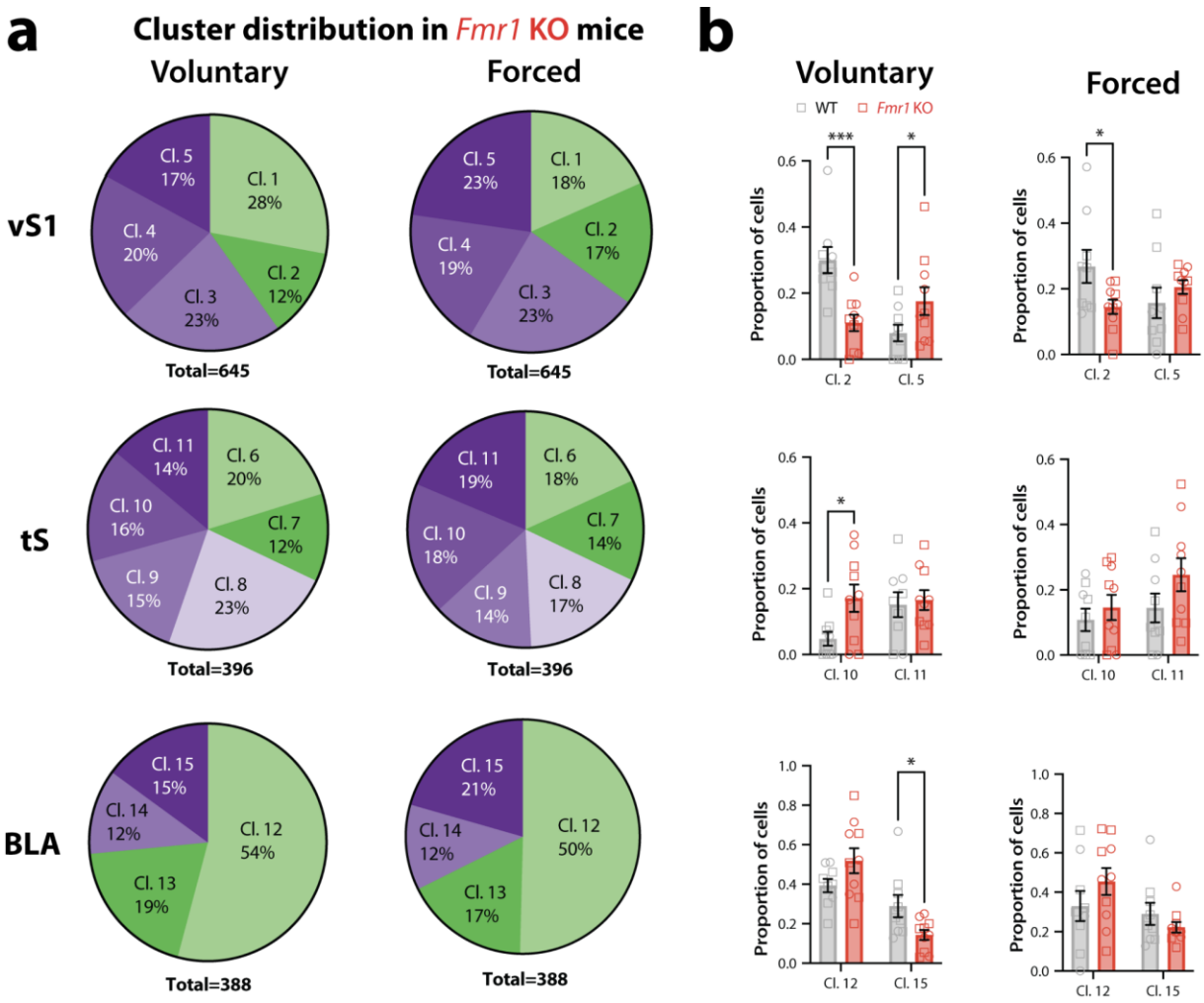
a
Cluster distribution in Fmr1 KO mice
Voluntary
Forced
vS1
Cl. 5 17%
Cl. 1 28%
Cl. 4 20%
Cl. 2 12%
Cl. 3 23%
Total=645
Cl. 5 23%
Cl. 1 18%
Cl. 2 17%
Cl. 4 19%
Cl. 3 23%
Total=645
tS
Cl. 11 14%
Cl. 6 20%
Cl. 10 16%
Cl. 7 12%
Cl. 9 15%
Cl. 8 23%
Total=396
Cl. 11 19%
Cl. 6 18%
Cl. 10 18%
Cl. 7 14%
Cl. 9 14%
Cl. 8 17%
Total=396
BLA
Cl. 15 15%
Cl. 14 12%
Cl. 12 54%
Cl. 13 19%
Total=388
Cl. 15 21%
Cl. 14 12%
Cl. 12 50%
Cl. 13 17%
Total=388
b
Voluntary
Forced
WT
Fmr1 KO
Proportion of cells
Cl. 2
Cl. 5
Cl. 10
Cl. 11
Cl. 12
Cl. 15

Supplementary Fig. 4-1.1: Proportion of total cells in each cluster differs within *Fmr1* KO and between WT and *Fmr1* KO mice.

a. Number of cells in each cluster as a proportion of total cells for vS1, tS and BLA from all *Fmr1* KO mice for voluntary touch (left). Number of cells in each cluster as a proportion of total cells for vS1, tS and BLA from all *Fmr1* KO mice for forced touch (right).

b. Number of cells in vS1 Cl. 2 & 5, tS Cl. 10 & 11 and BLA Cl. 12 & 15 as a proportion of total cells within the corresponding brain region per mouse for WT and *Fmr1* KO mice during voluntary touch (left). Number of cells in vS1 Cl. 2 & 5, tS Cl. 10 & 11 and BLA Cl. 12 & 15 as a proportion of total cells within the corresponding brain region per mouse for WT and *Fmr1* KO mice during forced touch (right). ***$p<0.01$, *$p<0.05$ for unpaired parametric t-test WT vs *Fmr1* KO for each cluster. Squares=males, circles=females.

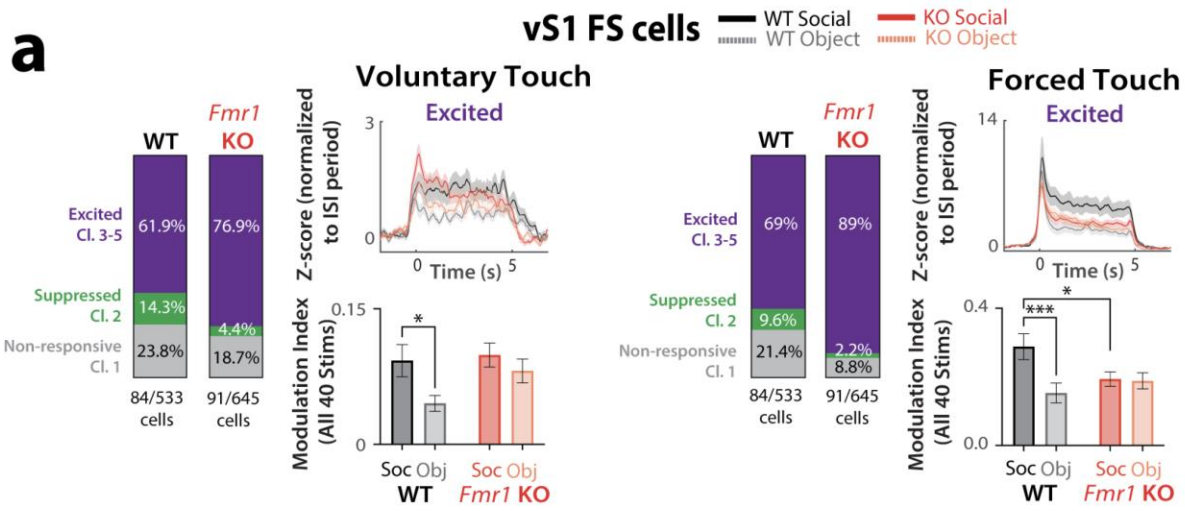
a
vS1 FS cells
WT Social
WT Object
KO Social
KO Object
Voluntary Touch
Forced Touch
WT
Fmr1 KO
Excited Cl. 3-5
Suppressed Cl. 2
Non-responsive Cl. 1
61.9%
76.9%
14.3%
4.4%
23.8%
18.7%
69%
89%
9.6%
2.2%
21.4%
8.8%
84/533 cells
91/645 cells
Excited
Z-score (normalized to ISI period)
Time (s)
Modulation Index (All 40 Stims)
Soc Obj
WT
Fmr1 KO

Supplementary Fig. 4-1.2: vS1 FS suppressed and excited cells show differences in modulation to voluntary and forced object touch in WT versus *Fmr1* KO mice.

a. Proportion of suppressed (Cl. 2) and excited cells (Cl. 3-5) as a total of all FS vS1 cells (84 FS cells for WT & 91 for *Fmr1* KO mice) for voluntary and forced touch in WT versus *Fmr1* KO mice. Z-score firing of vS1 FS excited cells during voluntary and forced social versus object touch for WT and *Fmr1* KO mice. Modulation index of vS1 FS excited cells to voluntary and forced social and object touch in WT versus *Fmr1* KO mice as an average of all 40 stimulations. *p<0.01, ***p<0.001 for two-way ANOVA with Bonferroni's.

4.3.2: Fmr1 KO mice show similar proportions of object and social preferring cells across brain regions compared to wild types, except for BLA excited cells

We then used ROC analyses to calculate the proportion of social and object preferring excited cells in *Fmr1* KO mice. We observed no significant differences in the proportion of social- and object-preferring cells even in the BLA, contrary to what we see in WT mice for forced touch (**Fig. 4-1f-g;** *Fmr1* KO BLA p=0.094). When compared to WT mice, the proportion of object- and social-preferring cells across brain regions was similar between genotypes except for tS during voluntary touch, where there was a higher proportion of object-preferring cells, and for vS1 during forced touch, where there were fewer social-preferring cells, in *Fmr1* KO mice (**Fig. 4-1f-g**; voluntary: tS excited WT vs *Fmr1* KO p=0.028; forced: vS1 suppressed WT vs *Fmr1* KO p=0.025). We also wondered if the degree to which neurons are object-preferring or social-preferring was different between genotypes. We therefore compared the absolute auROC values (including cells with no significant preference) in vS1, tS and BLA. We only found significant differences for vS1 cells excited by voluntary touch and vS1 cells suppressed by forced touch, such that those from *Fmr1* KO mice showed less preference for social touch compared to WT mice (**Fig. 4-1h;** WT vs. *Fmr1* KO p=0.002 and p=0.045, respectively). This suggests that vS1, tS and BLA neurons from *Fmr1* KO mice show less discrimination in their preference for social or object touch relative to WT controls.

When looking at these data from *Fmr1* KO mice, we surmise that, overall, neurons in vS1 and tS respond similarly to object and social touch, which matches how, behaviorally, they tend to display avoidance and AFEs to both types of touch. This is in sharp contrast to WT mice which can discriminate better between social vs. object touch presentations both behaviorally and at the level of neural firing in vS1 and tS. On the other hand, the BLA in both genotypes showed greater preference for forced object touch (and had more object preferring cells), which may be related to the fact that forced object touch reliably produced more avoidance/AFEs in mice of both genotypes (**Fig. 4-1c,g**).

4.3.3: Decoders based on orofacial motion or avoidance behaviors and AFEs from WT mice outperform those from Fmr1 KO mice in distinguishing touch context.

Based on the behavioral results (and the Neuropixels data) described above and from chapter 3, we hypothesized that a classifier trained on WT facial motion would outperform one trained on facial motion from *Fmr1* KO mice in decoding touch context. When we trained an SVM classifier on orofacial movements using 23 DLC labels on the animal's face, we observed no significant differences in decoding of touch context between voluntary and forced touch within each genotype (**Fig. 4-2a-c**).

Under voluntary conditions in WT, decoding accuracy was highest just before the platform stopped moving, which likely coincided with the onset of first contact by the whiskers (**Fig. 4-2c**, WT bef. vs dur. $p = 0.042$). Under forced conditions, decoding accuracy peaked when the platform stopped moving and the snout of the test mouse was in direct contact with the object/visitor mouse (**Fig. 4-2b)**.

With *Fmr1* KO mice, we expected to find lower accuracy in discriminating touch context since mice react similarly to object and social touch. Indeed, we observed that decoder performance from all face labels was lower for voluntary touch in *Fmr1* KO mice relative to WT controls (**Fig. Fig. 4-2c**, $p=0.069$), although we saw little difference for forced touch interactions ($p=0.876$). A decoder using only the whisker DLC labels from WT mice also performed better than a decoder from using whisker labels from *Fmr1* KO mice (**Fig. 4-2d**, WT vs. *Fmr1* KO voluntary $p=0.009$, forced $p=0.470$).

We found striking differences in how WT and *Fmr1* KO mice respond to social and object facial touch in both this chapter and chapter 2 (**Fig. 4-1a**)**.** Mice display certain AFEs and running avoidance to unwanted touch stimuli. We therefore tested how a SVM classifier trained on these behaviors might perform in decoding touch context (**Fig. 4-2e**). We also included eye saccades because gaze avoidance is prominent in autistic children and nearly universal in those with FXS[13-16], and mice are capable of making directed saccades to different sensory stimuli, including

touch[17,18]. Strikingly, we observed that, avoidance behaviors and AFEs can decode touch context far better (accuracy >80%) than orofacial movements. Decoding accuracy decreases slightly when the platform stops, and there were no differences between voluntary and forced touch in WTs (**Fig. 4-2f-g**, p=0.221). Decoder performance was slightly worse in *Fmr1* KO mice compared to WT controls for forced touch but the difference was not significant (**Fig. 4-2f-g**, p=0.172). Together, these results suggest that WT and *Fmr1* KO mice differ greatly in their ability to distinguish voluntary or forced social and object touch based on orofacial movements or aversive behaviors.

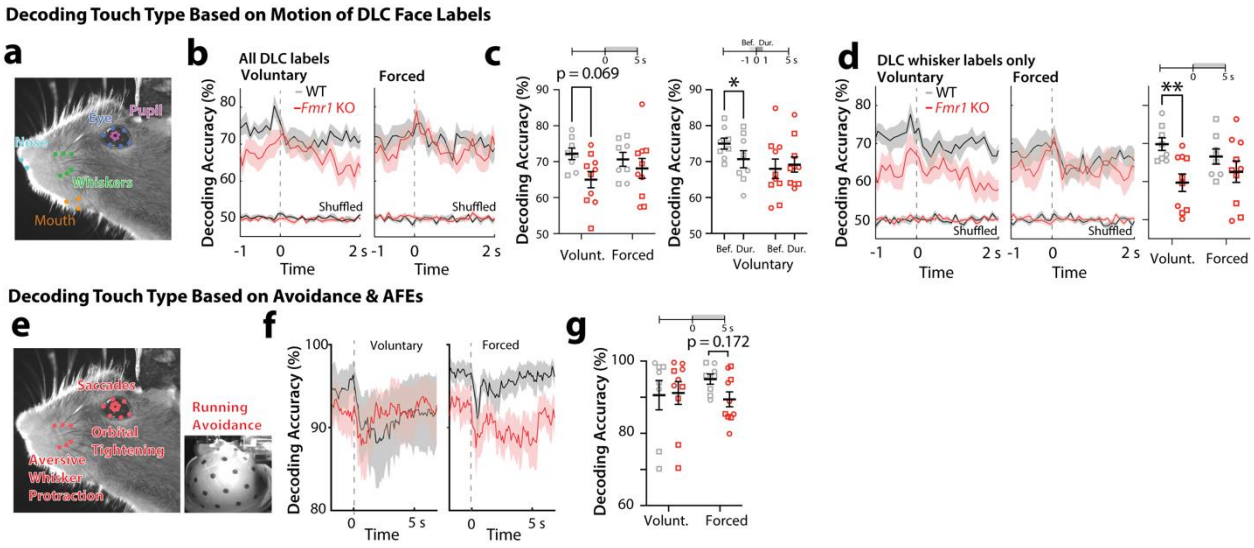
Decoding Touch Type Based on Motion of DLC Face Labels
a
Eye
Pupil
Nose
Whiskers
Mouth
b
All DLC labels
Voluntary
Forced
WT
Fmr1 KO
Shuffled
Decoding Accuracy (%)
Time
c
p = 0.069
*
Volunt.
Forced
Bef. Dur.
Voluntary
d
DLC whisker labels only
**
Decoding Touch Type Based on Avoidance & AFEs
e
Saccades
Orbital Tightening
Aversive Whisker Protraction
Running Avoidance
f
g
p = 0.172

Fig. 4-2: Orofacial movements and avoidance behaviors and AFEs perform worse at decoding context of touch in *Fmr1* KO mice compared to WTs.

a. Motion of features on the face of WT or *Fmr1* KO mice can be acquired by using DLC to label individual points and then using MATLAB to determine how these labels change their position over time.

b. Decoding accuracy for object versus social voluntary and forced touch using all 23 DLC labels across 100 ms time bins from 1 s before the onset of touch to 2 s after the onset of touch using an SVM classifier in WT and *Fmr1* KO mice.

c. Motion from DeepLabCut (DLC) labels on animal's face mildly lowers decoding accuracy for object and social touch in *Fmr1KO* mice compared to WT mice. WT mice show a decrease in decoding accuracy for before versus during voluntary touch whereas *Fmr1KO* mice consistently show low decoding accuracy at both time points. *p<0.05 for two-way ANOVA with Bonferroni's. Squares=males, circles=females. No mice were excluded according to ROUT's analysis.

d. Decoding accuracy for object versus social voluntary and forced touch using all whisker DLC labels across 100 ms time bins from 1 s before the onset of touch to 2 s after the onset of touch using an SVM classifier in WT and *Fmr1* KO mice. Motion from DLC labels on animal's whiskers significantly lowers decoding accuracy for voluntary object and social touch in *Fmr1KO* mice compared to WT mice. **p<0.01 for two-way ANOVA with Bonferroni's. Squares=males, circles=females. No mice were excluded according to ROUT's analysis.

e. Avoidance behaviors and AFEs of WT and *Fmr1* KO can be acquired by using DLC to label individual points and then using MATLAB measure these behaviors that can then be inputted into an SVM classifier.

f. Decoding accuracy for object versus social voluntary and forced touch using avoidance behaviors and AFEs across 100 ms time bins from 1 s before the onset of touch to 2 s after the onset of touch using an SVM classifier in WT and *Fmr1* KO mice.

g. Avoidance behaviors and AFEs show lower decoding accuracy for object and social touch in *Fmr1* KO mice compared to WT mice for forced touch. $p>0.05$ for two-way ANOVA with Bonferroni's. Squares=males, circles=females. No mice were excluded according to ROUT's analysis.

4.3.4: vS1, tS and BLA cells responsive to avoidance and AFEs are recruited more during forced touch and in social touch for Fmr1 KO mice.

Given that *Fmr1* KO mice are unable to distinguish social from object touch at the circuit, in vS1 and tS, and behavioral level, we finally asked if these regions recruit cells that respond to running avoidance and AFEs and if more of these cells are present in *Fmr1* KO mice. ROC analyses were used to identify cells that showed increased firing following the onset of either running avoidance, aversive whisker protraction or orbital tightening. The z-score firing of these cells was much lower during periods in which the animal displayed the opposite behavior (bouts of forward running instead of avoidance, backward running) or didn't display the behavior at all (bouts where AFEs were not present) (**Fig. 4-3a**).

We first assessed how prevalent these cells are during voluntary or forced touch regardless of if the voluntary or forced touch was from a novel object or stranger mouse. The percent of behaviorally relevant cells (i.e. cells that responded to avoidance running, whisker protraction or orbital tightening) in WT mice was higher in forced than voluntary touch particularly in vS1 and tS (**Fig. 4-3b,** vS1 p=0.063, tS p=0.037, BLA p=0.102).

Given that these behaviorally relevant cells were more prevalent in forced touch, we focused on this type of touch and investigated whether WT and *Fmr1* KO mice showed differences in the percentage of these cells for forced social versus object touch. Indeed, while WT mice consistently showed more of these cells for object than social touch (**Fig. 4-3c,** WT social vs. object vS1 p=0.026, tS p=0.098, BLA p =0.015), *Fmr1* KO mice had a similar percentage of these cells for both social and object touch (**Fig. 4-3c,** *Fmr1* KO social vs. object vS1 p=0.111, tS p=0.074, BLA p =0.121). These findings suggest more of these behaviorally relevant cells for avoidance running and AFEs are recruited for social touch in *Fmr1* KO mice.

Finally, while some cells in these brain regions may respond to only one type of aversive behavior over others, there could be cells in vS1, tS or BLA that show responsivity to more than one behavior. This would suggest that these cells are more likely recruited for aversive state

encoding of touch rather than a specific aversive behavior alone[19,20]. As a total of all behaviorally relevant cells, we found that a larger proportion of behaviorally relevant cells overlapped in *Fmr1* KO than in WT mice across brain regions (**Fig. 4-3d,** vS1 WT 14% vs *Fmr1* KO 39%, tS WT 17% vs *Fmr1* KO 37%, BLA WT 13% vs *Fmr1* KO 24%). When comparing the percentage of these cells responding to more than one behavior across mice, we saw minor increases, most notably in the BLA, in *Fmr1* KO relative to WT mice (**Fig. 4-3e,** BLA WT vs *Fmr1* KO p=0.134). Together, these findings suggest the vS1, tS and BLA cells may be recruited for encoding aversion more prominently in *Fmr1* KO mice.

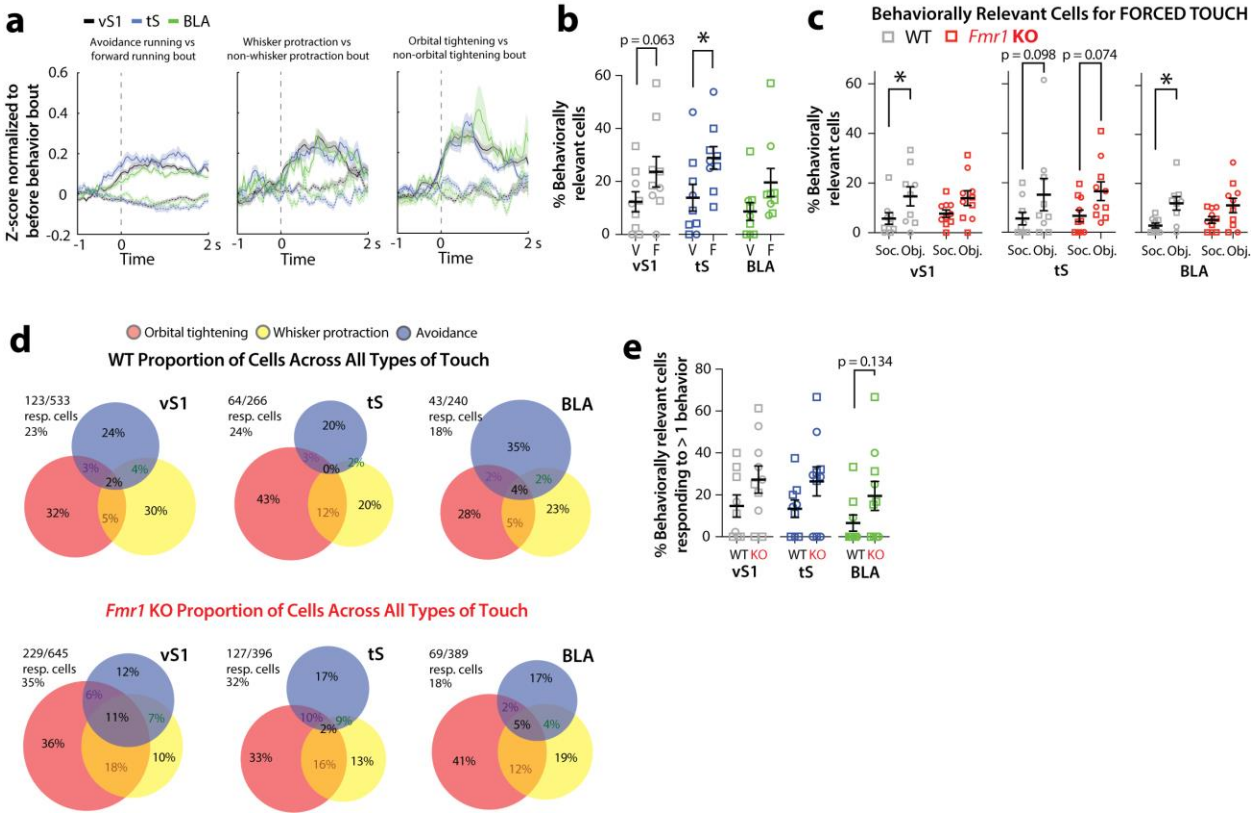
a
vS1 tS BLA
Avoidance running vs forward running bout
Whisker protraction vs non-whisker protraction bout
Orbital tightening vs non-orbital tightening bout
Z-score normalized to before behavior bout
Time
b
p = 0.063
% Behaviorally relevant cells
V F
vS1 tS BLA
c
Behaviorally Relevant Cells for FORCED TOUCH
WT Fmr1 KO
p = 0.098 p = 0.074
Soc. Obj.
vS1 tS BLA
d
Orbital tightening Whisker protraction Avoidance
WT Proportion of Cells Across All Types of Touch
123/533 resp. cells 23%
64/266 resp. cells 24%
43/240 resp. cells 18%
Fmr1 KO Proportion of Cells Across All Types of Touch
229/645 resp. cells 35%
127/396 resp. cells 32%
69/389 resp. cells 18%
e
% Behaviorally relevant cells responding to > 1 behavior
p = 0.134
WT KO

Fig. 4-3: *Fmr1* KO mice recruit more cells that respond to aversive behaviors during social touch and more cells encoding aversion relative to WT mice.

a. Z-score firing of vS1, tS and BLA cells that increase their firing during avoidance running (left), whisker protraction (middle) or orbital tightening (right). Dotted lines denote z-score firing of these behaviorally relevant cells during the opposite behavior or when the behavior is not occurring. Firing is aligned to 1 s before the onset of the behavior to 2 s after the onset of the behavior. Z-score firing was average from all bouts of behavior across all types of touch (voluntary or forced object or social touch)

b. Percentage of all behaviorally relevant cells (cells responding to avoidance running or AFEs) for vS1, tS and BLA during voluntary or forced touch (including all bouts of object and social touch). *$p<0.05$ for two-way ANOVA with Bonferroni's. Squares=males, circles=females.

c. Percentage of all behaviorally relevant cells (cells responding to avoidance running or AFEs) for vS1, tS and BLA during voluntary or forced social (Soc.) and object (Obj.) touch in WT versus *Fmr1* KO mice. *$p<0.05$ for two-way ANOVA with Bonferroni's. Squares=males, circles=females.

d. Venn diagram of all behaviorally relevant cells from all 9 WT or 10 *Fmr1* KO mice and the percentage of these cells in vS1, tS and BLA that show overlap in responding to more than one avoidance or aversive behavior. Behaviorally relevant cells were identified based on how they respond all bouts of behavior across all types of touch (voluntary or forced object or social touch).

e. Percentage of behaviorally relevant cells that respond to more than one avoidance or aversive behavior as total of all behaviorally relevant cells per mouse. Behaviorally relevant cells for each mouse were identified based on the method used in d. $p>0.05$ for two-way ANOVA with Bonferroni's. Squares=males, circles=females.

4.4: Discussion

In this chapter, we determined if the *Fmr1* KO model of autism differentially represents social and object touch in vS1, tS and BLA relative to WT mice. Our findings from this chapter suggest the following: 1. *Fmr1* KO mice shows differences in maladaptive behaviors and neuronal responses of vS1, tS and BLA cells to object and social touch relative to WT mice; 2. *Fmr1* KO mice are unable to discriminate between object and social touch primarily based on activity in vS1 and tS; 3. *Fmr1* KO facial motion is more similar during object and social touch; 4. vS1, tS and BLA contain subset of cells that preferentially respond during bouts of avoidance running or AFEs; 5. *Fmr1* KO mice have a slightly larger proportion of behaviorally relevant cells for avoidance and AFEs during forced social touch; 6. *Fmr1* KO mice tend to have more cells that may be recruited for aversive state encoding in vS1, tS and BLA.

4.4.1: Circuit differences for social touch in Fmr1 KO mice

Contrary to our results in WT mice, *Fmr1* KO mice show similar modulation of vS1, tS and BLA neurons by voluntary object and social touch, which matches their behavior: they exhibit similar degrees of running avoidance and AFEs in social and object touch. This was reflected in the reduced decoding accuracy in KO mice (compared to WT controls) for context when we used classifiers based on avoidance and aversive behaviors. On the other hand, under forced touch conditions, excited cells in tS and BLA of *Fmr1* KO are modulated far more by object touch than by social touch compared to WT mice.

Our findings first suggest that vS1 cells in *Fmr1* KO mice are unable to discriminate between the two distinct textures of a Falcon tube and a stranger mouse, particularly when the test mouse lacks the control of engaging in touch. *Fmr1* KO mice do show slower learning in discriminating different sensory stimuli and also hypersensitivity to innocuous tactile stimuli, which may reflect the inability of this model to distinguish two clearly distinct tactile stimuli in vS1[7,10]. ASD individuals also display similar sensory processing changes [3,10,21-23]. Furthermore, there are

a similar proportion of vS1 RS suppressed cells preferring forced social and object touch across *Fmr1* KO mice, further suggesting texture feature coding is impaired even when the texture of a stranger mouse is clearly distinguishable from a novel object.

The lack of discrimination between social and object touch extends to vS1 FS excited cells in *Fmr1* KO mice that show similar modulation to voluntary, and forced, social and object touch. In addition, *Fmr1* KO vS1 FS cells showed reduced modulation to forced social touch relative to WT mice, which may coincide with enhanced excitability of RS vS1 cells. A reduced density parvalbumin (PV) expressing interneurons has been reported in both FXS humans and in *Fmr1* KO mice, which could contribute to reduced inhibition of excitatory pyramidal vS1 neurons and neuronal adaptation to sensory information[10-12].

4.4.2: The role of tS and BLA in social touch aversion in ASD

Second, our findings in the neuronal responses of *Fmr1* KO mice posit that the modulation of tS and BLA cells by object and social touch in *Fmr1* KO mice correlates with the degree of avoidance and AFEs these animals exhibit to object and social touch. In voluntary touch, where *Fmr1* KO showed a similar manifestation of avoidance and AFEs to social and touch, tS (and BLA) excited cells were not differentially modulated by the two types of touch. However, in forced touch, while *Fmr1* KO mice did show a tendency towards more avoidance and AFEs relative to wild type mice for social touch, they also displayed slightly more aversion to forced object than social touch. This may explain the responses we observed in *Fmr1* KO tS and BLA excited cells for forced touch, where they are modulated more by forced object than social touch compared to WT mice. BLA excited cells in *Fmr1* KO mice did show a similar proportion of cells with preference to social and object touch, suggesting that there is still a lack of discriminability between these two contexts even in the forced condition.

Together, these findings suggest that the tS, which we described as being involved in salience encoding in chapter 3, places a similar weight in salience between social and object

touch in *Fmr1* KO mice. The responses of BLA across the different types of touch in *Fmr1* KO mice may reflect its role in encoding strong aversive stimuli, such as forced object touch. The neuronal responses in BLA suggest that social touch may also be encoded as a mildly aversive stimulus in the FXS model.

Both the tS and BLA have been implicated in ASD behavioral symptoms[24-26]. tS dopaminergic signaling is required for its role in salience encoding and reduced dopaminergic signaling in the tS strongly correlated with novelty aversion in ASD mice[27]. The tS is anatomically comparable to the caudate in primates and humans, and ASD individuals show altered development and hyperexcitability of the caudate[28-30]. Changes in excitability in the BLA have been attributed to fear learning, anxiety and social dysregulation in mouse models of FXS and ASD and ASD individuals[31-33].

4.4.3: Decoder performance for context discrimination worsens in ASD mice

Fmr1 KO mice are also worse at discriminating social and object touch based on orofacial movements, particularly in voluntary touch. Decoder performance decreases further when whisker motion alone is used for decoding context, suggesting an inability of *Fmr1* KO mice to generate unique whisking movements required for facial social touch with another animal. Individuals with autism also have difficulties displaying appropriate facial expressions within a social context[34].

While avoidance behaviors and AFEs of WT mice also indicate strong discriminability between social and object touch and even more so than orofacial movements, *Fmr1* KO mice show reduced decoding of social and object touch based on avoidance and AFEs, particularly for forced touch. Furthermore, reduced decoder performance in KOs was sustained throughout the period of touch. Together, *Fmr1* KO mice show clear deficits in sensory discrimination at both the behavioral and circuit level that has been previously reported in ASD models[5,10,35,36].

4.4.4: Aversive state encoding in vS1, tS and BLA

Next, the presence of vS1, tS and BLA cells that increase their firing to aversive behaviors in WT and *Fmr1* KO mice was surprising. tS and BLA both share connectivity with motor thalamic nuclei and cortices and dorsal striatal areas and they may fine-tune motor actions, such as how much mice exhibit avoidance or aversive behaviors, based on the salience and negative valence from touch[37-40]. However, we were surprised to find that vS1 also contains behaviorally relevant cells for avoidance and AFEs. These behaviors do affect the way in which the test mice may engage using their whiskers with a novel object or stranger mouse. For example, aversive whisker protraction would prevent the mouse from actively whisking, which drives vS1 activity[41].

While WT mice showed more behaviorally relevant cells for avoidance and AFEs in object than social touch, *Fmr1* KO mice recruited a similar proportion of these cells in vS1, tS and BLA for both types of touch. We theorize that the recruitment of more of these cells in *Fmr1* KO mice is due to these mice not perceiving social touch any differently than object touch, which is consistently aversive to animals across genotypes.

Finally, behaviorally relevant cells that respond to more than one aversive or avoidance behavior were more prominent in the vS1, tS and BLA of *Fmr1* KO mice. These cells likely contribute to aversive state encoding if they can respond to more than one behavior and would suggest that *Fmr1* KO mice are in a persistent aversive state relative to wild type mice across bouts of both social and object touch. Emotional dysregulation, or the inability to modulate emotions to be below certain threshold, is frequently observed in ASD individuals as they interact with their environment[42]. Emotional dysregulation has not been well documented in ASD mouse models, though our findings to provide the first indication that *Fmr1* KO mice cannot down-modulate aversion when responding to non-threatening social touch. Emotional dysregulation in response to sensory stimuli could be explored further given that novel machine learning techniques can now identify different emotional states beyond aversion and pleasure and at varying degrees in mice[43,44].

4.4.5: Limitations and future directions

While this chapter primarily focused on the circuit differences in the FXS model, other mouse models of ASD may diverge from the FXS model in how vS1, tS and BLA respond to social touch. In chapter 2, we demonstrated that MIA mice do not have persistent hyperarousal and do show milder AFEs relative to *Fmr1* KO mice. The divergence in behaviors in MIA mice from the *Fmr1* KO model suggest that the social touch may also be represented slightly differently in the MIA model. It is important to consider how other models of ASD differ in how they respond to social touch and how social touch is represented at a circuit level.

Although we provide evidence that vS1, tS and BLA neuronal responses to social and object touch are altered in *Fmr1* KO mice and this may correlate with more avoidance and AFEs, this does not directly link circuit changes to these increased behaviors. vS1, tS or BLA activity could be manipulated with chemogenetic stimulation or inhibition of all cells or optogenetic stimulation or inhibition of specific cell types in these regions to determine if circuit interventions can reduce avoidance and AFEs in *Fmr1* KO mice[45].

We do report that vS1, tS and BLA have cells that respond to specific avoidance and aversive behaviors during social and object touch using ROC analysis; however, these behaviors tend to coincide with the onset of touch and thus we cannot reliably confirm that these cells are responsive to the behaviors alone. One alternative analysis that can distinguish if specific neurons are encoding touch stimuli versus behaviors is a generalized linear model (GLM). GLMs can be used as encoding models to discern to what extent touch stimuli (social or object) and avoidance and AFEs in combination contribute to neural variability in vS1, tS and BLA[46].

In conclusion, this chapter demonstrated that vS1, tS and BLA cells in *Fmr1* KO mice are unable to discriminate between social and object touch with varying degrees. The inability to distinguish social and object touch also occurs at the behavioral level in *Fmr1* KO mice and may explain why they display similar avoidance and AFEs to both social and object touch. We also find the similar proportion of cells responding to aversive behaviors are recruited for social and

object touch. Together, increased aversive behaviors to social touch in *Fmr1* KO mice coincide with the inability to discriminate between social and object touch in cortical, striatal and amygdalar circuits.

4.5: References

1. Cascio, C.J., Moore, D., and McGlone, F. (2019). Social touch and human development. Dev Cogn Neurosci *35*, 5-11. 10.1016/j.dcn.2018.04.009.

2. Green, S.A., Hernandez, L.M., Bowman, H.C., Bookheimer, S.Y., and Dapretto, M. (2018). Sensory over-responsivity and social cognition in ASD: Effects of aversive sensory stimuli and attentional modulation on neural responses to social cues. Dev Cogn Neurosci *29*, 127-139. 10.1016/j.dcn.2017.02.005.

3. Robertson, C.E., and Baron-Cohen, S. (2017). Sensory perception in autism. Nat Rev Neurosci *18*, 671-684. 10.1038/nrn.2017.112.

4. Chari, T., Hernandez, A., and Portera-Cailliau, C. (2023). A Novel Head-Fixed Assay for Social Touch in Mice Uncovers Aversive Responses in Two Autism Models. J Neurosci *43*, 7158-7174. 10.1523/jneurosci.0226-23.2023.

5. Orefice, L.L., Zimmerman, A.L., Chirila, A.M., Sleboda, S.J., Head, J.P., and Ginty, D.D. (2016). Peripheral Mechanosensory Neuron Dysfunction Underlies Tactile and Behavioral Deficits in Mouse Models of ASDs. Cell *166*, 299-313. 10.1016/j.cell.2016.05.033.

6. The Dutch-Belgian Fragile Consortium, Bakker, C.E., Verheij, C., Willemsen, R., van der Helm, R., Oerlemans, F., Vermey, M., Bygrave, A., Hoogeveen, A., Oostra, B.A., et al. (1994). Fmr1 knockout mice: A model to study fragile X mental retardation. Cell *78*, 23-33. https://doi.org/10.1016/0092-8674(94)90569-X.

7. He, C.X., Cantu, D.A., Mantri, S.S., Zeiger, W.A., Goel, A., and Portera-Cailliau, C. (2017). Tactile Defensiveness and Impaired Adaptation of Neuronal Activity in the Fmr1 Knock-Out Mouse Model of Autism. J Neurosci *37*, 6475-6487. 10.1523/JNEUROSCI.0651-17.2017.

8. Werling, D.M., and Geschwind, D.H. (2013). Sex differences in autism spectrum disorders. Curr Opin Neurol *26*, 146-153. 10.1097/WCO.0b013e32835ee548.

9. Bartholomay, K.L., Lee, C.H., Bruno, J.L., Lightbody, A.A., and Reiss, A.L. (2019). Closing the Gender Gap in Fragile X Syndrome: Review on Females with FXS and Preliminary Research Findings. Brain Sci *9*. 10.3390/brainsci9010011.

10. Goel, A., Cantu, D.A., Guilfoyle, J., Chaudhari, G.R., Newadkar, A., Todisco, B., de Alba, D., Kourdougli, N., Schmitt, L.M., Pedapati, E., et al. (2018). Impaired perceptual learning in a mouse model of Fragile X syndrome is mediated by parvalbumin neuron dysfunction and is reversible. Nat Neurosci *21*, 1404-1411. 10.1038/s41593-018-0231-0.

11. Kourdougli, N., Suresh, A., Liu, B., Juarez, P., Lin, A., Chung, D.T., Graven Sams, A., Gandal, M.J., Martínez-Cerdeño, V., Buonomano, D.V., et al. (2023). Improvement of sensory deficits in fragile X mice by increasing cortical interneuron activity after the critical period. Neuron. 10.1016/j.neuron.2023.06.009.

12. Antoine, M.W., Langberg, T., Schnepel, P., and Feldman, D.E. (2019). Increased Excitation-Inhibition Ratio Stabilizes Synapse and Circuit Excitability in Four Autism Mouse Models. Neuron *101*, 648-661.e644. 10.1016/j.neuron.2018.12.026.

13. Stuart, N., Whitehouse, A., Palermo, R., Bothe, E., and Badcock, N. (2022). Eye Gaze in Autism Spectrum Disorder: A Review of Neural Evidence for the Eye Avoidance Hypothesis. J Autism Dev Disord. 10.1007/s10803-022-05443-z.

14. Kliemann, D., Dziobek, I., Hatri, A., Steimke, R., and Heekeren, H.R. (2010). Atypical reflexive gaze patterns on emotional faces in autism spectrum disorders. J Neurosci *30*, 12281-12287. 10.1523/jneurosci.0688-10.2010.

15. Cuve, H.C., Gao, Y., and Fuse, A. (2018). Is it avoidance or hypoarousal? A systematic review of emotion recognition, eye-tracking, and psychophysiological studies in young adults with autism spectrum conditions. Research in Autism Spectrum Disorders *55*, 1-13. https://doi.org/10.1016/j.rasd.2018.07.002.

16. Wilkinson, E.H., Britton, T.C., and Hall, S.S. (2022). Examining Phenotypic Differences in Gaze Avoidance Between Autism Spectrum Disorder and Fragile X Syndrome. Am J Intellect Dev Disabil *127*, 435-454. 10.1352/1944-7558-127.6.435.

17. Miura, S.K., and Scanziani, M. (2022). Distinguishing externally from saccade-induced motion in visual cortex. Nature *610*, 135-142. 10.1038/s41586-022-05196-w.

18. Zahler, S.H., Taylor, D.E., Wong, J.Y., Adams, J.M., and Feinberg, E.H. (2021). Superior colliculus drives stimulus-evoked directionally biased saccades and attempted head movements in head-fixed mice. Elife *10*. 10.7554/eLife.73081.

19. Gehrlach, D.A., Dolensek, N., Klein, A.S., Roy Chowdhury, R., Matthys, A., Junghänel, M., Gaitanos, T.N., Podgornik, A., Black, T.D., Reddy Vaka, N., et al. (2019). Aversive state processing in the posterior insular cortex. Nat Neurosci *22*, 1424-1437. 10.1038/s41593-019-0469-1.

20. Corder, G., Ahanonu, B., Grewe, B.F., Wang, D., Schnitzer, M.J., and Scherrer, G. (2019). An amygdalar neural ensemble that encodes the unpleasantness of pain. Science *363*, 276-281. 10.1126/science.aap8586.

21. Green, S.A., Hernandez, L., Tottenham, N., Krasileva, K., Bookheimer, S.Y., and Dapretto, M. (2015). Neurobiology of Sensory Overresponsivity in Youth With Autism Spectrum Disorders. JAMA Psychiatry *72*, 778-786. 10.1001/jamapsychiatry.2015.0737.

22. Puts, N.A., Wodka, E.L., Tommerdahl, M., Mostofsky, S.H., and Edden, R.A. (2014). Impaired tactile processing in children with autism spectrum disorder. J Neurophysiol *111*, 1803-1811. 10.1152/jn.00890.2013.

23. He, J.L., Wodka, E., Tommerdahl, M., Edden, R.A.E., Mikkelsen, M., Mostofsky, S.H., and Puts, N.A.J. (2021). Disorder-specific alterations of tactile sensitivity in neurodevelopmental disorders. Commun Biol *4*, 97. 10.1038/s42003-020-01592-y.

24. Fuccillo, M.V. (2016). Striatal Circuits as a Common Node for Autism Pathophysiology. Front Neurosci *10*, 27. 10.3389/fnins.2016.00027.

25. Wang, Z., Yueh, H., Chau, M., Veenstra-VanderWeele, J., and O'Reilly, K.C. (2023). Circuits underlying social function and dysfunction. Autism Res *16*, 1268-1288. 10.1002/aur.2978.

26. Krüttner, S., Falasconi, A., Valbuena, S., Galimberti, I., Bouwmeester, T., Arber, S., and Caroni, P. (2022). Absence of familiarity triggers hallmarks of autism in mouse model through aberrant tail-of-striatum and prelimbic cortex signaling. Neuron *110*, 1468-1482.e1465. 10.1016/j.neuron.2022.02.001.

27. Kohls, G., Schulte-Rüther, M., Nehrkorn, B., Müller, K., Fink, G.R., Kamp-Becker, I., Herpertz-Dahlmann, B., Schultz, R.T., and Konrad, K. (2013). Reward system dysfunction in autism spectrum disorders. Soc Cogn Affect Neurosci *8*, 565-572. 10.1093/scan/nss033.

28. Lee, K., An, S.Y., Park, J., Lee, S., and Kim, H.F. (2023). Anatomical and Functional Comparison of the Caudate Tail in Primates and the Tail of the Striatum in Rodents: Implications for Sensory Information Processing and Habitual Behavior. Mol Cells *46*, 461-469. 10.14348/molcells.2023.0051.

29. Schuetze, M., Park, M.T., Cho, I.Y., MacMaster, F.P., Chakravarty, M.M., and Bray, S.L. (2016). Morphological Alterations in the Thalamus, Striatum, and Pallidum in Autism Spectrum Disorder. Neuropsychopharmacology *41*, 2627-2637. 10.1038/npp.2016.64.

30. Adorjan, I., Ahmed, B., Feher, V., Torso, M., Krug, K., Esiri, M., Chance, S.A., and Szele, F.G. (2017). Calretinin interneuron density in the caudate nucleus is lower in autism spectrum disorder. Brain *140*, 2028-2040. 10.1093/brain/awx131.

31. Svalina, M.N., Rio, C.C., Kushner, J.K., Levy, A., Baca, S.M., Guthman, E.M., Opendak, M., Sullivan, R., Restrepo, D., and Huntsman, M.M. (2022). Basolateral amygdala hyperexcitability is associated with precocious developmental emergence of fear-learning in Fragile X Syndrome. J Neurosci *42*, 7294-7308. 10.1523/JNEUROSCI.1776-21.2022.

32. Fernandes, G., Mishra, P.K., Nawaz, M.S., Donlin-Asp, P.G., Rahman, M.M., Hazra, A., Kedia, S., Kayenaat, A., Songara, D., Wyllie, D.J.A., et al. (2021). Correction of amygdalar

dysfunction in a rat model of fragile X syndrome. Cell Rep *37*, 109805. 10.1016/j.celrep.2021.109805.

33. Kim, S., Kim, Y.E., Song, I., Ujihara, Y., Kim, N., Jiang, Y.H., Yin, H.H., Lee, T.H., and Kim, I.H. (2022). Neural circuit pathology driven by Shank3 mutation disrupts social behaviors. Cell Rep *39*, 110906. 10.1016/j.celrep.2022.110906.

34. Drimalla, H., Baskow, I., Behnia, B., Roepke, S., and Dziobek, I. (2021). Imitation and recognition of facial emotions in autism: a computer vision approach. Mol Autism *12*, 27. 10.1186/s13229-021-00430-0.

35. Michaelson, S.D., Ozkan, E.D., Aceti, M., Maity, S., Llamosas, N., Weldon, M., Mizrachi, E., Vaissiere, T., Gaffield, M.A., Christie, J.M., et al. (2018). SYNGAP1 heterozygosity disrupts sensory processing by reducing touch-related activity within somatosensory cortex circuits. Nat Neurosci *21*, 1-13. 10.1038/s41593-018-0268-0.

36. Chen, Q., Deister, C.A., Gao, X., Guo, B., Lynn-Jones, T., Chen, N., Wells, M.F., Liu, R., Goard, M.J., Dimidschstein, J., et al. (2020). Dysfunction of cortical GABAergic neurons leads to sensory hyper-reactivity in a Shank3 mouse model of ASD. Nat Neurosci *23*, 520-532. 10.1038/s41593-020-0598-6.

37. Valjent, E., and Gangarossa, G. (2021). The Tail of the Striatum: From Anatomy to Connectivity and Function. Trends Neurosci *44*, 203-214. 10.1016/j.tins.2020.10.016.

38. Hintiryan, H., Bowman, I., Johnson, D.L., Korobkova, L., Zhu, M., Khanjani, N., Gou, L., Gao, L., Yamashita, S., Bienkowski, M.S., et al. (2021). Connectivity characterization of the mouse basolateral amygdalar complex. Nat Commun *12*, 2859. 10.1038/s41467-021-22915-5.

39. Terburg, D., Scheggia, D., Triana Del Rio, R., Klumpers, F., Ciobanu, A.C., Morgan, B., Montoya, E.R., Bos, P.A., Giobellina, G., van den Burg, E.H., et al. (2018). The Basolateral Amygdala Is Essential for Rapid Escape: A Human and Rodent Study. Cell *175*, 723-735.e716. 10.1016/j.cell.2018.09.028.

40. Li, Z., Wei, J.X., Zhang, G.W., Huang, J.J., Zingg, B., Wang, X., Tao, H.W., and Zhang, L.I. (2021). Corticostriatal control of defense behavior in mice induced by auditory looming cues. Nat Commun *12*, 1040. 10.1038/s41467-021-21248-7.

41. de Kock, C.P., and Sakmann, B. (2009). Spiking in primary somatosensory cortex during natural whisking in awake head-restrained rats is cell-type specific. Proc Natl Acad Sci U S A *106*, 16446-16450. 10.1073/pnas.0904143106.

42. Dell'Osso, L., Massoni, L., Battaglini, S., De Felice, C., Nardi, B., Amatori, G., Cremone, I.M., and Carpita, B. (2023). Emotional dysregulation as a part of the autism spectrum continuum: a literature review from late childhood to adulthood. Front Psychiatry *14*, 1234518. 10.3389/fpsyt.2023.1234518.

43. Dolensek, N., Gehrlach, D.A., Klein, A.S., and Gogolla, N. (2020). Facial expressions of emotion states and their neuronal correlates in mice. Science *368*, 89-94. 10.1126/science.aaz9468.

44. Malezieux, M., Klein, A.S., and Gogolla, N. (2023). Neural Circuits for Emotion. Annu Rev Neurosci *46*, 211-231. 10.1146/annurev-neuro-111020-103314.

45. Aston-Jones, G., and Deisseroth, K. (2013). Recent advances in optogenetics and pharmacogenetics. Brain Res *1511*, 1-5. 10.1016/j.brainres.2013.01.026.

46. Kriegeskorte, N., and Douglas, P.K. (2019). Interpreting encoding and decoding models. Curr Opin Neurobiol *55*, 167-179. 10.1016/j.conb.2019.04.002.

CHAPTER 5: Discussion

5.1: Summary of results

Social touch between animals and humans is often considered pleasurable and comforting but can become perceived as aversive in certain contexts and particularly in individuals with ASD. However, it is not known why the brain would change its perception of social touch into something aversive. We hypothesized that this happens in ASD because relevant brain circuits for social touch, such vS1, tS and BLA, are unable to distinguish pleasurable social touch from aversive non-social touch.

To interrogate these brain circuits, we needed to look at social touch aversion using mouse models of ASD. However, aversion to social touch has not been studied in depth with these models and the circuits required for the perception of social touch are not fully characterized.

We conducted initial experiments to assess if mouse models of ASD display aversive behaviors to social touch in a novel head-fixed behavioral assay that we designed[1]. In this assay, test mice would voluntarily engage via the whiskers with a novel object or stranger mouse or would be forced to engage with either stimulus via their snouts. With this assay, we could gauge the extent to which two different mouse models of ASD display avoidance or AFEs to social or non-social touch when they have some control in engaging with the stimulus (voluntary touch) versus when they are forced into contact with their snout and many whiskers touching the stimulus (forced touch). The assay also allowed us to repeat bouts of voluntary, and forced, object and social touch in a trial-based manner. Both the genetic *Fmr1* KO and environmental MIA model of ASD displayed greater avoidance to 5 bouts of voluntary and forced social touch compared to healthy controls. Furthermore, forced touch is perceived as more aversive than voluntary touch. Both ASD models expressed AFEs more so during just forced social touch compared to controls. We did observe some divergence in the behavioral manifestations from these models in which the FXS model displayed persistent hyperarousal (via pupil size) to social touch and this was not the case for the MIA model. Overall, our findings

showed that ASD models are unable to down-modulate aversion to social touch compared to controls and thus show similar levels of avoidance and AFEs to both social and object touch.

As this novel behavioral assay allowed us to quantify social touch aversion and show differences in ASD models relative to controls, we used the assay to identify brain regions that were strongly modulated by social touch. Although there were brain-wide changes in activity in response to social touch, including regions involved in aversive encoding, we focused on recording neuronal activity from just the vS1, tS and BLA[2-12]. All these regions were modulated more by social than object touch, could be targeted simultaneously for in vivo electrophysiological recordings with silicon probes and may contribute to valence encoding of social touch based on their known functional roles[2,4,5,10,12-18].

Our initial set of electrophysiological recordings were done in WT mice to determine how vS1, tS and BLA typically encode social touch relative to object touch and how neuronal responses differ between voluntary and forced touch. We found that vS1 activity represents texture encoding since vS1 cells preferentially fired more to social than object regardless of if the touch was voluntary or forced. tS activity, on the other hand, reflects salience encoding since firing was greater for voluntary social than object touch, but the opposite for forced touch. Finally, the BLA did not show major differences in firing between social and object touch but may be involved in encoding aversive sensory stimuli since there were a larger proportion of BLA cells preferring object touch. WT mice can distinguish between social and object touch in these circuits and in their behavior, specifically their whisker movements.

Since WT mice vS1, tS and BLA circuits respond very differently to social and object touch in, we hypothesized these circuits in the *Fmr1* KO model of ASD show more similar responses to these two types of touch and contributes the inability of the FXS model to down-modulate social touch aversion. In our subsequent electrophysiological recordings in *Fmr1* KO mice, vS1 displayed similar firing to voluntary, and forced, social and object touch. While tS activity was also similar between voluntary social and object touch, both tS and BLA cells were

modulated more by forced object than social touch like WT mice. Not only did these circuits show similar responses to social and object touch, *Fmr1* KO were unable to distinguish social and object touch as well as WT mice based on their behavior. Finally, we observed the *Fmr1* KO have similar proportion of vS1, tS and BLA cells that respond to aversive behaviors between social and object touch. It is clear from these findings that *Fmr1* KO vS1, tS and BLA neuronal circuits are unable to perceive social and object touch differently and this correlates with increased aversion to social touch in *Fmr1* KO mice.

5.2: Neural basis of social touch aversion in ASD

How does pleasurable social touch become perceived as aversive in ASD? We propose a mechanism in which sensory perception is perturbed in ASD, this contributes to aberrant emotional encoding of social touch in subcortical regions and leads to social touch aversion.

Our findings clearly show that vS1, important for whisker-mediated touch, can distinguish between social and object touch in WT mice. The difference in encoding of social versus non-social touch early in the somatosensory pathway may be necessary for perception of social touch as pleasurable in prefrontal or subcortical regions that connect with vS1. However, vS1 in the FXS mouse model of ASD does not perceive social touch any differently from object touch. Reduced sensory discrimination is consistent with other studies in ASD mouse models and individuals with ASD[19-23]. Poorer perceptual discrimination of touch stimuli is partly dependent on tactile hypersensitivity, such that vS1 activity is heightened for all types of textures and textures of different salience or valence become indistinguishable[24-28]. As a result, social touch that is typically pleasurable would not be perceived any differently to touch from a Falcon tube or toy mouse, that is aversive to mice, in vS1.

How might tactile-relevant information from vS1 transfer over to the tS and BLA where we also observed differences in the encoding of social versus non-social touch? The majority of long-range connections for vS1 are with other sensory or motor cortices, sensory thalamic

nuclei and prefrontal areas[29]. However, the tS does receive some input directly from primary sensory cortices and also receives input from sensory thalamic nuclei, including the ventral posteromedial nucleus (VPM), which is the thalamic relay for touch stimuli[10]. The tS integrates stimuli across all sensory modalities, including touch, and is excited by both rewarding or aversive stimuli, which relates to its role in salience encoding[10,18,30,31]. This may explain why tS activity in wild type mice is modulated more so by voluntary social than object touch, but the opposite happens in forced touch. In voluntary touch, the test mouse has the flexibility to engage in touch by palpating its whiskers. As such, voluntary social touch may be more salient because it is more pleasurable than voluntary object touch, which is only mildly aversive. In forced touch, social touch may still be considered somewhat pleasurable but the salience of social touch is outweighed by the strong aversion to forced object touch. We postulate that social and non-social touch are indistinguishable in the tS of *Fmr1* KO mice and perceived as having the same level of salience. This is supported by the fact that *Fmr1* KO mice show similar tS activity to voluntary social and object touch. It is also likely that the tS represents both social and object touch as equally salient since ASD mice display a similar degree of aversion to social and object touch. Efferent projections from the tS relay to other basal ganglia regions, thereby allowing for subsequent motor actions including aversive behaviors[10].

The tS alone likely does not contribute to the emergence of aversion to social touch in ASD. This is evidenced by the fact that the TRAP experiments revealed multiple brain regions highly modulated by social touch and vS1 and BLA also show cells that increase their firing to avoidance running and AFEs. How might the BLA contribute to social touch aversion? Our findings showed that, for the most part, the BLA is not differentially modulated by social or object touch both in wild type and *Fmr1* KO mice. This is surprising given that the BLA is known for encoding both aversive and social stimuli and our TRAP experiments demonstrated that BLA activity was significantly more modulated by social than object touch[4,17]. One hypothesis is that BLA activity integrates multisensory social information and is already driven by the social

context such that social touch doesn't drive activity further[32]. Furthermore, BLA activity is only further tuned by touch that is strongly aversive, such as forced touch. Indeed, while WT animals show more object-preferring cells in the BLA for forced touch, *Fmr1* KO mice show a similar proportion of social and object-preferring BLA cells that translates to more similar levels of aversion to social and object touch. BLA does share connectivity with multiple sensory cortices, including somatosensory, and could directly encode aversive sensory stimuli, but there isn't evidence of strong connectivity between BLA and tS[33,34]. It is more likely that the BLA converges on similar motor systems as the tS, including dorsal striatal areas, to drive aversive motor behaviors to social touch in ASD mice[33].

Together, vS1, tS and BLA may be part of a larger circuit mechanism in ASD mice that perceives both social and non-social touch stimuli, which are clearly distinct in texture, salience and emotional valence, as aversive. This contributes to more avoidance and AFEs to social touch and increased aversion to social touch in ASD mice relative to WTs.

5.3: Future directions

5.3.1: Modified social touch behavioral assay

The novel behavioral assay we designed and described in chapter 2 can uncover aversive responses to social touch in mouse models of ASD. However, one of the main limitations of this assay is that it is not naturalistic. Even in voluntary touch where test mice have the flexibility to engage in touch, these mice are still controlled by the experimenter to be within a certain distance of the stranger mouse or novel object. Would ASD mice prefer shorter durations, farther distances or fewer bouts of social touch if they were given full agency to control the duration, distance or number of bouts of touch?

One advantage of our novel behavioral assay is that it can be easily modified such that the test mouse could control the movement of the platform via a lever press. Head-fixed test mice can learn to associate the lever press with the platform movement through reward

learning[35]. Upon associating the level press with the movement of the platform for a food or water reward, the reward can be replaced with a stranger mouse or novel object. The experimenter would then be able to quantify how often the test mouse moves the platform, the distance at which the test mouse engages in touch and the duration of touch. Presumably, if touch from another mouse is perceived as rewarding then the test mouse would more frequently lever press to move the platform forward. Social touch interactions would no longer be trial-based but complex, aversive behaviors and in vivo recordings could still be acquired. This modified behavioral assay would assess the motivation to engage in social touch in ASD mice.

5.3.2: Encoding of social facial touch across multiple brain regions

While vS1, tS and BLA are encoding features of social touch, including social touch aversion, these brain regions alone do not comprise the neural circuit for social touch perception especially given their connectivity with multiple cortical and subcortical brain regions. The TRAP experiments we described in chapter 3 also show that ACCx, NAc, InsCx, CeA, MeA, PVT and PvtH are all highly modulated by social touch and there is likely additional prefrontal, striatal, thalamic and hypothalamic brain regions that behave similarly.

Chronic implantations of multiple Neuropixels probes in a single mouse would allow us to record from many of these brain regions simultaneously. This was not considered feasible for the past few years since most chronic implantations were bulky relative to the size of mice[36,37]. By 3D-printing smaller casings that can hold multiple probes and that are relatively light when implanted on mice, simultaneous recordings with up to 6 probes in the brain across multiple days are now possible[38]. By recording from multiple brain regions with Neuropixels, it is possible to assess the functional connectivity of these regions as mice receive voluntary and forced social touch and how connectivity changes in mouse models of ASD[39].

5.3.3: Manipulation of vS1, tS and BLA activity

Our findings of altered activity in the vS1, tS and BLA of the FXS mouse model during social touch may be associated with social touch aversion but cannot be directly linked to increased avoidance and AFEs to social touch. Neuronal activity in these brain regions could be manipulated with either chemogenetics or optogenetics to see if manipulating activity reduces avoidance and AFEs in ASD mouse models. Both manipulations can be done in a time-dependent manner, although optogenetics is much more precise in temporal specificity and can be used to target specific cell types[40].

Either manipulation can also be done simultaneously with chronic Neuropixels recordings; however, electrophysiological recordings are sensitive to light artefacts with optogenetic stimulation[41].

5.3.4: Encoding model to discern how touch and behaviors contribute to neural variability

Although we found the vS1, tS and BLA can encode avoidance and aversive behaviors, the responses of these cells to these behaviors are not disentangled from social or object touch. Avoidance and aversive behaviors typically occur when the test mice receive touch such that it is unclear if neural variability in these regions are due to the presence of touch stimuli or the behaviors.

One method that can circumvent this caveat is an encoding model. GLMs can be used as encoding models in which stimuli and behaviors can be used as predictors for neural activity. Typically, a GLM with a Poisson or Gaussian distribution is used for electrophysiological data to predict action potential spike count (or firing rate) of each neuron from these predictors[42]. A modified linear encoding model that uses ridge regression leverages time-shifted versions of stimuli or behavior predictors to determine if neural variability is better explained when predictors are shifted backwards or forwards by a certain time delay relative to neuronal activity

over time[43]. Using an encoding model, we could more accurately gauge whether vS1, tS or BLA consists of cells that uniquely encode aversive behaviors, touch stimuli or both.

5.4: References

1. Chari, T., Hernandez, A., and Portera-Cailliau, C. (2023). A Novel Head-Fixed Assay for Social Touch in Mice Uncovers Aversive Responses in Two Autism Models. J Neurosci *43*, 7158-7174. 10.1523/jneurosci.0226-23.2023.

2. Terburg, D., Scheggia, D., Triana Del Rio, R., Klumpers, F., Ciobanu, A.C., Morgan, B., Montoya, E.R., Bos, P.A., Giobellina, G., van den Burg, E.H., et al. (2018). The Basolateral Amygdala Is Essential for Rapid Escape: A Human and Rodent Study. Cell *175*, 723-735.e716. 10.1016/j.cell.2018.09.028.

3. Sengupta, A., Yau, J.O.Y., Jean-Richard-Dit-Bressel, P., Liu, Y., Millan, E.Z., Power, J.M., and McNally, G.P. (2018). Basolateral Amygdala Neurons Maintain Aversive Emotional Salience. J Neurosci *38*, 3001-3012. 10.1523/jneurosci.2460-17.2017.

4. Corder, G., Ahanonu, B., Grewe, B.F., Wang, D., Schnitzer, M.J., and Scherrer, G. (2019). An amygdalar neural ensemble that encodes the unpleasantness of pain. Science *363*, 276-281. 10.1126/science.aap8586.

5. Allsop, S.A., Wichmann, R., Mills, F., Burgos-Robles, A., Chang, C.J., Felix-Ortiz, A.C., Vienne, A., Beyeler, A., Izadmehr, E.M., Glober, G., et al. (2018). Corticoamygdala Transfer of Socially Derived Information Gates Observational Learning. Cell *173*, 1329-1342.e1318. 10.1016/j.cell.2018.04.004.

6. Wu, Y.E., Dang, J., Kingsbury, L., Zhang, M., Sun, F., Hu, R.K., and Hong, W. (2021). Neural control of affiliative touch in prosocial interaction. Nature *599*, 262-267. 10.1038/s41586-021-03962-w.

7. Li, Y., Mathis, A., Grewe, B.F., Osterhout, J.A., Ahanonu, B., Schnitzer, M.J., Murthy, V.N., and Dulac, C. (2017). Neuronal Representation of Social Information in the Medial Amygdala of Awake Behaving Mice. Cell *171*, 1176-1190.e1117. 10.1016/j.cell.2017.10.015.

8. Gao, C., Leng, Y., Ma, J., Rooke, V., Rodriguez-Gonzalez, S., Ramakrishnan, C., Deisseroth, K., and Penzo, M.A. (2020). Two genetically, anatomically and functionally distinct

cell types segregate across anteroposterior axis of paraventricular thalamus. Nat Neurosci *23*, 217-228. 10.1038/s41593-019-0572-3.

9. Gehrlach, D.A., Dolensek, N., Klein, A.S., Roy Chowdhury, R., Matthys, A., Junghänel, M., Gaitanos, T.N., Podgornik, A., Black, T.D., Reddy Vaka, N., et al. (2019). Aversive state processing in the posterior insular cortex. Nat Neurosci *22*, 1424-1437. 10.1038/s41593-019-0469-1.

10. Valjent, E., and Gangarossa, G. (2021). The Tail of the Striatum: From Anatomy to Connectivity and Function. Trends Neurosci *44*, 203-214. 10.1016/j.tins.2020.10.016.

11. de Kloet, S.F., Bruinsma, B., Terra, H., Heistek, T.S., Passchier, E.M.J., van den Berg, A.R., Luchicchi, A., Min, R., Pattij, T., and Mansvelder, H.D. (2021). Bi-directional regulation of cognitive control by distinct prefrontal cortical output neurons to thalamus and striatum. Nat Commun *12*, 1994. 10.1038/s41467-021-22260-7.

12. Krüttner, S., Falasconi, A., Valbuena, S., Galimberti, I., Bouwmeester, T., Arber, S., and Caroni, P. (2022). Absence of familiarity triggers hallmarks of autism in mouse model through aberrant tail-of-striatum and prelimbic cortex signaling. Neuron *110*, 1468-1482.e1465. 10.1016/j.neuron.2022.02.001.

13. Bobrov, E., Wolfe, J., Rao, R.P., and Brecht, M. (2014). The representation of social facial touch in rat barrel cortex. Curr Biol *24*, 109-115. 10.1016/j.cub.2013.11.049.

14. Ebbesen, C.L., Bobrov, E., Rao, R.P., and Brecht, M. (2019). Highly structured, partner-sex- and subject-sex-dependent cortical responses during social facial touch. Nat Commun *10*, 4634. 10.1038/s41467-019-12511-z.

15. Wolfe, J., Mende, C., and Brecht, M. (2011). Social facial touch in rats. Behav Neurosci *125*, 900-910. 10.1037/a0026165.

16. Tye, K.M. (2018). Neural Circuit Motifs in Valence Processing. Neuron *100*, 436-452. 10.1016/j.neuron.2018.10.001.

17. Fustiñana, M.S., Eichlisberger, T., Bouwmeester, T., Bitterman, Y., and Lüthi, A. (2021). State-dependent encoding of exploratory behaviour in the amygdala. Nature. 10.1038/s41586-021-03301-z.

18. Akiti, K., Tsutsui-Kimura, I., Xie, Y., Mathis, A., Markowitz, J.E., Anyoha, R., Datta, S.R., Mathis, M.W., Uchida, N., and Watabe-Uchida, M. (2022). Striatal dopamine explains novelty-induced behavioral dynamics and individual variability in threat prediction. Neuron *110*, 3789-3804.e3789. 10.1016/j.neuron.2022.08.022.

19. Goel, A., Cantu, D.A., Guilfoyle, J., Chaudhari, G.R., Newadkar, A., Todisco, B., de Alba, D., Kourdougli, N., Schmitt, L.M., Pedapati, E., et al. (2018). Impaired perceptual learning in a mouse model of Fragile X syndrome is mediated by parvalbumin neuron dysfunction and is reversible. Nat Neurosci *21*, 1404-1411. 10.1038/s41593-018-0231-0.

20. Lee Masson, H., Pillet, I., Amelynck, S., Van De Plas, S., Hendriks, M., Op de Beeck, H., and Boets, B. (2019). Intact neural representations of affective meaning of touch but lack of embodied resonance in autism: a multi-voxel pattern analysis study. Mol Autism *10*, 39. 10.1186/s13229-019-0294-0.

21. Puts, N.A., Wodka, E.L., Tommerdahl, M., Mostofsky, S.H., and Edden, R.A. (2014). Impaired tactile processing in children with autism spectrum disorder. J Neurophysiol *111*, 1803-1811. 10.1152/jn.00890.2013.

22. Cascio, C.J., Moana-Filho, E.J., Guest, S., Nebel, M.B., Weisner, J., Baranek, G.T., and Essick, G.K. (2012). Perceptual and neural response to affective tactile texture stimulation in adults with autism spectrum disorders. Autism Res *5*, 231-244. 10.1002/aur.1224.

23. Clements, C.C., Zoltowski, A.R., Yankowitz, L.D., Yerys, B.E., Schultz, R.T., and Herrington, J.D. (2018). Evaluation of the Social Motivation Hypothesis of Autism: A Systematic Review and Meta-analysis. JAMA Psychiatry *75*, 797-808. 10.1001/jamapsychiatry.2018.1100.

24. He, C.X., Cantu, D.A., Mantri, S.S., Zeiger, W.A., Goel, A., and Portera-Cailliau, C. (2017). Tactile Defensiveness and Impaired Adaptation of Neuronal Activity in the Fmr1 Knock-Out Mouse Model of Autism. J Neurosci *37*, 6475-6487. 10.1523/jneurosci.0651-17.2017.

25. Chen, Q., Deister, C.A., Gao, X., Guo, B., Lynn-Jones, T., Chen, N., Wells, M.F., Liu, R., Goard, M.J., Dimidschstein, J., et al. (2020). Dysfunction of cortical GABAergic neurons leads to sensory hyper-reactivity in a Shank3 mouse model of ASD. Nat Neurosci *23*, 520-532. 10.1038/s41593-020-0598-6.

26. Green, S.A., Hernandez, L.M., Bowman, H.C., Bookheimer, S.Y., and Dapretto, M. (2018). Sensory over-responsivity and social cognition in ASD: Effects of aversive sensory stimuli and attentional modulation on neural responses to social cues. Dev Cogn Neurosci *29*, 127-139. 10.1016/j.dcn.2017.02.005.

27. Kojovic, N., Ben Hadid, L., Franchini, M., and Schaer, M. (2019). Sensory Processing Issues and Their Association with Social Difficulties in Children with Autism Spectrum Disorders. J Clin Med *8*. 10.3390/jcm8101508.

28. Hamilton, A., and Pelphrey, K. (2018). Sensory and social features of autism - can they be integrated? Dev Cogn Neurosci *29*, 1-3. 10.1016/j.dcn.2018.02.009.

29. Petersen, C.C. (2007). The functional organization of the barrel cortex. Neuron *56*, 339-355. 10.1016/j.neuron.2007.09.017.

30. Gangarossa, G., Castell, L., Castro, L., Tarot, P., Veyrunes, F., Vincent, P., Bertaso, F., and Valjent, E. (2019). Contrasting patterns of ERK activation in the tail of the striatum in response to aversive and rewarding signals. J Neurochem *151*, 204-226. 10.1111/jnc.14804.

31. Li, Z., Wei, J.X., Zhang, G.W., Huang, J.J., Zingg, B., Wang, X., Tao, H.W., and Zhang, L.I. (2021). Corticostriatal control of defense behavior in mice induced by auditory looming cues. Nat Commun *12*, 1040. 10.1038/s41467-021-21248-7.

32. Mazuski, C., and O'Keefe, J. (2022). Representation of ethological events by basolateral amygdala neurons. Cell Rep *39*, 110921. 10.1016/j.celrep.2022.110921.

33. Hintiryan, H., Bowman, I., Johnson, D.L., Korobkova, L., Zhu, M., Khanjani, N., Gou, L., Gao, L., Yamashita, S., Bienkowski, M.S., et al. (2021). Connectivity characterization of the mouse basolateral amygdalar complex. Nat Commun *12*, 2859. 10.1038/s41467-021-22915-5.

34. Menegas, W., Bergan, J.F., Ogawa, S.K., Isogai, Y., Umadevi Venkataraju, K., Osten, P., Uchida, N., and Watabe-Uchida, M. (2015). Dopamine neurons projecting to the posterior striatum form an anatomically distinct subclass. Elife *4*, e10032. 10.7554/eLife.10032.

35. Guo, Z.V., Hires, S.A., Li, N., O'Connor, D.H., Komiyama, T., Ophir, E., Huber, D., Bonardi, C., Morandell, K., Gutnisky, D., et al. (2014). Procedures for behavioral experiments in head-fixed mice. PLoS One *9*, e88678. 10.1371/journal.pone.0088678.

36. Juavinett, A.L., Bekheet, G., and Churchland, A.K. (2019). Chronically implanted Neuropixels probes enable high-yield recordings in freely moving mice. Elife *8*. 10.7554/eLife.47188.

37. Luo, T.Z., Bondy, A.G., Gupta, D., Elliott, V.A., Kopec, C.D., and Brody, C.D. (2020). An approach for long-term, multi-probe Neuropixels recordings in unrestrained rats. Elife *9*. 10.7554/eLife.59716.

38. Melin, M.D., Churchland, A.K., and Couto, J. (2023). Large scale, simultaneous chronic neural recordings from multiple brain areas. bioRxiv. 10.1101/2023.12.22.572441.

39. Jia, X., Siegle, J.H., Durand, S., Heller, G., Ramirez, T.K., Koch, C., and Olsen, S.R. (2022). Multi-regional module-based signal transmission in mouse visual cortex. Neuron *110*, 1585-1598.e1589. 10.1016/j.neuron.2022.01.027.

40. Aston-Jones, G., and Deisseroth, K. (2013). Recent advances in optogenetics and pharmacogenetics. Brain Res *1511*, 1-5. 10.1016/j.brainres.2013.01.026.

41. Steinmetz, N.A., Koch, C., Harris, K.D., and Carandini, M. (2018). Challenges and opportunities for large-scale electrophysiology with Neuropixels probes. Curr Opin Neurobiol *50*, 92-100. 10.1016/j.conb.2018.01.009.

42. Pillow, J.W., Shlens, J., Paninski, L., Sher, A., Litke, A.M., Chichilnisky, E.J., and Simoncelli, E.P. (2008). Spatio-temporal correlations and visual signalling in a complete neuronal population. Nature *454*, 995-999. 10.1038/nature07140.

43. Musall, S., Kaufman, M.T., Juavinett, A.L., Gluf, S., and Churchland, A.K. (2019). Single-trial neural dynamics are dominated by richly varied movements. Nat Neurosci *22*, 1677-1686. 10.1038/s41593-019-0502-4.